Posttargeting Events in Cotranslational Translocation Through the Sec61 Complex: a Thesis

POSTTARGETING EVENTS IN COTRANSLATIONAL TRANSLOCATION THROUGH THE SEC61 COMPLEX

A Thesis Presented

By

Zhiliang Cheng

Submitted to the faculty of the University of Massachusetts Medical School in partial fulfillment of the requirements for the degree of

DOCTOR OF PHILOSOPHY IN BIOCHEMISTRY AND MOLECULAR PHARMACOLOGY

March 2006

POSTTARGETING EVENTS IN COTRANSLATIONAL TRANSLOCATION THROUGH THE SEC61 COMPLEX

A Thesis Presented

By

Zhiliang Cheng

Approved as to style and content by:

Dr. Anthony Carruthers, Chairman of the Committee

Dr. Lila Gierasch

Dr. Duane Jenness

Dr. Kendall Knight

Dr. Mary Munson

Dr. Reid Gilmore, Thesis advisor

Dr. Anthony Carruthers, Dean of
Graduate School of Biomedical Sciences

Dedicated to my parents, Nianchao Cheng and Yunyu Hu,

for their selfless, priceless and endless love

ACKNOWLEDGEMENT

I would like to express deep respect and appreciation to a great person and scientist, my thesis advisor, Dr. Reid Gilmore. His dedication to the work, incredible intelligence and insightful advice inspired and guided me through my graduate study.

I also want to thank my beautiful wife, Ying Jiang, for her love and support, and for being my best friend and soul mate. Ying was also my colleague in lab and contributed as much as I did to the work in chapter III.

All the members in Gilmore's lab provided priceless help and support during my thesis research. I owe millions of thanks to Elisabet Mandon, Daniel Kelleher, Catalina Ruiz, Steven Trueman, and Sanhamitra Mylavarapu.

I am very grateful to all the members in my thesis advisory committee, Drs. Anthony Carruthers, Lila Gierasch, Duane Jenness, Kendall Knight, and Mary Munson. Thanks to them for keeping me on the right track and providing great advice along the way.

ABSTRACT

The cytoplasmic surface of Sec61p is the binding site for the ribosome and has been proposed to interact with the signal recognition particle receptor during targeting of the ribosome nascent chain complex to the translocation channel. Point mutations in cytoplasmic loops six (L6) and eight (L8) of yeast Sec61p cause reductions in growth rates and defects in translocation of nascent polypeptides that utilize the cotranslational translocation pathway. Sec61 heterotrimers isolated from the L8 *sec61* mutants have a greatly reduced affinity for 80S ribosomes. Cytoplasmic accumulation of protein precursors demonstrates that the initial contact between the large ribosomal subunit and the Sec61 complex is important for efficient insertion of a nascent polypeptide into the translocation pore. In contrast, point mutations in L6 of Sec61p inhibit cotranslational translocation without significantly reducing the ribosome binding activity, indicating that the L6 and L8 *sec61* mutants impact different steps in the cotranslational translocation pathway.

Integral membrane proteins are cotranslationally inserted into the endoplasmic reticulum via the protein translocation channel, which mediates the translocation of lumenal domains, retention of cytosolic domains and integration of transmembrane spans into the phospholipid bilayer. We analyzed the in vivo kinetics of integration of model membrane proteins in *Saccharomyces cerevisiae* using ubiquitin translocation assay reporters. A signal anchor sequence from a type II membrane protein gates the translocon pore less rapidly than a cleavable signal sequence from a secretory protein. Transmembrane spans and lumenal domains are exposed to the cytosol during integration of a polytopic membrane protein. The conformational changes in the translocon that

permit opening of the lumenal and lateral channel gates occur less rapidly than elongation of the nascent polypeptide. Cytosolic exposure of transmembrane spans and lumenal domains poses a challenge to the fidelity of membrane protein integration.

TABLE OF CONTENTS

List of Figures

List of Abbreviations

CPY	carboxypeptidase Y
DPAPB	dipeptidylaminopeptidase B
DPAPB-HA	HA-tagged DPAPB
Endo H	endoglycosidase H
5-FOA	5-fluoroorotic acid
PK-RM	puromycin-high salt-washed rough microsomes
RNC	ribosome nascent chain complex
SR	SRP receptor
SRP	signal recognition particle
SSB	signal sequence binding site
TM	transmembrane
Tm	tunicamycin
Ub	ubiquitin
Ub*	I3G, I13G Ub mutant
UBPs	ubiquitin specific proteases
UTA	ubiquitin translocation assay

CHAPTER I

Introduction

Signal hypothesis and signal sequence

The complex organization of eukaryotic cells is characterized by their many interactive subcellular compartments. These membrane-enclosed organelles have distinct functions as defined by the proteins located inside the lumen and the membrane. Proteins are synthesized by ribosomes in the cytoplasm of cells. Newly synthesized proteins that won't remain in the cytoplasm, such as secretory and membrane proteins, have to be transported to their final destinations. Polypeptides cannot move freely across the hydrophobic barrier formed by a membrane. Therefore, there must be specific mechanisms to govern the transport of polypeptides. It has been determined that the endoplasmic reticulum (ER) is the first step of the polypeptide transport mechanism (pathway) for many proteins (Siekevitz and Palade, 1960). After translocation into the ER lumen, polypeptides are then subsequently transported to the Golgi apparatus. During translocation through these organelles, proteins undergo post-translocational modifications in ER and Golgi that facilitate their maturation and further transportation. Although protein translocation was first recognized in the ER of eukaryotes, a similar process is also utilized in prokaryotic organisms to integrate membrane proteins or secrete proteins into the periplasmic space.

One of the mechanisms to transport the nascent polypeptide chain across the ER membrane was first revealed in studies on the biosynthesis of secretory proteins (Redman and Sabatini, 1966; Redman et al., 1966). This process was originally called the "vectorial discharge of nascent polypeptides". In this mechanism, the transfer of proteins across the membrane

occurs concurrently with protein synthesis. The process also requires the binding of ribosomes to some receptor proteins on the rough ER membrane. This concurrent relationship between protein translation and translocation is now widely known as "cotranslational translocation".

After the discovery of ER protein translocation, one major question to address is how the fate of the polypeptides is determined. Why do some proteins remain in the cytoplasm while others are transported into the ER lumen? The ribosome is unlikely to be the decision-maker since free and membrane-bound ribosomes are identical in their composition and structure. There are several pieces of evidence suggesting that the nascent polypeptide may play a major role in determining its own fate. First, after the amino-terminal portion of the nascent chain emerges from the ribosome, the ribosome is targeted to the membrane. Then the nascent polypeptide is protected from exogenous proteases by the membrane-bound ribosome unless the membrane is dissolved by detergents (Sabatini and Blobel, 1970). Second, ribosome binding to the receptors on the ER membrane can be disrupted by high salt concentration. On the contrary, ribosomes which contain long nascent polypeptides can only be removed from the membranes when nascent chains are released from ribosomes by puromycin (Adelman et al., 1973a; Adelman et al., 1973b). These findings suggest the nascent polypeptide, especially the N-terminal portion, is important for targeting to the ER membrane. Therefore, in 1971, it was postulated by Blobel (Blobel and Sabatini, 1971) that the secret code determining the fate of the protein is contained in the N-terminal segment of the nascent polypeptide. In 1975, the "signal hypothesis" was proposed by Blobel and Dobberstein to explain the polysome-membrane interaction mediated by the signal sequence. It was proposed that secretory proteins contain an N-terminal signal sequence that is not present in non-secretory proteins. Although the initiation of synthesis of all proteins occurs in the cytoplasm, proteins with signal sequences will be

directed to the ER membrane while proteins that lack signal sequences will remain in the cytoplasm (Fig. 1A). A model was also proposed in the "signal hypothesis" for the formation of a tunnel in the membrane through which the nascent chains would be transferred. The emerging signal sequence may recruit two or more membrane receptor proteins to form a tunnel in the membrane. Association of receptor proteins may also provide binding sites for the ribosome (Fig. 1B). Binding of the ribosome not only links the polypeptide exit tunnel with the newly formed membrane tunnel but also stabilizes the association of receptor proteins. The translation of a nascent chain will then continue on the bound ribosome until the nascent chain is released and vectorially discharged into the ER lumen. After discharge of the completed chain, the ribosome is then detached from the membrane and can restart translation of another mRNA (Fig. 1A). The first evidence supporting this hypothesis came from the study of mRNA-dependent in vitro synthesis of secretory proteins. In the absence of microsomal membranes, translation products contain extra N-terminal segments missing in products found inside the microsomal lumen (Blobel and Dobberstein, 1975a; Blobel and Dobberstein, 1975b). Furthermore, mutations within signal segments result in defects in the passage of polypeptides across the membrane (Bedouelle et al., 1980). The essence of this "signal hypothesis" turned out to be correct. Secretory proteins have N-terminal signal sequences that direct nascent polypeptide transport across the ER membrane.

A typical signal sequence consists of a stretch of 7-15 hydrophobic residues, which are likely to adopt an α-helical conformation. Frequently, the hydrophobic core of a signal sequence is flanked by a few positively charged residues near the amino- terminal end and polar amino acids at the carboxy-terminal end (Von Heijne, 1990). The amino acid composition of a signal sequence is highly variable as long as the hydrophobic core is conserved. Its hydrophobicity and

Fig 1. The "Signal Hypothesis". A hypothetical model proposed by Blobel and Dobberstein in 1975. (A). Illustration of the essential features of the signal hypothesis. The initiation of synthesis of all proteins occurs in the cytoplasm. Proteins that lack signal sequences will remain in the cytoplasm, while proteins with signal sequences will be directed to the ER membrane while. The translation of a nascent chain will then continue on the bound ribosome until the nascent chain is released and vectorially discharged into the ER lumen. After discharge of the completed chain, the ribosome is then detached from the membrane. (B) Hypothetical model for the formation of a transient tunnel in the membrane. The emerging signal sequence may recruit two or more membrane receptor proteins to form a tunnel in the membrane. Association of receptor proteins may also provide binding sites for the ribosome. Binding of the ribosome not only links the polypeptide exit tunnel with the newly formed membrane tunnel but also stabilizes the association of receptor proteins. Ribosome binding sites on the receptor proteins are indicated by cones. Channel binding sites on the ribosome are indicated by notches. The figure and the legend are adapted from (Blobel and Dobberstein, 1975a).

A

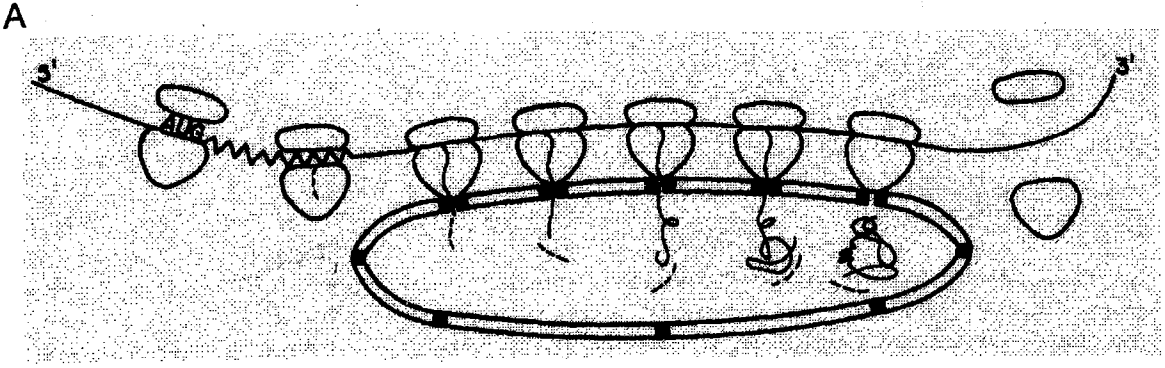

B

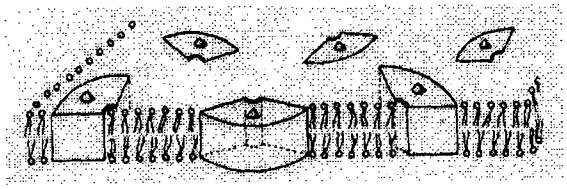

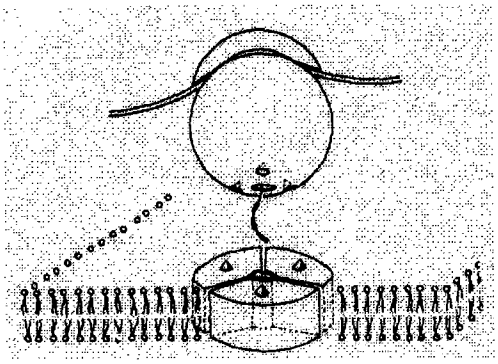

conformational features rather than specific primary sequence, are required to carry out the targeting function.

Overview of Cotranslational translocation

Upon the emergence of the nascent chain from the ribosome, the signal recognition particle (SRP), a conserved ribonucleoprotein particle, recognizes and binds the signal sequence to form the RNC (ribosome-nascent chain)-SRP complex (Fig. 2, step 1 and 2). When binding to the signal sequence, SRP also interacts with the ribosome (Walter and Blobel, 1981) causing the retardation of peptide elongation. Next, the RNC-SRP complex is targeted to the ER membrane (Fig. 2, step 3) by the interaction with the SRP receptor (SR), a heterodimeric membrane protein (Gilmore et al., 1982b). The interaction between SR and the RNC-SRP complex results in both the GTP-dependent dissociation of the nascent polypeptide from SRP (Connolly et al., 1991) and the transfer of the signal sequence to the channel (Fig. 2, step 4). This interaction may also trigger the rearrangement of SRP relative to the ribosome, since the binding site for SRP on the ribosome overlaps with the binding site for the Sec61 complex on the ribosome (Halic et al., 2004). The dissociation of the signal sequence from SRP is inhibited in the absence of a functional translocon (Song et al., 2000), suggesting that the Sec61 complex regulates the GTP hydrolysis cycle of the SRP-SR. This regulation may provide a mechanism to insure the direct insertion of the signal sequence into the translocation channel upon release from SRP. After the signal sequence is released from SRP and inserted into the channel, the nascent chain can then be translocated while protein synthesis resumes (Fig. 2, step 5). Upon termination of translation, the ribosome can then leave the channel (Fig. 2, step 6).

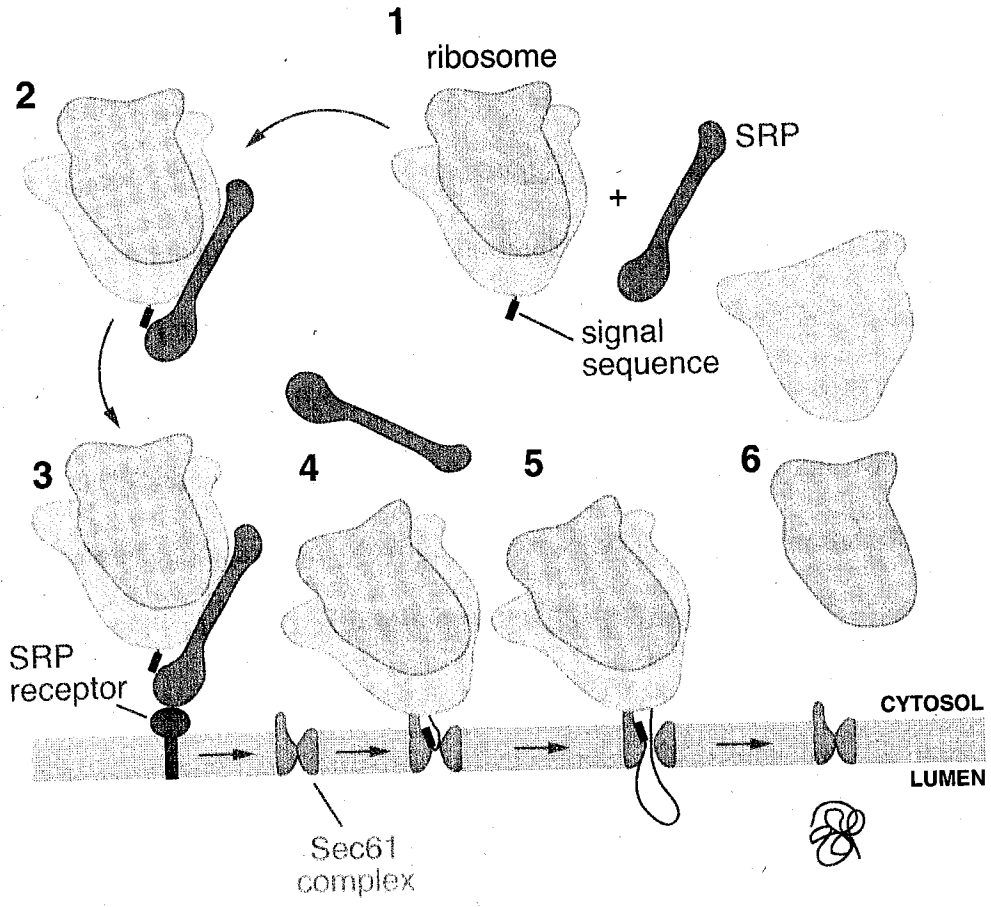

Osborne AR, et al. 2005.
Annu. Rev. Cell Dev. Biol. 21:529–50

Fig 2. Cotranslational translocation of a secretory protein. The scheme shows different steps in the translocation of a eukaryotic secretory protein. For details see the text. The figure is taken from (Osborne et al., 2005) and the legend is adapted from the original.

SRP

An 11S ribonucleoprotein (RNP) named SRP was identified to be the binding factor for the signal sequence in the mammalian system (Walter et al., 1981). This particle shows three main activities in cotranslational targeting: 1) it binds to the signal sequence; 2) it slows down peptide elongation; 3) it interacts with SRP receptor and transfers the RNC to the translocon. Mammalian SRP contains a 7S RNA molecule and six proteins (SRP9, SRP14, SRP19, SRP54, SRP68, SRP72) (Walter and Blobel, 1980; Walter and Blobel, 1982). The 300-nucleotide RNA adopts an elongated conformation, providing the structural backbone for the SRP proteins. SRP can be divided into two major functional units: the S and Alu domains. The S domain functions in signal sequence recognition and interaction with SR. It includes the middle part of the 7S SRP RNA in addition to four proteins: SRP19, SRP54, SRP68 and SRP72. The Alu domain, which contributes to the elongation arrest activity, contains the 5' and 3' segments of the SRP RNA along with the heterodimer SRP9/SRP14. In the S domain, the most important subunit is the highly conserved subunit, SRP54 protein. This subunit is responsible for both signal sequence recognition and RNC targeting to the membrane. SRP54 contains three domains: the N-terminal domain (N), the GTPase domain (G) and a methionine-rich C-terminal domain (M). The ras-like G domain is closely related to another GTPase domain located in the SRP receptor subunit, SRα. The N and G domains are structurally and functionally coupled (NG domain) to mediate the interaction with the SRP receptor (SR). Cross-linking studies demonstrate that the M domain contains the signal sequence binding site. Crystal structures of the M domain have also been solved (Batey and Doudna, 2002; Batey et al., 2000) revealing a deep groove in the M domain which may be responsible for signal sequence binding. This groove is surrounded by conserved

hydrophobic residues on one side and a flexible finger loop on the other side. The conformational flexibility of the groove may explain the ability to bind signal peptides of various lengths and sequences. The detailed structural basis for the recognition and binding of the signal sequence awaits further structural study of the SRP54-signal sequence complex.

High-resolution X-ray structures of the SRP and cryo-EM structures of SRP bound to RNCs have revealed detailed information about the interaction of SRP with both the ribosome and SR (Andrews et al., 1987; Halic et al., 2004). SRP has a kinked conformation with a hinge connecting two domains. SRP stretches from the polypeptide exit site of the large ribosomal subunit (S domain) to the elongation factor-binding site in the interface between two ribosomal subunits (Alu domain). The recognition of the signal sequence by the S domain may lead to a conformational change that places the Alu domain further into the intersubunit space, which in turn could cause elongation arrest by competition with elongation factors (Fig. 3). This theory agrees with the observation that SRP has a much higher affinity for the ribosome in the presence of signal sequence (Walter et al., 1981).

Archaeal SRP contains SRP19, SRP54 and an RNA molecule of similar size and conformation. Bacterial SRP only has one SRP54 homologue (Ffh) and a shorter 4.5S RNA molecule. In vitro translocation assays show bacterial SRP can functionally replace mammalian SRP (Powers and Walter, 1997). This confirms the essential role of SRP54 and also suggests additional regulatory roles for the other subunits.

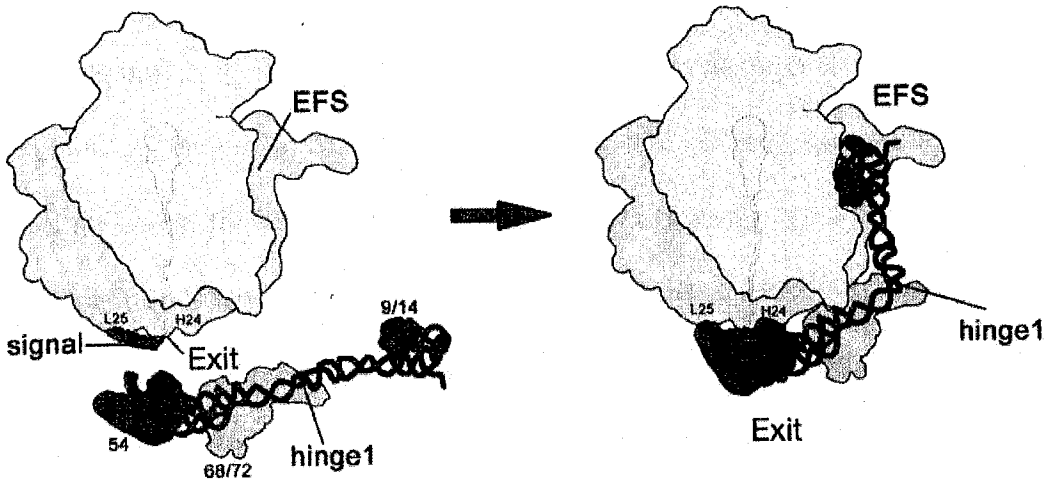

Fig 3. Signal sequence-dependent SRP-ribosome interaction. On signal sequence binding by SRP54, a kinked conformation of SRP involving possibly SRP68/72 and a rotation around hinge 1 is stabilized. As a result, SRP interacts with the ribosome, stretching from the peptide exit (S domain) to the elongation-factor-binding site in the intersubunit space (Alu domain), where it causes elongation arrest by competition with elongation factors. The 40S small ribosomal subunit is shown in yellow, 60S large ribosomal subunit in blue, the signal sequence in green and SRP in red. Exit, peptide tunnel exit; EFS, elongation-factor-binding site. The figure and the legend are taken from (Halic et al., 2004)

SRP receptor

The mammalian SRP receptor is a heterodimer consisting of two GTPases, the SRα and the SRβ subunits (Connolly and Gilmore, 1989; Miller et al., 1995; Tajima et al., 1986). The existence of a receptor for SRP on the ER membrane was first suggested (Walter et al., 1979) when translocation activity was restored by adding a proteolytic fragment back to protease treated-microsomal membranes. This fragment was later identified to be a digestion product from a 70kd protein (SRα), which can release the elongation arrest induced by SRP (Gilmore et al., 1982a; Gilmore et al., 1982b). SRα is a peripheral membrane protein anchored to the ER membrane via its interactions with SRβ. SRα contains an NG domain that is homologous to the NG domain in SRP54. The association between the two NG domains initiates the docking of the RNC to the membrane. The GTPase domains in SRα and SRP54 are required for the dissociation of SRP54 from the signal sequence. SRα also contains an N-terminal SRX domain that interacts with SRβ. Furthermore, biosensor experiments have revealed that SRα also has high affinity for the ribosome (Mandon et al., 2003) and that the ribosome binding site can be mapped to the N-terminal segment of SRα. Such an interaction may accelerate the targeting of RNCs to the rough ER, while the SRP-SR interaction insures the fidelity of the targeting. SRβ consists of a cytosolic Arf-like GTPase domain and an N-terminal transmembrane helix. Multiple mutations in the GTP-binding site compromise the association between SRα and SRβ (Ogg et al., 1998). Surprisingly, SRβ without the TM span still can recruit SRP-RNCs to the ER membrane (Ogg et al., 1998), suggesting the existence of specific binding sites for SRβ on the membrane. The bacterial SR (FtsY) has a single subunit, which is homologous to the N and G domains of SRα (Bernstein et al., 1989). FstY also contains an N-terminal acidic (A) domain,

which interacts directly with the phospholipids of the plasma membrane (Luirink et al., 1994; Powers and Walter, 1997).

Sec61 complex

After being targeted to the ER membrane, polypeptides have to be transported across the membrane. It is now known that the central component of the translocation channel is a heterotrimeric complex of membrane proteins, called the Sec61p complex (Sec61α, Sec61β, Sec61γ) in eukaryotes and the SecYEG complex in prokaryotes. The α subunit of the complex in *S. cerevisiae* was first discovered in a genetic screen for defects in secretory protein translocation into the ER membrane and was subsequently named Sec61p (Deshaies and Schekman, 1987). The temperature-sensitive alleles of Sec61p cause translocation defects at the nonpermissive temperature (Stirling et al., 1992). The bacterial homolog (SecY) of Sec61p (Ito et al., 1983) was also identified in genetic screens whereas the mammalian homologue (Sec61α) was identified by photo-crosslinking experiments (Görlich et al., 1992). These α subunits, encoded by essential genes, share an identical topology of ten transmembrane spans (Akiyama and Ito, 1987; Görlich et al., 1992) as well as significant sequence similarity among species.

The γ subunit (Sec61γ in mammals, Sss1p in *S. cerevisiae* and SecE in bacteria) of the Sec61 complex is also encoded by an essential gene (Esnault et al., 1993). Overexpression of Sss1p can suppress the translocation defect of the temperature-sensitive *sec61-2* mutant. Repression of Sss1p expression blocks translocation of secretory, vacuolar, and membrane proteins. The γ subunit has a single transmembrane (TM) span in eukaryotes and archaebacteria, while its homologue in eubacteria has three TM spans. The conserved, essential region however, consists of a single TM span (C-terminal TM in eubacteria) and several surrounding residues (Hartmann et al., 1994).

The β subunits of the heterotrimer do not show similarity in sequence and topology between the eubacterial subunit (SecGp, two TMs), the archaebacterial subunit (Secβ, one TM) and its eukaryotic counterparts (Sec61β in mammals and Sbh1p in yeast, one TM) (Panzner et al., 1995). These subunits are not required for cell viability and protein translocation, yet exhibit a large stimulatory effect in an in vitro translocation assay (Kalies et al., 1998).

The purified Sec61 complex and the SR are the only required membrane components for the in vitro translocation of some proteins into proteoliposomes (Görlich and Rapoport, 1993). Site-specific photo-crosslinking experiments have shown that the translocating polypeptide is located in a membrane environment, which is formed almost exclusively from Sec61α during polypeptide transfer across the ER membrane (Mothes et al., 1994). These results suggest that Sec61α, the major subunit in the Sec61p complex, forms the protein transport channel. When native mammalian ER membranes, as well as the purified Sec61p complex in detergent solution were viewed by electron microscopy, ring-shaped particles were observed with a volume and mass suggesting assembly from 3-4 Sec61 heterotrimers (Hanein et al., 1996).

Initially, it was thought that the channel would be formed by the interface between three or four Sec61 heterotrimers. In contrast to this theory, the recent X-ray structure of the SecYEβ complex from *Methanococcus jannaschii* has suggested that one copy of Sec61 heterotrimer is sufficient to serve as the translocation channel (Van den Berg et al., 2004). As seen in the X-ray crystal structure, the ten transmembrane segments of the α subunit (SecY) can be divided into two linked halves, each consisting of five TM spans. The two halves are clamped together by the γ subunit (SecE) (Fig. 4A). The SecY TMs form an hourglass like interior containing a ring of hydrophobic residues at its constriction. A short helix (TM2a), that is part of the second TM segment, occupies the luminal exit of the channel and could serve as a moveable plug of the

channel (Fig. 4B). Wrapped by both β (Secβ) and γ subunits, the α subunit can only open the two halves laterally in one direction, with the hinge for the motion being the loop between TM5 and TM6 (Fig. 4C). Previous crosslinking experiments (Plath et al., 1998) have suggested that the binding site for the signal sequence of nascent polypeptides is located between TM2 and TM7. The X-ray structure shows that these two TMs are in opposite halves of the α subunit and lateral opening of the channel would allow the intercalation of the signal sequence between TM2 and TM7. Binding of the signal sequence may trigger opening of the channel by destabilizing the closed conformation of the channel. The plug is proposed to move towards to the back of α subunit where the C-terminus of γ subunit is located (Fig. 4D). Movement of the plug would open the channel towards the lumen and allows the polypeptide movement across the membrane. Moreover, opening the channel from the lateral exit also allows the partitioning of transmembrane domains of membrane proteins into the lipid. The Sec61 complex in eukaryotes likely has a similar structure because the α subunits are well conserved between the archae and eukaryotic translocation channels.

Although one copy of the Sec61 heterotrimer may serve as the translocation pore, the native channel is likely formed by more than one Sec61 complex. When visualized by electron microscopy, the size of the channel suggests an oligomer of three to four copies of the Sec61 complex (Hanein et al., 1996). Three-dimensional EM reconstructions of the ribosome-Sec61 complex and the RNC-Sec61 complex have revealed four stalklike connections between the channel and the ribosome (Beckmann et al., 2001; Morgan et al., 2002), which is consistent with the presence of three to four Sec61 heterotrimers per channel. On the contrary, fitting the SecYEβ X-ray structure into the electron density map of the 2D crystal structure of the *E. coli*

Fig 4. Architecture of the translocation channel and proposed mechanism of its gating. (A, B) Top view (A) and cross-sectional view (B) of the closed channel. Transmembrane segments 1–5 and 6–10 of the α-subunit are shown in blue and red, respectively. The β- and γ-subunits are shown in gray. The hydrophobic pore-ring residues are shown in green and TM2a (plug) in dark green. (C, D) (Van den Berg et al., 2004) (C) Top views with faces of the helices (TM2b, TM3, TM7 and TM8) that form the signal-sequence-binding site and the lateral gate highlighted. The plug is colored in green. The hydrophobic core of the signal sequence probably forms a helix, modeled as a magenta cylinder, which intercalates between TM2b and TM7 above the plug. Intercalation requires opening the front surface, as indicated by the broken arrows, with the hinge for the motion being the loop between TM5 and TM6 at the back of the molecule (5/6 hinge). A solid arrow pointing to the magenta circle indicates schematically how a TM of a nascent membrane protein would exit the channel into lipid. (D) View from the side with the front half of the model cut away. The modeled plug movement towards the γ-subunit (magenta) is indicated. The figure was created by combining figures from (Rapoport et al., 2004) (A, B) and (Van den Berg et al., 2004) (C, D). The legend is adapted from the original.

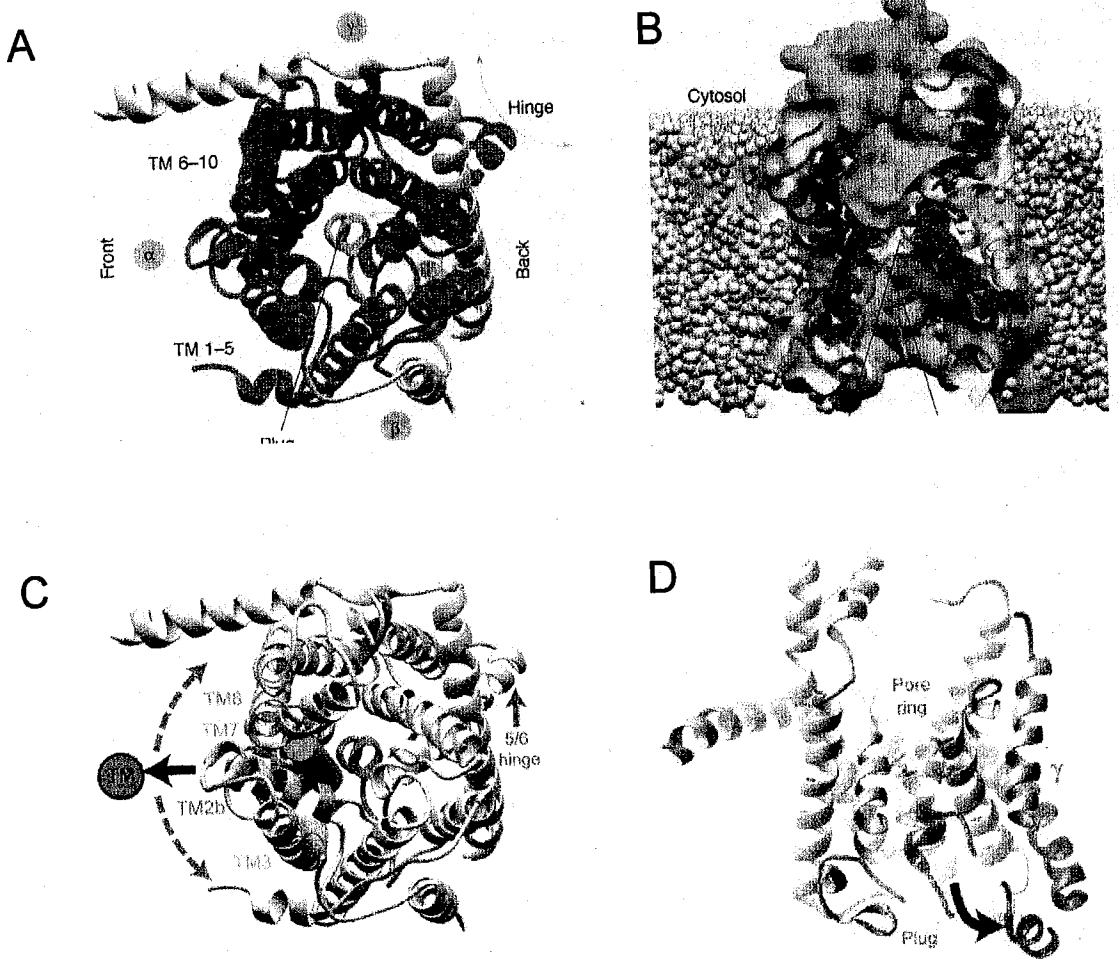
A
Hinge
TM 6–10
Front
Back
TM 1–5
B
Cytosol
C
TM8
TM7
5/6
hinge
TM2b
TM3
D
Pore
ring
γ
Plug

SecYEG complex, determined by EM (Breyton et al., 2002), suggests that the SecYEG complex is dimer. Not only is the number of the Sec61 heterotrimers per channel unclear, but the arrangement of the Sec61 complexes in the channel is also under debate. The exit of transmembrane domains from the channel would suggest the lateral gate of the Sec61 complex faces the phospholipids. A back-to-back orientation of two SecYEG complexes was observed in two-dimensional crystals. However, a recent cryo-EM reconstruction of the E. coli channel bound to a translating ribosome favors a front-to-front arrangement with lateral gates in contact (Mitra et al., 2005). The role of the non-translocating Sec61 complexes in the translocon during the translocation reaction is not understood. Oligomerization of Sec61 heterotrimers may be required to recruit important components such as the OST, TRAM, to the translocation site or to provide a high affinity binding site for the ribosome.

SRP-independent pathway

A posttranslational translocation pathway was first revealed in yeast when an in vitro translocation assay showed that prepro-alpha-factor, a soluble secretory protein, can be translocated into yeast microsomal membranes after the completion of translation (Hansen et al., 1986; Waters and Blobel, 1986). Later, it was observed that yeast cells can tolerate mutations that block the cotranslational targeting pathway (Hann and Walter, 1991). This confirmed the in vivo existence of a posttranslational pathway. Although both pathways may be present in prokaryotes and eukaryotes, the relative contributions of the two pathways are different. In yeast, partitioning of nascent polypeptides between the co-and posttranslational pathways is governed by the relative hydrophobicity of the signal sequence (Ng et al., 1996). Proteins containing a more hydrophobic signal sequence (e.g. membrane proteins) are selected for the cotranslational pathway. Conversely, proteins with a less hydrophobic signal (e.g. many secreted

proteins) are directed to the posttranslational pathway. In prokaryotes, posttranslational translocation is mainly utilized to transport outer membrane proteins and periplasmic proteins, while Ffh and FtsY are required for integration of inner membrane proteins (Koch et al., 1999; Ulbrandt et al., 1997). In the case of mammals, cotranslational translocation is the predominant pathway while a subset of low molecular weight proteins (usually fewer than 70 residues) can be transported posttranslationally (Zimmermann et al., 1990).

Overview of posttranslational translocation pathway

In a posttranslational translocation pathway, preventing premature folding of a fully translated polypeptide is critical, since folded proteins are too large to be transported across the channel. Genetic experiments revealed that the Hsp70 family of heat shock proteins (hsp) is involved in the posttranslational pathway. Depletion of a subset of Hsp70 (Ssa1-Ssa4) results in the accumulation of precursor proteins in the cytoplasm (Deshaies et al., 1988). Additionally, highly purified Hsp70 proteins have been shown to stimulate the in vitro translocation of prepro-α-factor, which was synthesized by a wheat germ translation system (Chirico et al., 1988). This translocation-stimulating activity can be mimicked by destabilizing precursor proteins with either urea or point mutations, suggesting the fully translated polypeptides are held in an unfolded state by the interaction with Hsp70 to maintain a translocation competent conformation (Fig. 5, step 1). In *Saccharomyces cerevisiae*, Ydj1p, a DnaJ homolog localized to the cytoplasm and the peripheral ER, associates with Ssa1p (Hsp70 protein) to regulate the chaperones activity (Caplan et al., 1992). The interaction between Ydj1p and Ssa1p releases the chaperones from secretory protein precursors before the translocation can occur (Brodsky et al., 1998).

Studies in yeast have shown that post-translational translocation can be reproduced with reconstituted proteoliposomes containing the SEC complex, which consists of the Sec61

complex plus the tetrameric Sec62/63 complex (Deshaies et al., 1991; Panzner et al., 1995) and a lumenal chaperone (BiP in mammals and Kar2p in yeast), a member of the Hsp70 family of ATPases. Results from cross-linking studies have suggested that in the posttranslational pathway, the recognition and insertion of the signal sequence is mediated by Sec61p and two subunits of Sec62/63 complex: Sec72p (Feldheim and Schekman, 1994) and Sec62p (Müsch et al., 1992). Movement of polypeptides across the membrane is facilitated by BiP. ATP-bound BiP interacts with the ER membrane via contact with the lumenal J domain of Sec63p. This interaction stimulates ATP hydrolysis, which in turn enhances the binding of BiP to the polypeptide (Fig. 5, step 2). A hypothetical model was proposed for the in vivo function of BiP (Matlack et al., 1999). When a nascent polypeptide emerges into the ER lumenal, BiP binds to the nascent polypeptide and prevents its movement back into the cytosol. Every time a new segment is exposed, another BiP molecule would bind until the nascent polypeptide completely crosses the membrane. Thus, BiP is proposed to act as a ratchet and provide the driving force for posttranslational translocation (Fig. 5, step 3). After translocation is complete, BiP dissociates from the polypeptide and becomes available for binding to another nascent chain (Fig. 5, step 4 and 5).

Sec62/63 complex

The Sec62/63 complex consists of Sec62p, Sec63p, Sec71p and Sec72p. The Sec61 complex associates with the Sec62/63 complex to form a seven-component SEC complex. SEC62 and SEC63 were first identified in a genetic selection for mutant yeast cells that fail to translocate a signal peptide-cytosolic enzyme hybrid protein (Deshaies and Schekman, 1989; Rothblatt et al., 1989). Sec62p and Sec63p span the ER membrane two and three times

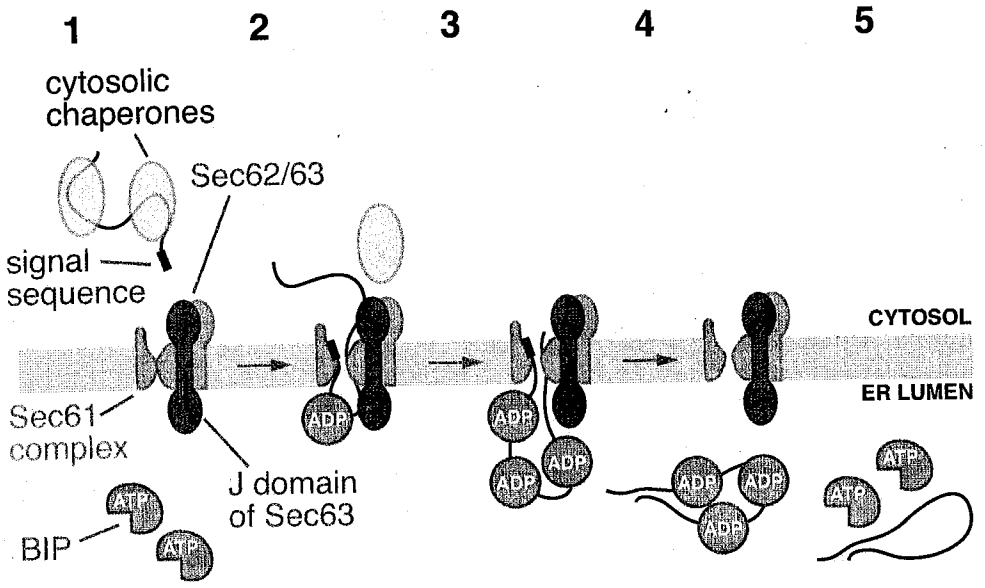

Osborne AR, et al. 2005.
Annu. Rev. Cell Dev. Biol. 21:529–50

Fig 5. Posttranslational translocation in eukaryotes. The scheme shows different steps in posttranslational translocation of a eukaryotic secretory protein. For details see text. The figure is taken from (Osborne et al., 2005). The legend is adapted from the original.

respectively. Both genes are essential for cell viability. On the contrary, Sec71p and Sec72p are not essential proteins. These proteins were also identified in genetic selection to isolate mutations that inhibit membrane protein insertion into the ER membrane of *Saccharomyces cerevisiae* (Green et al., 1992). Sec71p, the only glycoprotein in the complex, spans the membrane once. Sec71p null strains are temperature-sensitive for growth. Accumulation of precursors in Sec71p null cells is observed at the permissive temperature and becomes more severe at the restrictive temperature (Feldheim et al., 1993). Deletion of Sec71p also causes rapid degradation of Sec72p, suggesting that the two subunits interact with each other (Fang and Green, 1994). Sec72p is a peripheral membrane protein tightly associated on the cytoplasmic side of the ER. Sec72 null cells are viable but accumulate a subset of precursor proteins (Feldheim and Schekman, 1994).

Sec63p contains a lumenal J domain that is a homologue of *E. coli* DnaJ protein (Sadler et al., 1989). The J domain in Sec63p functions to recruit the lumenal chaperon Kar2p (BiP), a homologue of DnaK in *E. coli*, to the membrane. Other than the J domain, the precise functions of those subunits in Sec62/63 complex remain unclear.

Ssh1p complex

The yeast Ssh1p complex consists of Ssh1p (a distantly related Sec61p homolog), Sbh2p (Sbh1p homolog) and Sss1p (Finke et al., 1996). Ssh1p is only ~32% identical in sequence to yeast Sec61p and mammalian Sec61α (Fig. 6), while the latter two are more closely related to each other (~55% sequence identity). Unlike Sec61p, Ssh1p is not essential for cell viability as an *ssh1*Δ strain shows only a slight growth defect. The Ssh1p complex interacts with membrane-bound ribosomes (Finke et al., 1996), which is consistent with the high sequence identity between the cytoplasmic loops of yeast Ssh1p and Sec61p (Fig. 6). The Ssh1p complex does not

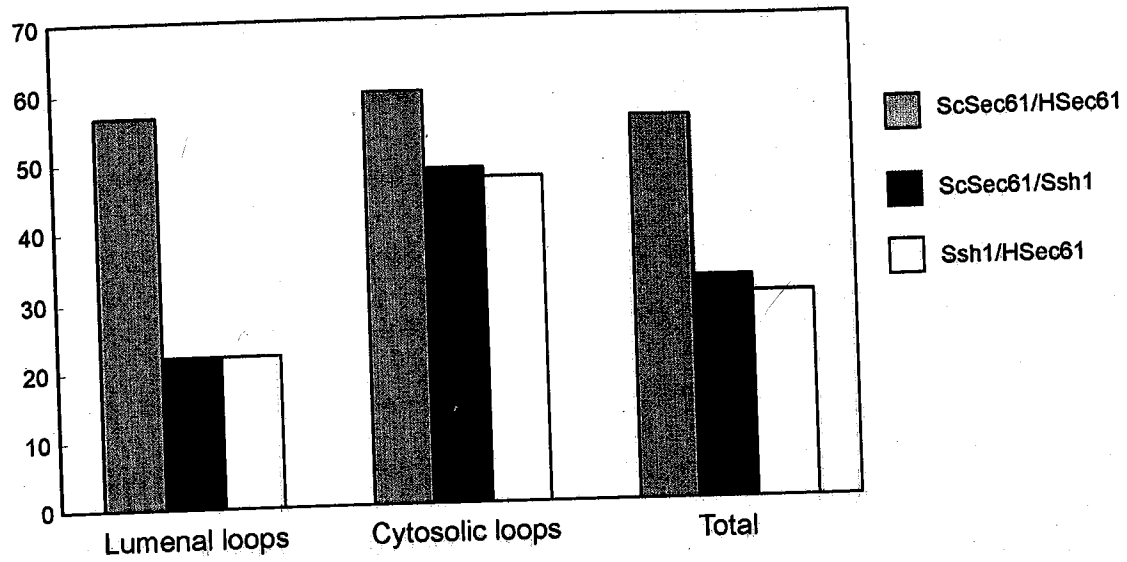

Fig 6. Sequence comparison of *S. cerevisiae* Sec61p, Ssh1p and human Sec61α. The sequence identity (%) between Sec61p and Sec61α (gray bar), between Sec61p and Ssh1p (black bar), between Ssh1p and Sec61α (white bar) are shown.

associate with the Sec62/63 complex (Finke et al., 1996), hence, overexpression of Ssh1p cannot compensate for loss of Sec61p. Ssh1p may interact with the signal sequences of cotranslational translocation substrates and with SRβ (Wittke et al., 2002). These results suggest that the Ssh1p complex functions as an auxiliary translocon specific for the cotranslational pathway. In mammals, a second gene which shows 95% identity to Sec61α has been identified (Görlich et al., 1992). Its expression level and function remain unclear.

Integration of membrane proteins during translocation

Most membrane proteins in eukaryotic cells are integrated into the ER membrane before they are subsequently transported to their sites of function. The signal that binds SRP and directs membrane proteins to the ER membrane can be either a cleavable signal sequence or the first transmembrane span. Integration of membrane proteins is considerably more complicated than translocation of secretory proteins, since only the lumenal regions of a membrane protein are translocated across the membrane. The transmembrane segments have to be eventually exposed to the phospholipid bilayer. During the integration of membrane proteins, Sec61 channels have to deal with some challenging tasks, such as the orientation of the TMs, binding the TMs and releasing the TMs into the lipid phase.

While a cleavable signal sequence inserts into the channel in the N_{cyt}-C_{lum} orientation, a TM span may assume a final topology with either a cytoplasmic N- and a lumenal C-terminus (N_{cyt}-C_{lum}) or with the opposite orientation (N_{lum}-C_{cyt}) (Fig. 7, i). The insertion orientation of a TM span is primarily influenced by the charge distribution of the flanking residues (Beltzer et al., 1991) in accordance with the "positive inside" rule (Hartmann et al., 1989). The more positive flanking segment is generally in the cytoplasm. The uneven charge distribution likely affects the orientation of a TM span by an interaction with the charged head groups of phospholipids as well

as charged protein residues at or near the translocon. Additional factors also contribute to the adoption of correct topology. N-terminal sequences preceding the first TM are exposed to the cytosol before the docking of RNCs to the channel. Rapid folding of an N-terminal domain will prevent the translocation of the N terminus, thus, favoring a type II (N_{cyt}- C_{lum}) orientation (Denzer et al., 1995). Moreover, the hydrophobicity of a TM segment also affects its orientation, which was suggested by both in vitro (Sato et al., 1990) and in vivo (Wahlberg and Spiess, 1997) experiments. Extending the hydrophobic core of a single-TM protein would favor the translocation of the N-terminus. Although various mechanisms have been proposed (for review (Goder and Spiess, 2001)), how a TM span achieves the correct orientation during the membrane protein integration remains unclear.

Site-specific incorporation of photoactivatable amino acid analogues (Heinrich et al., 2000; Heinrich and Rapoport, 2003; Mothes et al., 1997; Sadlish et al., 2005) or fluorescent reporters (Liao et al., 1997; Woolhead et al., 2004) into nascent membrane proteins that are encoded by termination codon-deficient mRNA molecules has allowed a mechanistic analysis of membrane protein integration. Sequential events in membrane protein biosynthesis have been investigated by the analysis of these in vitro-assembled integration intermediates. Photocrosslinking experiments have shown that the Sec61 heterotrimer has a primary binding site for the signal sequence (Plath et al., 1998). This binding site, formed by TM2b and TM7 of Sec61α, is located at the interface of the channel and the lipid bilayer. Later it was proposed that a single TM span binds to the same site in the Sec61 complex (Heinrich and Rapoport, 2003; Sadlish et al., 2005). The X-ray crystal structure of the closed-conformation of the *M. jannaschii* SecYEβ complex indicates that TM2 and TM7 are located at the front of the channel (the mouth of the "clamshell"), which is the only surface of the Sec61 heterotrimer that can open to the lipid

bilayer. When intercalated between TM2 and TM7, the TM span of nascent polypeptides can make contact with the lipid (Fig. 4C). The existence of such protein-lipid contact soon after the insertion of a TM span is supported by crosslinking experiments (Heinrich et al., 2000; Mothes et al., 1997). The opening of the lateral gate between TM2 and TM7 is critical for the lateral movement of a hydrophobic TM into the lipid bilayer. The hydrophobicity of a TM may determine how fast it can be released from the channel. A more hydrophobic TM partitions into the lipid rapidly, while a less hydrophobic TM stays close to the channel for an extended time period (Heinrich et al., 2000). Other factors, such as the flanking sequences may also play a role (McCormick et al., 2003).

Very little is known about the integration of polytopic membrane proteins. The insertion of multi-TM proteins occurs sequentially and the final topology is primarily determined by the insertion orientation of the initial TM span (Fig. 7, ii and iii). Individual TM spans must sequentially move from the transport pore to the signal sequence-binding site, and exit through the lateral gate of the channel into the membrane bilayer (Heinrich et al., 2000; Sadlish et al., 2005). Conformational changes in the Sec61 heterotrimeric complex that facilitate the lateral moment of TM spans between these three distinct environments and mediate the gating of the central pore in the translocon are not well understood.

Fig 7. Integration of membrane proteins of different topology. **(a)** Three stages of integration of a membrane protein with a cleavable signal sequence. (i) The signal sequence (green) has emerged from the ribosome (blue) and has inserted as a loop into the Sec61 channel (brown). (ii) At chain elongation, the signal sequence has been cleaved by signal peptidase (scissors), and a transmembrane segment (TM; red stripes) is synthesized by the ribosome. (iii) The TM (red) has emerged from the ribosome, and has left the channel sideways and entered lipid. **(b, c)** Three stages of integration of a membrane protein with a non-cleaved first TM that adopts N_{cyt}-C_{lum} **(b)** or N_{lum}-C_{cyt} **(c)** orientation. (i) The first TM has emerged from the ribosome and has inserted into the Sec61 channel. (ii) The first TM has left the channel sideways and entered lipid, and a second TM is synthesized. (iii) The second TM has emerged from the ribosome, and has left the channel and entered lipid. The figure is taken from (Rapoport et al., 2004). The legend is adapted from the original.

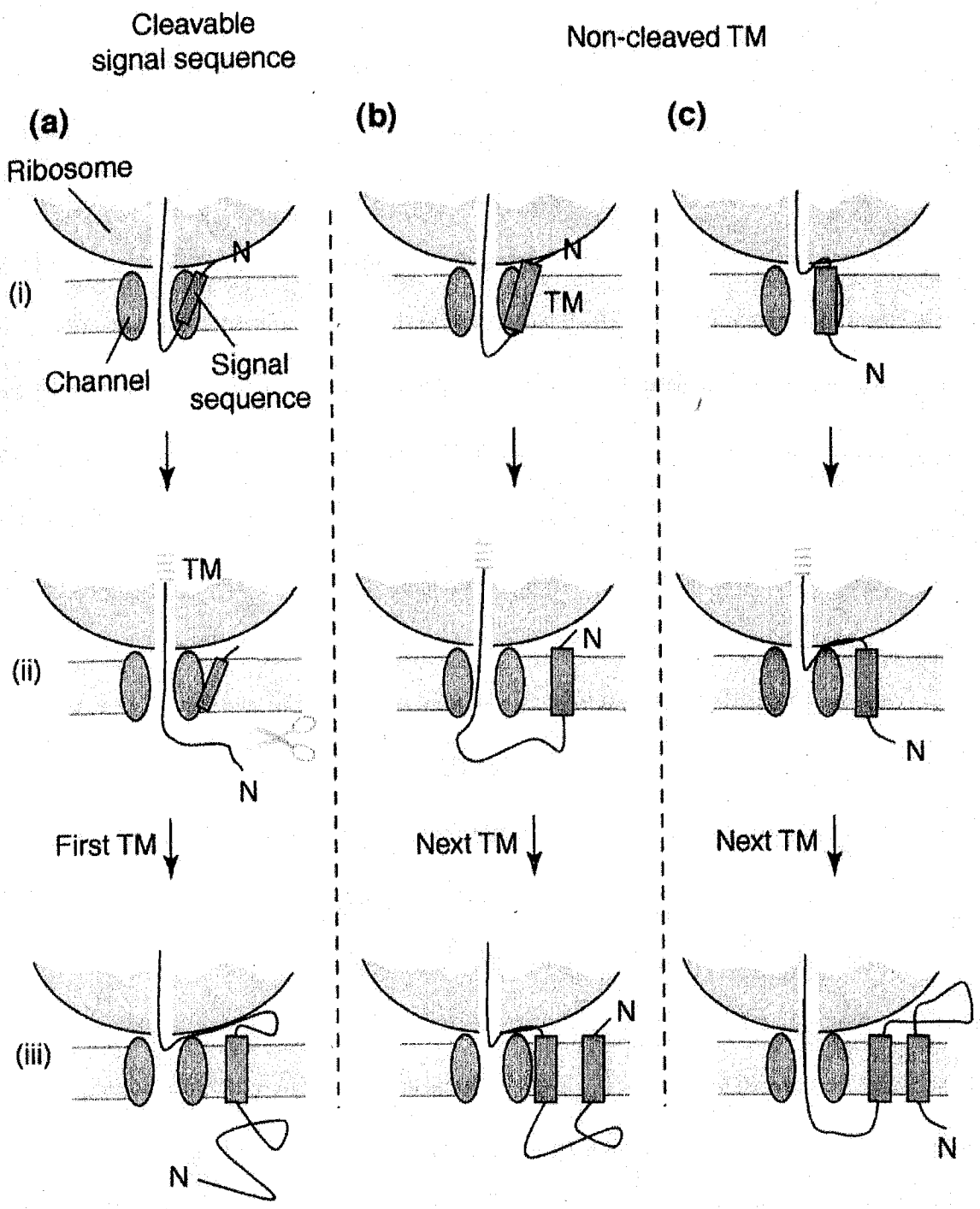
Cleavable
signal sequence
Non-cleaved TM
(a)
(b)
(c)
Ribosome
N
(i)
Channel
Signal
sequence
TM
(ii)
First TM
Next TM
Next TM
(iii)

Enclosed work

The research reported here has two parts. First, we have identified residues in L6 and L8 of Sec61p that are critical for the cotranslational translocation pathway, as well as defined segments of Sec61p that interact with the ribosome and possibly with the SR. Point mutations in cytoplasmic loops six (L6) and eight (L8) of yeast Sec61p cause reductions in growth rates and defects in translocation of nascent polypeptides that utilize the cotranslational translocation pathway. Sec61 heterotrimers isolated from the L8 *sec61* mutants have a greatly reduced affinity for 80S ribosomes. In contrast, point mutations in L6 of Sec61p inhibit cotranslational translocation without significantly reducing the ribosome binding activity, indicating that the L6 and L8 *sec61* mutants impact different steps in the cotranslational translocation pathway.

Secondly, ubiquitin translocation assays (UTA) were utilized to study in vivo kinetics of the targeting and integration of membrane proteins. Radiolabel experiments show that translocon gating is delayed in L6 and L8 *sec61* mutants. The results indicate that yeast cells adapt to defects in cotranslational translocation by increasing the flux through the SEC complex. Our studies define the time window for translocon gating by the RNC, which is a slow step relative to the in vivo rate of polypeptide elongation. The model for the integration of polytopic membrane proteins is also refined by our in vivo analysis with UTA reporters. Translocation of the lumenal domain can be affected by the orientation of a N_{cyt}-C_{lum} TM and the movement of a TM into the lipid bilayer. A long lumenal loop facilitates rapid insertion of the following TM by allowing both events to occur before the following TM emerges from the ribosome. On the contrary, a long cytosolic loop retards the translocation of the following TM since the channel is closed during the translation of a cytosolic loop.

Isolation and characterization of the *sec61* L8 mutants were done by Ying Jiang. Ribosome binding assays were performed by Dr. Elisabet C. Mandon.

CHAPTER II

Experimental Procedures

Plasmid and Strain Constructions for the *sec61* L6 and L8 mutants

The strains used to express the *sec61* L6 and L8 mutants are derived from BWY12 (*MATα, trp1-1, ade2, leu2-3, 112, ura3, his3-11, can1 sec61::HIS3*[pBW7]); provided by C. Stirling, University of Manchester, Manchester, UK). The *SSH1* gene in BWY12 was disrupted to obtain RGY400. PCR using the plasmid pFA6a-KanMX4 as a template (Wach et al., 1994) was used to generate a DNA fragment containing a kanamycin resistance gene flanked by 5' (nucleotides -203 to -1) and 3' (nucleotides 1224 to 1470) regions from the *SSH1* gene. Following transformation of BWY12, G418 resistant colonies were selected and disruption of the *SSH1* gene was confirmed by PCR. Transformation of RGY400 and BWY12 with pGAL-Kar2GFP (derived from pDN182) yielded RGY401 and RGY402 respectively.

An N-terminal His_6-FLAG tag was added to Sbh1p using a two-step PCR-based gene disruption method. The *SBH1* gene in RGY400 was disrupted using a linear DNA fragment encoding the hygromycin B resistance gene (hph) gene derived from plasmid pAG32 (Goldstein and McCusker, 1999) flanked by 5' (-198 to -1) and 3' (249 to 528) *SBH1* noncoding regions. Integration of the disruption construct into the *SBH1* locus to obtain RGY403 was confirmed by PCR analysis of hygromycin B resistant transformants. RGY403 was transformed with a linear DNA fragment containing the following segments: (a) the 5' noncoding region of the *SBH1* gene, (b) the Sbh1p coding sequence with a His_6-FLAG tag inserted after the initiation codon, (c) the heterologous *TRP1* gene from *K. lactis* (derived by PCR amplification of the plasmid pYM3 (Knop et al., 1999) and (d) the 3' *SBH1* noncoding segment. Integration of the construct

into the *SBH1* locus to obtain RGY404 was confirmed by PCR analysis of trp^+ hygromycin B^- sensitive transformants. Expression of epitope-tagged Sbh1p was confirmed by protein immunoblotting.

Cassette Mutagenesis of Sec61

Restriction sites (Pst1 to SacI, XhoI to SalI) in the polylinker of pRS315 were removed by sequential rounds of double digestion, filling in with T4 DNA polymerase followed by blunt end ligation and plasmid isolation. The resulting plasmid is designated pRS315ΔRS. Silent unique restriction sites for SalI (nt 810 relative to the ATG initiation codon), SacII (nt 825), SpeI (nt 862) and AatII (nt 901) were introduced into the coding sequence of SEC61 by PCR amplification of the plasmid pBW11 (Wilkinson et al., 1996) using a QuikChange mutagenesis kit (Stratagene) and synthetic oligonucleotide primers. Digestion of the resulting plasmid with HindIII yielded a 3.2 kb fragment which was cloned into the HindIII site of pRS315ΔRS to obtain the plasmid designated pZCSEC61-L6. Unique restriction sites for BamHI (nt 1111), BglII (nt 1145), XhoI (nt 1163), NcoI (nt 1196), SacI (nt 1241) and PstI (nt 1263) were introduced into plasmid pZCSEC61-L6 by the same procedure to obtain the plasmid designated pZCSEC61-L6L8. The NcoI site in the L8 coding region causes a substitution (G399A) at a non-conserved residue in Sec61p (see Fig. 10A). The G399A mutation does not cause growth or translocation defects (not shown).

Oligonucleotides that were 32-fold degenerate at a single codon (NNG/C on the sense strand, G/CNN on the nonsense strand) were designed to span the gap between unique restriction sites in pZCSEC61-L6 or pZCSEC61-L6L8. The oligonucleotides were annealed and ligated to double-digested ZCSEC61-L6 or pZCSEC61-L6L8 to introduce mutations in L6 or L8 respectively. *E.*

coli (DH5α) was transformed with the resulting plasmid pools, and 40-60 transformants were selected for plasmid isolation and DNA sequencing.

RGY401, RGY402 and RGY404 were transformed with the pZCSEC61-L6 or pZCSEC61-L6L8 derivatives, and Leu^+ Trp^+ prototrophs were selected on synthetic defined media (SD) plates supplemented with uracil and adenine. Several transformants for each point mutant were streaked onto 5-FOA plates and incubated for 2 d at 30°C to select colonies that had lost pBW7. Yeast L6 and L8 *sec61* mutants were maintained on SEG media (synthetic minimal media containing 2% ethanol and 3% glycerol) to select against ρ- cells.

Immunoprecipitation of radiolabeled proteins and protein immunoblots

Yeast strains bearing pZCSEC61-L6 or pZCSEC61-L6L8 derivatives were transformed with the URA3 marked plasmid pDN317 which encodes DPAPB-HA under control of the glyceraldehyde 3-phosphate dehydrogenase promoter (Ng et al., 1996). DPAPB-HA expression is roughly10-fold greater than endogenous DPAPB.

After growth at 30°C in SEG media to mid-log phase (0.2 to 0.6 OD at 600 nm) yeast were collected by centrifugation and resuspended in SD media and grown for 4 h at 30°C. Yeast cells were collected by centrifugation and resuspended in fresh SD media at a density of 6 A_{600}/ml and pulse-labeled for 7 min with Tran-^{35}S-label (100 μCi/OD). In pulse-chase experiments, the chase was initiated by adding unlabeled cysteine and methionine to a final concentration of 0.6 mg/ml. Radiolabeling experiments were terminated by the addition of an equal volume of ice-cold 20 mM NaN_3, followed by freezing in liquid nitrogen. Rapid lysis of cells with glass beads and immunoprecipitation of yeast proteins was done as described (Rothblatt and Schekman, 1989). Spheroplasts, prepared as described below from cells grown in

SD media for 4 h at 30°C, were allowed to recover for 15 min in SD media adjusted to 1.2 M sorbitol prior to pulse-labeling.

Total protein extracts were prepared as described (Arnold and Wittrup, 1994) from cells after 4 h of growth at 30 °C in SD media. Aliquots of the protein extracts were digested with Endo H (New England Biolabs) prior to CPY immunoblots. Proteins were resolved by PAGE in SDS, transferred to PVDF membranes, and incubated with polyclonal or monoclonal antibodies. Peroxidase-labeled second antibodies were visualized using an ECL Western blotting detection kit (Amersham Corp.).

Degradation of CPY*$_{HA}$, expressed from the plasmid pDN431, was evaluated using a cycloheximide-chase protocol (Spear and Ng, 2003). Cell extracts prepared at 30 min intervals after adjustment of the culture to 100 μg/ml cycloheximide were resolved by SDS-PAGE for protein immunoblot analysis using anti-HA monoclonal antibodies. Densitometric scans of protein immunoblots were used to determine the half-life for p1 CPY*$_{HA}$.

Growth curves and frequency of petite phenotype

For serial dilution experiments, yeast strains were grown in SEG media at 30°C to mid-log phase. After dilution of cells to 0.1 OD at 600 nm, 5 μl aliquots of 10-fold serial dilutions were spotted onto YPD plates that were incubated at 30 or 37°C for 2 days. RGY402 *(ssh1Δ)* did not show a colony sectoring phenotype when grown on YPD plates, in contrast to a previous report (Wilkinson et al., 2001).

Yeast cells grown to mid-log phase in YPEG media were harvested by centrifugation and transferred to YPD media for subsequent growth at 30°C. The yeast cells were diluted into fresh media when the A_{600} reached 0.8-1 OD. After 20 generations of growth, the cells were diluted

and plated onto YPD-agar. After two days, 208 colonies were tested for respiratory competence by replica plating colonies onto YPD and YPEG plates.

Cell fractionation and purification of Sec61p complexes

5 g of yeast cells grown in YPD media at 25°C to a density of 1.8 OD at 600 nm were collected by centrifugation, chilled to 4° C, adjusted to 10 mM NaN_3 and converted to spheroplasts with Zymolase (ICN) as described (Walworth and Novick, 1987). Spheroplasts were centrifuged for 10 min at 0.5 Kg, and broken by resuspension in 10 ml of 10 mM triethanolamine-acetate pH 7.2, 0.8 M sorbitol, 1mM EDTA using a serological pipette. Microsomes were isolated from spheroplast lysates as described (Goud et al., 1988). Puromycin high salt-stripped membranes (PK-RM) were prepared from yeast microsomes as described (Görlich and Rapoport, 1993). Spheroplast lysates from *sec61L6DDD* cells were fractionated as described (Gerrard et al., 2000).

Purification of the Sec61 complex was facilitated by construction of a strain (RGY404) that expresses His_6-FLAG-Sbh1p. The plasmid shuffle procedure was repeated to allow purification of the L6 and L8 *sec61* mutants from RGY404 derivatives. The Sec61 complex was purified from digitonin-solubilized PK-RM by sequential chromatography on Con-A Sepharose, Ni-NTA agarose, Q-Sepharose fast flow and SP-Sepharose fast flow using chromatography conditions described previously (Panzner et al., 1995) and standard chromatography methods for Ni-NTA agarose. The Sec complex is resolved from Sec61 heterotrimers by Con-A chromatography. Purification of Sec61 heterotrimers was monitored by coomassie blue staining after SDS-PAGE and by protein immunoblot analysis using anti-FLAG and anti-Sec61p antibodies. Point mutations in Sec61p do not destablize the Sec61p-Sbh1p-Sss1p heterotrimer. The Sec61-proteoliposomes were prepared as described (Song et al., 2000).

Ribosome binding to yeast PKRM, Sec61 proteoliposomes or Sec61 heterotrimers

Ribosomes were isolated from wild type yeast as described (Beckmann et al., 1997). Loosely associated proteins were separated from 80S ribosomes by two sequential centrifugations through a high salt-sucrose cushion followed by sucrose density gradient (10-30%) centrifugation and resuspension in 50 mM triethanolamine-acetate pH 7.5, 150 mM KOAc, 5 mM $Mg(OAc)_2$. Binding of ^{125}I-labeled ribosomes to PK-RM or Sec61-proteoliposomes was assayed as described previously (Mandon et al., 2003; Raden et al., 2000). Membrane or proteoliposome-bound and unbound ribosomes were separated by gel filtration chromatography (Raden et al., 2000). The cosedimentation assay to measure binding of purified Sec61p heterotrimers to ribosomes in detergent solution was performed as described (Prinz et al., 2000a).

Strains construction for ubiquitin translocation assay

Yeast strains were derived from BWY12 (*MATα, trp1-1, ade2, leu2-3,112, ura3, his3-11, can1 sec61::HIS3*[pBW7]); provided by C. Stirling, University of Manchester, Manchester, UK). Expression of L6 and L8 *sec61* mutants in RGY400 (BWY12 *ssh1Δ)* has been described as above (Cheng et al., 2005).

To generate a null allele of SRP54, a 1700bp SalI-SacI fragment from the plasmid pAG32 (Goldstein and McCusker, 1999) containing a hygromycin B resistance (*Hph*) gene was inserted between 5' (nucleotides -434 to -1) and 3' (nucleotides 1627 to 1927) regions from the *SRP54* gene. The resulted DNA fragment was used to disrupt the *SRP54* gene in BWY100 ((*MATa/MATα, trp1-1/ trp1-1, ade2/ade2, leu2-3,112/leu2-3,112, ura3/ura3, his3-11/his3-11, can1/can1 sec61::HIS3/SEC61*) (Wilkinson et al., 2000). Hygromycin B resistant diploids were transformed with pBW7 (*SEC61 URA3*) and sporulated. The Hph^+ His^+ Ura^+ haploids (RGY407) were selected and disruption of the *SRP54* gene was confirmed by PCR.

A hygromycin B resistance (Hph) gene flanked by 5' (bp, –512 to –1) and 3' (bp, 736-941) regions of *SRP102* gene was used to transform BWY100. Hygromycin B resistant diploids were transformed with pJY01 (*SEC61, SRP102, URA3*) and sporulated. The Hph^+ His^+ Ura^+ haploids (YJY101) were selected and the disruption of *SRP102* gene was confirmed by PCR. YJY101 was transformed with pZC511 [*SEC61, srp102(K51I), LEU2*] (Ogg et al., 1998). The Leu^+ Ura^- prototrophs (ZCY108) were selected on SD media containing 5-fluoroorotic acid.

Construction of UTA reporter plasmids

The plasmids described here are derived from the $Suc2_{277}$-Ub-Ura3p UTA reporter (construct IV, (Johnsson and Varshavsky, 1994)). In the Dpa2p-Ub-Ura3p reporter ((Mason et al., 2000); pJEY117 provided by J. Brown, University of Newcastle) the invertase (Suc2p) coding sequence has been replaced with DNA encoding residues 1-310 of DPAPB. The resulting construct has a BglII site immediately upstream of the start codon, with reporter protein expression under control of the P_{CUP1} promoter. DNA encoding a HA_3 epitope tag was appended to the construct to obtain the plasmid pZC401-4 ($Dap2_{310}$-Ub-Ura3-HA). Point mutations (I3G and I13G) were introduced into the Ub coding sequence to produce Ub*, a folding-defective form of Ub (Johnsson and Varshavsky, 1994). Shorter spacer segments (49, 104, or 149 residues) between the DPAPB TM span ($Dap2_{30-45}$) and the Ub domain were obtained by PCR amplification of plasmid pJEY117 using a sense primer containing the BglII site upstream of the start codon, and antisense primers containing a SalI site. The BglII-SalI digested PCR products were ligated into BglII-SalI digested pZC401-4. The DPA-Nub reporter was derived from DPA49. The Dap2p-derived portion of the DPA-Nub reporter contains the following sequence: $Dap2_{1-94}$-Ub_{1-34}-L-Q-$Dap2_{49-94}$.

A BglII-SalI digested PCR product encoding $Suc2_{1-53}$ or $Suc2_{1-79}$ was ligated into BglII-SalI digested pZC401-4 to obtain the Suc2-33 and Suc2-59 reporters. Suc2-295 was produced by replacing the coding sequence for $Dap2_{1-48}$ in pZC401-4 with sequences encoding $Suc2_{1-53}$.

Recombinant PCR was used to construct the 3TM series of reporters. The Dap2p-derived portion of the 3TM49 reporter contains the following sequence: $(Dap2_{1-68})$-E-$(Dap2_{30-45})$-K-R-$(Dap2_{10-94})$. Acidic (E69) and basic (K86 and R87) residues flanking TM2 in this construct were added to favor the 3TM (N_{cyt}-C_{lum}) topology according to the "positive-inside" rule (Hartmann et al., 1989).

An XhoI site (encoding L-E) was inserted between codons 68 and 69 of the 3TM reporters to obtain p3TM-XhoI. A BglII-XhoI digested PCR product encoding $Dap2_{1-194}$ was ligated into BglII-XhoI digested p3TM-XhoI to obtain the L1-IN series of reporters. The Dap2p-derived portion of L1-IN49 reporter contains the following sequence: $(Dap2_{1-194})$-L-E-E-$(Dap2_{30-45})$-K-R-$(Dap2_{10-94})$. A PstI site (encoding L-Q) was introduced between codons 93 and 94 of the 3TM reporters to obtain p3TM-PstI. A PstI digested PCR product encoding $Dap2_{49-148}$ was ligated into PstI-digested p3TM-PstI to obtain the L2-IN series of reporters. The Dap2p-derived portion of L2-IN49 reporter contains the following sequence: $(Dap2_{1-68})$-E-$(Dap2_{30-45})$-K-R-$(Dap2_{10-15})$-LQ-$(Dap2_{49-148})$-LQ-$(Dap2_{16-94})$.

The S2TM series of UTA reporters was obtained by replacing the $(Dap2_{1-68})$ segment in p3TM-XhoI with a BglII-XhoI digested PCR product encoding $Suc2_{1-79}$. The protein sequence that precedes the Ub-Ura3-HA reporter domain in S2TM49 is $(Suc2_{1-79})$-L-E-E-$(Dap2_{30-45})$-K-R-$(Dap2_{10-94})$. The protein sequence that precedes the Ub-URA3-HA reporter domain in SL1-IN49 reporter is $(Suc2_{1-53})$-$(Dap2_{49-194})$-L-E-E-$(Dap2_{30-45})$-K-R-$(Dap2_{10-94})$.

Immunoprecipitation of radiolabeled UTA reporters

The pulse labeling and rapid lysis of yeast strains expressing UTA reporters were performed as described above. *N*-ethylmaleimide (NEM) was added in the lysis buffer to a final concentration of 50 mM to inhibit endogenous UBPs (Johnsson and Varshavsky, 1994). Immunoprecipitation of cleaved and uncleaved UTA reporters was performed using anti-HA antibodies (Rothblatt and Schekman, 1989). Labeling cells in the presence of cycloheximide was performed as above except that the cells were preincubated for 10 min in growth medium containing 0.5 μg/ml cycloheximide before pulse labeling. The inhibition of translation by cycloheximide was determined by counting total TCA-insoluble ^{35}S. The volume of labeled cells and the exposure times for autoradiograms were doubled to compensate for a 4-fold reduction in protein synthesis in CHX-treated cells.

Quantification of UTA reporter cleavage

Immunoprecipitated proteins were resolved by PAGE in SDS, and the radioactive bands detected with a BioRad FX Molecular Imager. Reporter cleavage (%) was calculated using the following equation: % = 100*Ura3-HA* F_{Met} /(intact reporter+ Ura3-HA * F_{Met}) where (F_{met}) is a correction factor to account for loss of radioactivity upon reporter cleavage. Non-glycosylated DPA-reporters (Fig. 22) were observed in mutant cells, and represent non-translocated uncleaved reporters. The distribution of methionine and cysteine residues in the intact UTA reporter and the Ub-Ura3-HA fragment was determined. Given that Tran^{35}S-label has a 4-5 fold higher concentration of methionine than cysteine, the four cysteine residues in Ura3 were treated as one methionine during calculation of F_{met}. Correction factors (F_{Met}) have different values in the Ub fusions with different length of spacers. For instance, the values for DPA3TM series were 1.25 (3TM49), 1.375 (3TM103 and 149) and 1.5 (3TM265).

CHAPTER III

Identification of cytoplasmic residues of Sec61p involved in ribosome binding and cotranslational translocation

Introduction

Translocation of proteins across the rough endoplasmic reticulum can occur by cotranslational or posttranslational pathways. The signal sequence of a protein that is translocated by the cotranslational pathway is recognized by the signal recognition particle (SRP) as the nascent chain emerges from the polypeptide exit site on the large ribosomal subunit (Halic et al., 2004; Walter and Johnson, 1994). Targeting to the RER is mediated by the interaction between the SRP-ribosome nascent chain (RNC) complex and the SRP receptor (SR) (Mandon et al., 2003), which initiates a GTPase cycle that culminates in attachment of the RNC to the protein translocation channel (Song et al., 2000). In *S. cerevisiae*, proteins that are translocated by the posttranslational pathway are not targeted to the Sec61 translocation channel by SRP (Fig. 8), but are instead delivered to the SEC complex by cytosolic Hsp70 proteins (as reviewed in (Corsi and Schekman, 1996). Translocons that mediate cotranslational translocation are oligomers formed from 3-4 copies of a Sec61 heterotrimer (Beckmann et al., 2001; Morgan et al., 2002) that is in turn composed of Sec61p, Sbh1p and Sss1p (Panzner et al., 1995). The Sec complex is composed of a Sec61 translocon plus the Sec62/Sec63 complex (Deshaies et al., 1991; Panzner et al., 1995). Yeast Ssh1p, a distantly related homologue of Sec61p (Fig. 8), assembles with Sbh2p and Sss1p to form an auxiliary translocon that is specific for the cotranslational pathway (Finke et al., 1996; Wittke et al., 2002). Ssh1p translocons are not incorporated into the Sec complex (Finke et al., 1996), hence overexpression of Ssh1p cannot compensate for loss of Sec61p.

The relative contributions of the co- and posttranslational pathways to precursor transport across the RER have been extensively investigated in *S. cerevisiae*. Partitioning of nascent polypeptides between the targeting pathways is governed by the relative hydrophobicity of the signal sequence (Ng et al., 1996), with SRP selecting more hydrophobic signals for the cotranslational pathway (Fig. 8). Although the cotranslational pathway is the predominant pathway in vertebrate organisms, SRP and the SR are dispensable in *S. cerevisiae* (Hann and Walter, 1991; Ogg et al., 1992).

The predicted topology of yeast Sec61p in the ER (Wilkinson et al., 1996) has now been refined by the structural determination of the archaebacterial translocation channel SecYEβ (Van den Berg et al., 2004). The N and C-terminus of Sec61p and the even numbered loops (L2, L4, L6 and L8) that separate the 10 membrane spans face the cytoplasm. Proteolytic mapping experiments of canine Sec61α indicated that L6 and L8 are highly exposed on the cytoplasmic surface of the Sec61 complex (Song et al., 2000). Proteolysis of canine Sec61α in L6 and L8 inhibits SRP-dependent translocation activity (Song et al., 2000) and eliminates ribosome binding to the translocon (Raden et al., 2000). Nonetheless, the detailed mechanism that allows transfer of the RNC from the GTP-bound conformation of the SRP-SR complex to the translocon is not well understood. The ribosome-binding site on the translocation channel had not been mapped with precision. Because L6 and L8 have a net positive charge it was not clear whether specific residues, as opposed to the overall charge distribution, were important for the ribosome binding affinity of the Sec61 complex. Here, we have identified residues in L6 and L8 of Sec61p that are critical for the cotranslational translocation pathway, and defined segments of Sec61p that interact with the ribosome and possibly interact with the SRP receptor.

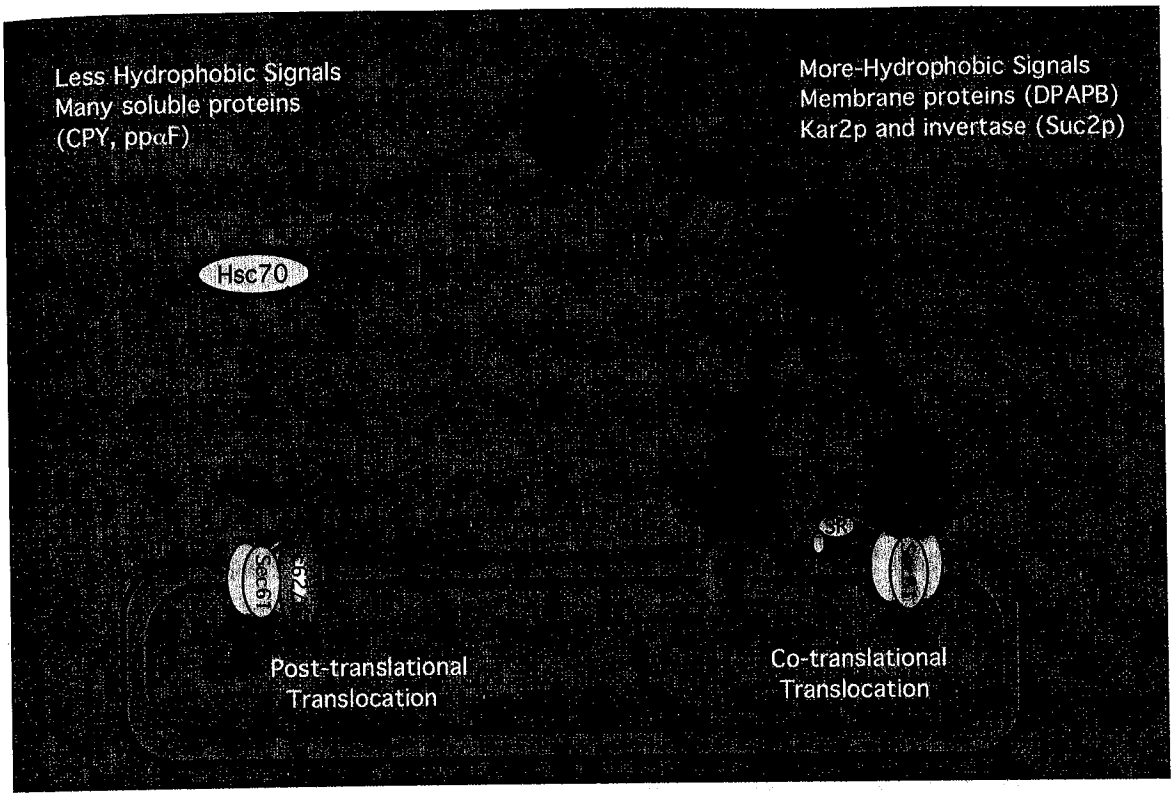

Fig 8. Two translocation pathways in *S. cerevisiae*. The scheme shows different steps in cotranslational and posttranslational translocation in yeast. For details see text.

Results

Mutagenesis of cytosolic loops of Sec61p

A sequence comparison of L6 of Sec61 from diverse eukaryotes reveals a high degree of amino acid identity particularly in the segments that are proximal to transmembrane spans 6 and 7 (Fig. 9A). A seven-residue loop, which connects two β-strands in the *M. jannashii* SecY structure (Van den Berg et al., 2004), contains several highly conserved polar residues (K273, R275 and Q277). These three residues, together with G276 and K284 were selected for site directed mutagenesis in *S. cerevisiae* Sec61p. The haploid BWY12 was chosen as a starting strain to analyze yeast *sec61* mutants using a plasmid shuffle procedure. In BWY12, a *HIS3*-marked disruption of the essential *SEC61* gene is rescued by the *URA3* marked CEN plasmid pBW7 that encodes Sec61p. We disrupted the non-essential *SSH1* gene to provide a sensitized genetic background for the analysis of the Sec61p mutants. Although the initial description of an *ssh1Δ* strain noted a minor decrease in growth rate (Finke et al., 1996), a more recent study reported that a yeast strain lacking Ssh1p rapidly acquires a petite phenotype when grown on a fermentable carbon source, and displays severe defects in protein translocation and dislocation when maintained on a non-fermentable carbon source (Wilkinson et al., 2001). As shown below, the growth phenotype of our *ssh1Δ* strain (RGY401) was consistent with the initial report (Finke et al., 1996), hence this strain was suitable for the analysis of L6 and L8 *sec61* mutants. For example, when RGY401 cells are grown on glucose containing media (YPD or SD), petite cells (ρ^-) arise at a low frequency (~0.3%/cell division).

RGY401 (*ssh1Δ*) and RGY402 (*SSH1*) were transformed with *LEU2* marked plasmids encoding *sec61* point mutants, and plated on media containing 5-FOA to select against retention of pBW7 (Fig. 9B). Positive and negative controls for the screen are based upon the

observations that Ssh1p is nonessential (*SEC61ssh1Δ* is viable), and that expression of Ssh1p cannot suppress a *sec61* null (*sec61R275*SSH1* is not viable). Amino acid substitutions at R275 cause a growth rate defect in the absence, but not in the presence, of Ssh1p. Differences in growth rate were evaluated by plating serial dilutions of cells onto YPD (Fig. 9C) or YPEG plates. With the exception of lysine (*sec61R275Kssh1Δ*), amino acid substitutions at R275 cause obvious reductions in growth rate at 30°C that are accentuated at 37°C, and not apparent at 18°C (not shown). Reductions in the growth rates of the mutants relative to RGY401 or RGY402 were slightly less obvious on YPEG plates (not shown). The effects of L6 point mutations are summarized in Fig. 9D. Substitutions that reverse the charge (R275D or R275E) or substitute an aliphatic or aromatic amino acid for arginine cause a severe growth defect. Less severe growth defects were caused by substitutions of polar (R275S, R275T) or positively charged amino acids (R275H). A wider variety of substitutions were tolerated at K273 and G276. The triple charge-reversal mutant (*sec61K273D, R275D, K284D ssh1Δ*) designated *sec61L6DDD* has a more severe growth defect than *sec61R275Dssh1Δ* (not shown).

Several conserved residues between R389 and E407 were selected for mutagenesis based upon a sequence comparison of the L8 region of eukaryotic Sec61 (Fig. 10A). The structure of *M. jannashii* SecY indicates that four of these residues (G404, K405, R406 and E407) are located in the tip of the L8 loop between two α-helices that project into the cytoplasm from the membrane surface. Point mutations in L8 did not cause a growth rate defect in strains that express Ssh1p (Fig. 10B). Serial dilution experiments (Fig. 10C) demonstrated that mutations at K405, R406 and to a lesser extent K396 cause growth rate defects (Fig. 10D). Substitutions at the other tested residues had little or no effect including a two-residue deletion (R389ΔD390Δ).

Figure 9. Point mutations in L6 of Sec61p. (A) Secondary structure of L6 (*M. jannaschii* SecY) and sequence alignment between eukaryotic and *M. jannaschii* L6 segments. Identities are boxed and asterisks indicate residues subjected to mutagenesis. (B) Yeast strains RGY401 (*ssh1Δ*) and RGY402 (*SSH1*) that had been transformed with plasmids expressing wild type or mutant (R275*, R275S, R275L or R275G) alleles of Sec61p were streaked on 5-FOA plates and allowed to grow for 2 d at 30°C. Sec61R275* has a termination codon at position 275. (C, D) Growth rates of L6 *sec61* mutants were compared by serial dilution analysis (C) as described in the Materials and Methods and used to assign the L6 *sec61ssh1Δ* mutants to a growth phenotype category (D).

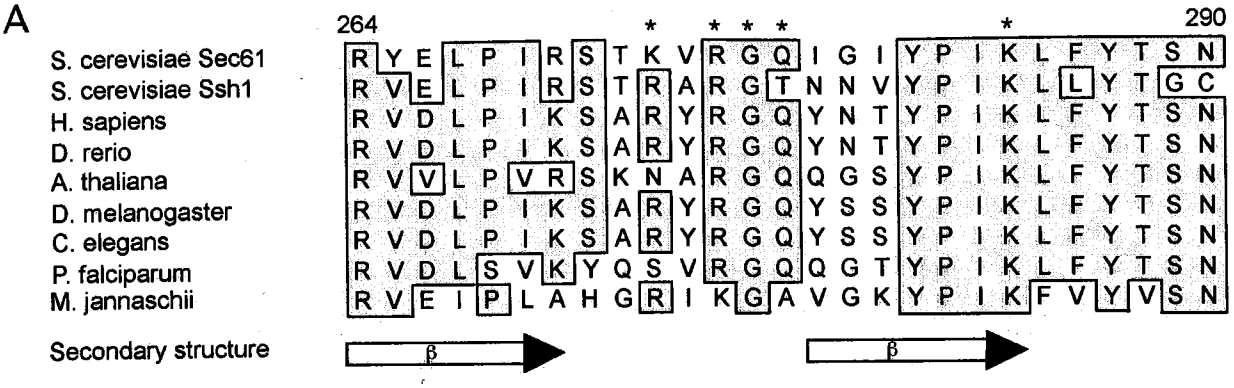
A
264
290
S. cerevisiae Sec61
S. cerevisiae Ssh1
H. sapiens
D. rerio
A. thaliana
D. melanogaster
C. elegans
P. falciparum
M. jannaschii
Secondary structure
β
β

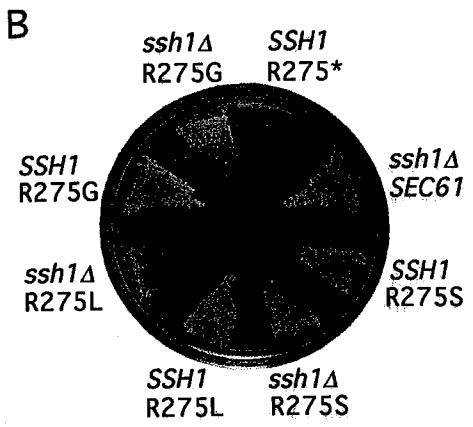
B
ssh1Δ R275G
SSH1 R275*
SSH1 R275G
ssh1Δ SEC61
ssh1Δ R275L
SSH1 R275S
SSH1 R275L
ssh1Δ R275S

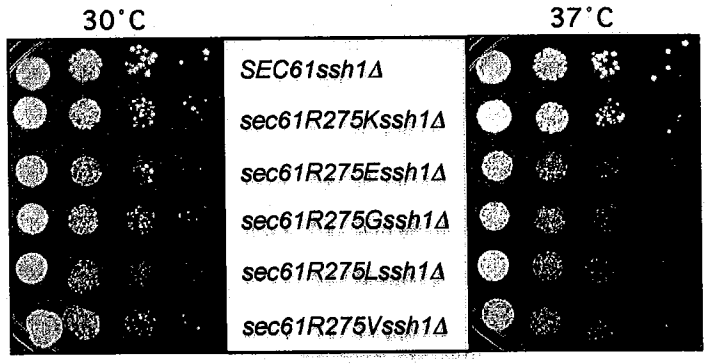
C
30°C
37°C
SEC61ssh1Δ
sec61R275Kssh1Δ
sec61R275Essh1Δ
sec61R275Gssh1Δ
sec61R275Lssh1Δ
sec61R275Vssh1Δ

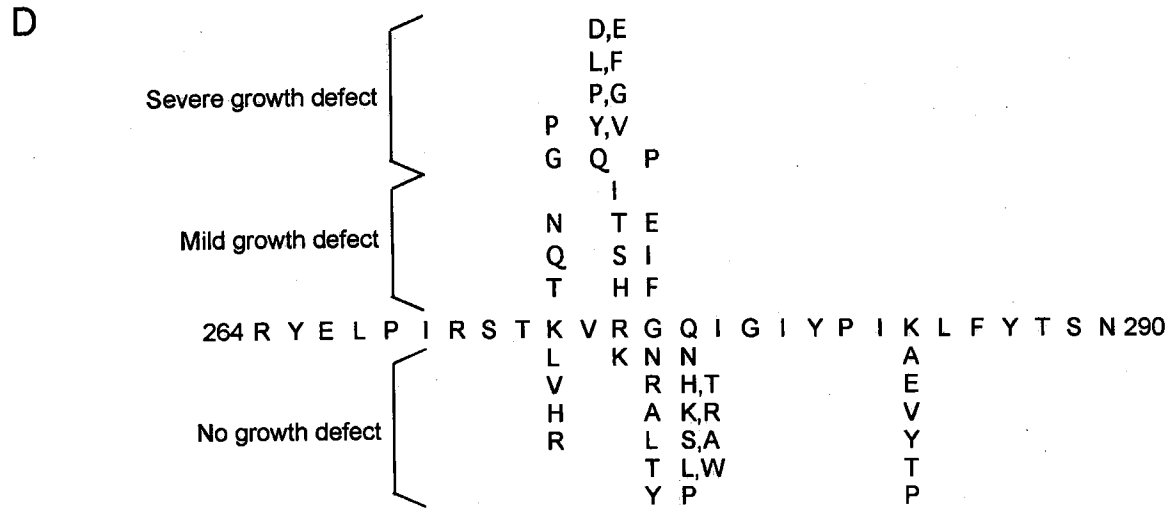
D
Severe growth defect
Mild growth defect
No growth defect
264 R Y E L P I R S T K V R G Q I G I Y P I K L F Y T S N 290
D,E
L,F
P,G
P Y,V
G Q P
I
N T E
Q S I
T H F
L K N N A
V R H,T E
H A K,R V
R L S,A Y
T L,W T
Y P P

Figure 10. Point mutations in L8 of Sec61p. (A) Secondary structure of L8 (*M. jannaschii* SecY) and sequence alignment between eukaryotic and *M. jannaschii* L8 segments. Identities are boxed and asterisks indicate residues subjected to mutagenesis. (B) Yeast strains RGY401 (*ssh1Δ*) and RGY402 (*SSH1*) that had been transformed with plasmids expressing wild type *SEC61*, or mutant alleles (R406*, R406E, L6L8EE (R275E, R406E) or K396D) of Sec61p were streaked onto 5-FOA plates and allowed to grow for 2 d at 30°C. (C, D) Serial dilution experiments were performed as described in Fig. 8C and used to assign the L8 *sec61ssh1Δ* mutants to a growth phenotype category (D).

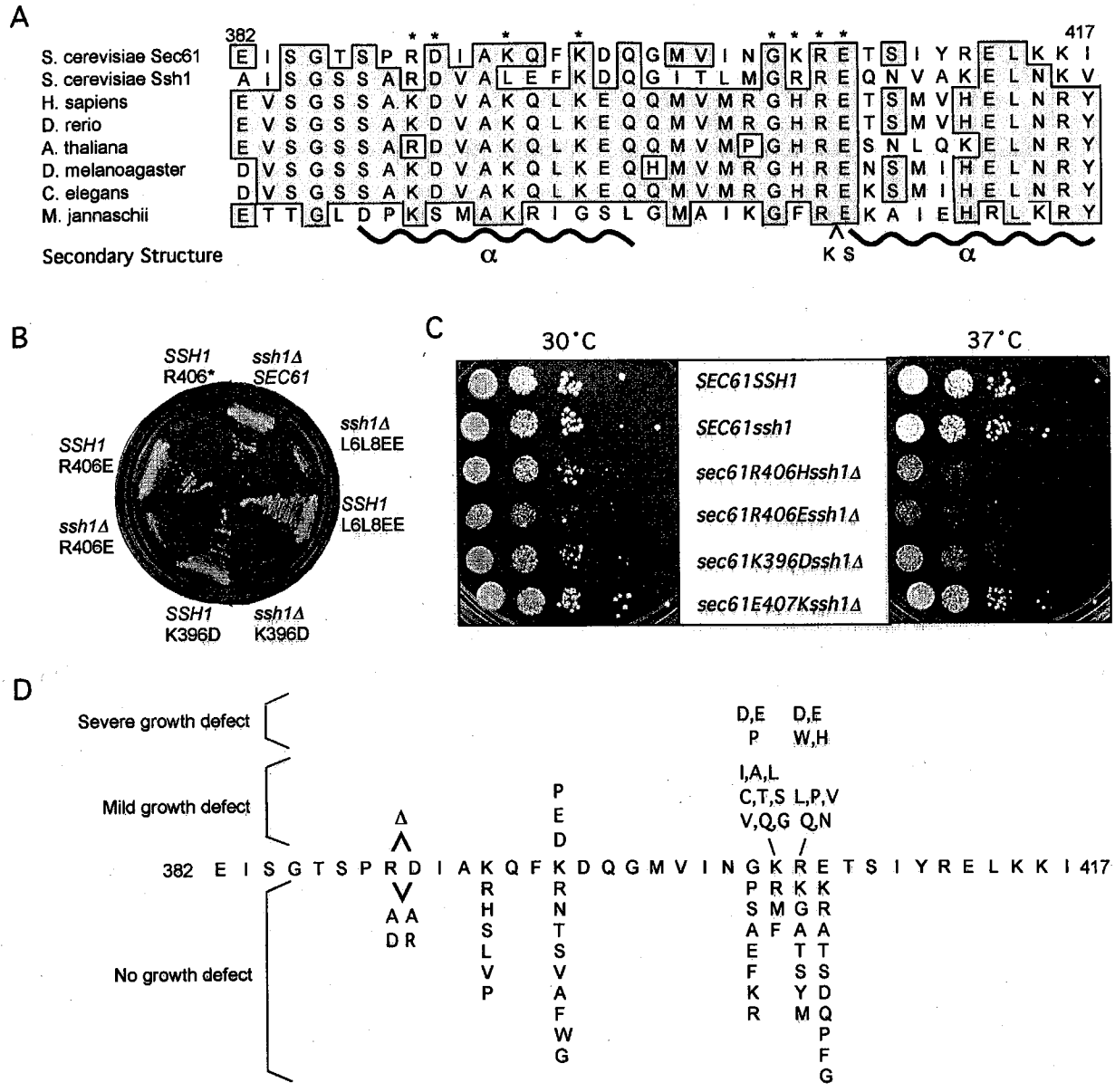
A
382
417
S. cerevisiae Sec61
S. cerevisiae Ssh1
H. sapiens
D. rerio
A. thaliana
D. melanoagaster
C. elegans
M. jannaschii
Secondary Structure
α
K S
α
B
SSH1 R406*
ssh1Δ SEC61
ssh1Δ L6L8EE
SSH1 R406E
SSH1 L6L8EE
ssh1Δ R406E
SSH1 K396D
ssh1Δ K396D
C
30°C
37°C
SEC61SSH1
SEC61ssh1
sec61R406Hssh1Δ
sec61R406Essh1Δ
sec61K396Dssh1Δ
sec61E407Kssh1Δ
D
Severe growth defect
Mild growth defect
No growth defect
382 E I S G T S P R D I A K Q F K D Q G M V I N G K R E T S I Y R E L K K I 417
D,E P
D,E W,H
I,A,L C,T,S V,Q,G
L,P,V Q,N
Δ
A A D R
R H S L V P
P E D R N T S V A F W G
P S A E F K R
R M F
K G A T S Y M
K R A T S D Q P F G

A double mutant (L6L8EE) that combined two severe L6 and L8 mutations (*R275E and R406E*) was suppressed by expression of Ssh1p (Fig. 10B).

Yeast strains with the *ade2* mutation turn red after growth in YPD for more than two days (Fig. 11A, R275R). This phenotype is due to accumulation of a red pigment, which is the oxidative metabolite of an intermediate in the biosynthetic pathway of adenine. Higher percentages of white colonies are observed in the *sec61* mutants (Fig. 11A). One mechanism that can cause loss of the red pigment is a loss of mitochondrial respiration. Although additional mutations preceding the *ADE2* step in the biosynthetic pathway of adenine (e.g. *ade2 ade3* double mutants) also prevent formation of the red pigment, such mutations should occur at a much lower rate. To determine the rate of respiration loss, yeast cells were first grown in YPEG media containing nonfermentable carbon sources, then shifted to YPD media for ~20 generations. Cells were diluted onto YPD plates and replicated to YPEG plates after two days. The percentages of colonies that are unable to grow on YPEG plates were calculated. RGY401 derivatives expressing L6 or L8 *sec61* mutants lose respiratory competence at a 3-10 fold higher frequency (~1-3% per generation) than the parental *ssh1Δ* strain.

To study mitochondrial morphology in wild-type and *sec61* mutants, cells were transformed with a plasmid (B742, provided by J. Shaw, University of Utah) encoding mitochondria-targeted GFP. After cells were shifted from YPEG media to YPD media, mitochondria in wild-type strain show a staining pattern of interconnected dots and short tubes around the cortex of the cells (Fig. 11B), which is the normal mitochondrial morphology in yeast cells (Shaw and Nunnari, 2002). Mitochondria in L6 and L8 *sec61* mutants undergo morphology changes after the shift, featuring elongated tubes and clusters of bright dots that are not evenly distributed in the cells. These phenotypes indicate defects in the dynamic fusion and fission pathway of

CHAPTER V

Discussion

Alleles of *sec61* that selectively interfere with the cotranslational translocation pathway have not been described previously. Although proteolytic mapping experiments suggested that L6 and L8 are specifically involved in SRP-dependent translocation activity (Song et al., 2000), the ribosome-binding sites on Sec61p had not been mapped with precision. Cassette mutagenesis of the L6 and L8 segments of Sec61p allowed the isolation of a novel class of *sec61* mutants that are primarily defective in the cotranslational translocation pathway.

The structure of SecYEβ had not been solved when we selected residues in L6 and L8 of Sec61p for site-directed mutagenesis. The transmembrane and loop domains of Sec61p were defined based on the predicted membrane topology of the protein (Wilkinson et al., 1996). Highly conserved, charged residues in the middle region of L6 and L8 were selected for mutagenesis. The growth and translocation defects caused by mutations in L6 and L8 demonstrate that these cytosolic loops are critical for cotranslational translocation. The X-ray structure of *M. jannaschii* SecYEβ (Van den Berg et al., 2004) confirmed that most of those residues are located at the tip of the two loops, highly exposed and oriented towards the cytosol. The effect of the L6 and L8 point mutations on the cotranslational translocation pathway was confirmed using ubiquitin translocation assays (UTA), which show that L6 and L8 mutations cause a delay in the gating of the Sec61p complex by DPA RNCs.

As seen in the SecYEβ structure, L6 and L8 project ~20Å into the cytosol from the membrane surface (Fig. 20A). When viewed from the top, the critical residues in L6 and L8 define a triangular surface with vertexes separated by 15-20 Å (Fig. 20D). Our observations

agree with the results from the three-dimensional EM reconstruction of the ribosome-Sec61 complex and the RNC-Sec61 complex, which revealed a ~15 Å gap between the channel and the ribosome that is bridged by four stalklike connections with diameters of ~20 Å. As expected, the mutations in positively charged residues on L8 caused reductions in ribosome-bind activity, suggesting that salt bridges between the basic side chains on Sec61p and the phosphodiester backbone of the 25S rRNA are critical for ribosome attachment.

Surprisingly, L6 mutants do not cause a significant reduction in ribosome-binding affinity, suggesting that point mutations in L6 may affect a different step in the attachment of the RNC complex to the channel. One possibility is that L6 serves as the marker for an unoccupied translocon. L6 may interact with the posttargeting intermediate (SR-SRP-RNC complex) to facilitate the transfer of the RNC to the channel after the dissociation of SRP from the signal sequence. The existence of a binding partner for SR on the ER membrane is supported by the observation that deletion of the TM span from SRβ does not prevent the binding of SR to the ER membrane (Ogg et al., 1998). Investigation of the interaction between SR and the Sec61p complex will provide more insight into the cotranslational targeting pathway.

Previous research has suggested that the Ssh1 complex is an auxiliary channel that is specific for cotranslational pathway (Finke et al., 1996). Ubiquitin translocation assays using DPA series of UTA reporters provided direct evidence to support the specific involvement of Ssh1p in cotranslational pathway. Elimination of the Ssh1p translocon increases the plateau value for reporter cleavage, which is consistent with a decrease in the number of translocons for cotranslational substrates. Moreover, *sec61* mutants in the *SSH1* background display a marked decrease in reporter cleavage, indicating that the Ssh1 complex rescues translocation defects in the mutants by providing an additional translocon for the cotranslational translocation pathway.

Expression of Ssh1p eliminates both co- and posttranslational transport defects caused by the L6 and L8 *sec61* mutants, supporting the theory that the kinetic delay in the posttranslational pathway was caused by accumulation of SRP-dependent substrates in the cytosol. The physiological reason why *S. cerevisiae* express an additional cotranslational translocon (the Ssh1p complex) remains unclear. The Ssh1p complex may provide a mechanism to balance precursor flux between two targeting pathways or regulate cotranslational translocation without affecting posttranslational translocation. Further biochemical and structural studies of the Ssh1p complex may shed light on how Ssh1p translocons function in vivo.

SRP pathway mutants (e.g. *srp54*Δ, *srp101*Δ), as well as our L6 and L8 mutants are able to adapt to defects in the cotranslational translocation pathway. The adaptation of *srp54*Δ correlates with the induction of cytosolic chaperones and reductions in protein synthesis rate (Mutka and Walter, 2001), which suggests a dynamic partitioning of nascent polypeptides between the two targeting pathways. This hypothesis was supported using the DPA series of UTA reporters, which provide a powerful tool to distinguish between the two targeting pathways. Surprisingly, *srp54*Δ strain translocates polypeptides by cotranslational as well as posttranslational translocation pathway. Further research is required to determine how RNCs are targeted to the translocon in the absence of SRP54.

Few previous studies have investigated the kinetics of membrane protein integration in vivo. In the second part of my thesis, I have used UTA reporters derived from the type II integral membrane protein DPAPB to analyze cotranslational integration of membrane proteins into the yeast endoplasmic reticulum. Our in vivo analysis with UTA reporters defined the time window for gating of the channel by the RNC. The study also reveals that one or more of the events that precede RNC gating of the translocon are slow relative to the in vivo rate of

polypeptide elongation in a eukaryotic cell. The delay causes the transient exposure of downstream lumenal sequences to the cytosol. The slow steps may be the conformational changes in Sec61p that allow signal sequence insertion and gating of the transport pore. A longer delay was observed for the insertion of a TM span in the type II (N_{cyt}-C_{lum}) orientation. Here, the rate-limiting step appears to be a nascent chain length-dependent event that permits the adoption of the type II topology. Our ubiquitin translocation assays provide insight into the kinetics of RNC targeting to the channel, which was not revealed in previous in vitro assays that utilize elongation arrested RNCs.

Integration of multi-pass integral membrane proteins is considerably more complicated than integration of a type II membrane protein. Current models describe an orderly and stepwise integration of membrane spanning segments, translocation of lumenal loops and retention of cytoplasmic loops in a process that is tightly coupled to elongation of the nascent polypeptide. Analysis of the 3TM series of UTA reporters revealed an unanticipated cytoplasmic exposure of reporter domains that follow TM3, which is also integrated in the N_{cyt}-C_{lum} orientation. Several steps that may cause the delay in the transport of the lumenal domain could be the insertion of a TM span in the type II orientation, the availability of the signal sequence binding site and the closing of the channel. If the binding site is still occupied by a preceding TM when a new TM emerges from the ribosome, the insertion of the following TM could be delayed. Continued elongation of the polypeptide results in cytoplasmic exposure of the lumenal domain.

Having a long lumenal loop allows the preceding N_{cyt}-C_{lum} TM to adopt the correct topology, exit the channel and leave the SSB site open, hence facilitating the insertion of the following TMs and the lumenal domain. Expansion of a cytosolic loop would allow the exit of the previous TM long before the insertion of a following N_{cyt}-C_{lum} TM. When unoccupied by the

polypeptide, the channel may be closed by the TM2a plug. The insertion of the follow TM would require reopening of the channel. Moreover, accommodating a large cytosolic loop in the ribosome-channel connection may interfere with the interaction between the ribosome and the channel.

More UTA reporters derived from the DPA 3TM reporters could be constructed to provide deeper understanding into the integration of membrane proteins. As discussed, integration of multi-pass membrane proteins can be complicated by different steps. UTA reporters that combine the L1 and L2 insertion could be used to selectively study the insertion of TM3. Expansion of both loops will allow the previous two TMs to achieve the correct topology and exit the channel, so that the insertion of TM3 won't be delayed by the integration of early segments of the reporter. It would also be interesting to construct 3TM UTA reporters in which TM3 is replaced by a signal sequence. As we know, a signal sequence can rapidly bind the channel in N_{cyt}-C_{lum} orientation if the binding site in the translocon is available. Although proteins with a signal sequence following several TMs have not be found in nature, study of these UTA reporters with various length of loop 2 will provide more information about the time required for the preceding TM to leave the channel and render the binding sites available. UTA reporters containing two TMs (a N_{lum}-C_{cyt} TM followed by a N_{cyt}-C_{lum} TM) can also be used to study whether a delay in the insertion of an N_{cyt}-C_{lum} TM span also exits in other types of membrane proteins.

It would also be interesting to study the mechanism that prevents premature folding of a lumenal domain or aggregation of TM spans in the cytosol. Folding of a reporter domain that is derived from a cytosolic protein (e.g. Ura3) may reduce the fidelity of membrane protein integration. To address this possibility, the reporter segment Ura3 could be replaced with a

segment derived from the lumenal domain of DPAPB. Monitoring the integration of this new UTA reporter will reveal whether the lumenal domains of membrane proteins are maintained in a translocation-competent state to prevent premature folding. Cytosolic chaperones may assist in the cotranslational integration of polytopic membrane proteins. Another possibility is that native membrane proteins have intrinsic sequences that would cause pauses during translation. Pausing may allow the previous TM to adopt the correct orientation, bind to the SSB site and exit the channel through the lateral exit. Further study on cytosolic chaperones as well as "pause signals" in membrane proteins will reveal the mechanism that maintains the fidelity of membrane protein integration.

CHAPTER VI

References

Adelman, M.R., G. Blobel, and D.D. Sabatini. 1973a. An improved cell fractionation procedure for preparation of rat liver microsomes. *J. Cell Biol.* 56:191-205.

Adelman, M.R., D.D. Sabatini, and G. Blobel. 1973b. Ribosome-membrane interaction. Nondestructive disassembly of rat liver rough microsomes into ribosomal and membrane components. *J. Cell Biol.* 56:206-229.

Akiyama, Y., and K. Ito. 1987. Topology analysis of the SecY protein, an integral membrane protein involved in protein export in *Escherichia coli*. *EMBO J.* 6:3465-3470.

Andrews, D., P. Walter, and F.P. Ottensmeyer. 1987. Evidence for an extended 7SL RNA structure in the signal recognition particle. *EMBO J.* 6:3471-3477.

Arnold, C.E., and K.D. Wittrup. 1994. The stress response to loss of signal recognition particle function in Saccharomyces cerevisiae. *J Biol Chem.* 269:30412-30418.

Batey, R.T., and J.A. Doudna. 2002. Structural and Energetic Analysis of Metal Ions Essential to SRP Signal Recognition Domain Assembly. *Biochemistry.* 41:11703-11710.

Batey, R.T., R.P. Rambo, L. Lucast, B. Rha, and J.A. Doudna. 2000. Crystal structure of the ribonucleoprotein core of the signal recognition particle. *Science.* 287:1232-1239.

Baxter, B.K., P. James, T. Evans, and E.A. Craig. 1996. *SSI1* encodes a novel Hsp70 of the *Saccharomyces cerevisiae* endoplasmic reticulum. *Mol. Cell. Biol.* 16:6444-6456.

Beckmann, R., D. Bubeck, R. Grassucci, P. Penczek, A. Verschoor, G. Blobel, and J. Frank. 1997. Alignment of conduits for the nascent polypeptide chain in the ribosome-Sec61 complex. *Science.* 278:2123-2126.

Beckmann, R., C.M. Spahn, N. Eswar, J. Helmers, P.A. Penczek, A. Sali, J. Frank, and G. Blobel. 2001. Architecture of the protein-conducting channel associated with the translating 80S ribosome. *Cell.* 107:361-372.

Bedouelle, H., P. Bassford, A. Fowler, I. Zabin, J. Beckwith, and M. Hofung. 1980. Mutations which alter the function of the maltose binding protein of *Eschericia coli. Nature (London).* 285:78-81.

Beltzer, J.P., K. Fiedler, C. Fuhrer, I. Geffen, C. Handschin, H.P. Wessels, and M. Spiess. 1991. Charged residues are major determinants of the transmembrane orientation of a signal-anchor sequence. *J. Biol. Chem.* 266:973-978.

Bernstein, H.D., M.A. Poritz, K. Strub, P.J. Hoben, S. Brenner, and P. Walter. 1989. Model for signal sequence recognition from amino-acid sequence of 54K subunit of signal recognition particle. *Nature.* 340:482-6.

Blobel, G., and B. Dobberstein. 1975a. Transfer of proteins across membranes. I. Presence of proteolytic processed and unprocessed nascent immunoglobulin light chains on membrane bound ribosomes of murine myeloma. *J. Cell Biol.* 67:835-851.

Blobel, G., and B. Dobberstein. 1975b. Transfer of proteins across membranes. II Reconstitution of functional rough microsomes from heterologous components. *J. Cell Biol.* 67:852-862.

Blobel, G., and D.D. Sabatini. 1971. Ribosome-membrane interaction in eukaryotic cells. *Biomembranes.* 2:193-195.

Breyton, C., W. Haase, T.A. Rapoport, W. Kuhlbrandt, and I. Collinson. 2002. Three-dimensional structure of the bacterial protein-translocation complex SecYEG. *Nature.* 418:662-5.

Brodsky, J.L., J.G. Lawrence, and A.J. Caplan. 1998. Mutations in the cytosolic DnaJ homologue, YDJ1, delay and compromise the efficient translation of heterologous proteins in yeast. *Biochemistry*. 37:18045-18055.

Caplan, A.J., D.M. Cyr, and M.G. Douglas. 1992. YDJ1p facilitates polypeptide translocation across different intracellular membranes by a conserved mechanism. *Cell*. 71:1143-1155.

Cheng, Z., Y. Jiang, E.C. Mandon, and R. Gilmore. 2005. Identification of cytoplasmic residues of Sec61p involved in ribosome binding and cotranslational translocation. *J. Cell Biol.* 168:67-77.

Chirico, W.J., M.G. Waters, and G. Blobel. 1988. 70K heat shock related proteins stimulate protein translocation into microsomes. *Nature*. 322:805-810.

Connolly, T., P. Collins, and R. Gilmore. 1989. Access of proteinase K to partially translocated nascent polypeptides in intact and detergent-solubilized membranes. *J Cell Biol.* 108:299-307.

Connolly, T., and R. Gilmore. 1989. The signal recognition particle receptor mediates the GTP-dependent displacement of SRP from the signal sequence of the nascent polypeptide. *Cell*. 57:599-610.

Connolly, T., P.J. Rapiejko, and R. Gilmore. 1991. Requirement of GTP hydrolysis for dissociation of the signal recognition particle from its receptor. *Science*. 252:1171-1173.

Corsi, A.K., and R. Schekman. 1996. Mechanism of polypeptide translocation into the endoplasmic reticulum. *J. Biol. Chem.* 271:30299-30302.

Crowley, K.S., G.D. Reinhart, and A.E. Johnson. 1993. The signal sequence moves through a ribosomal tunnel into a noncytoplasmic aqueous environment at the ER membrane early in translocation. *Cell.* 73:1101-1115.

Denzer, A.J., C.E. Nabholz, and M. Spiess. 1995. Transmembrane orientation of signal anchor proteins is affected by the folding state but not the size of the N-terminal domain. *EMBO J.* 14:6311-6317.

Deshaies, R.J., B.D. Koch, M. Werner-Washburne, E.A. Craig, and R. Schekman. 1988. A subfamily of stress proteins facilitates translocation of secretory and mitochondrial precursor polypeptides. *Nature.* 332:800-805.

Deshaies, R.J., S.L. Sanders, D.A. Feldheim, and R. Schekman. 1991. Assembly of yeast Sec proteins involved in translocation into the endoplasmic reticulum into a membrane-bound multisubunit complex. *Nature.* 349:806-808.

Deshaies, R.J., and R. Schekman. 1987. A yeast mutant defective at an early stage in import of secretory protein precursors into the endoplasmic reticulum. *J. Cell Biol.* 105:633-645.

Deshaies, R.J., and R. Schekman. 1989. Sec62 encodes a putative membrane protein required for protein translocation into the yeast endoplasmic reticulum. *J. Cell Biol.* 109:2653-2664.

Do, H., D. Falcone, L. J., D.W. Andrews, and A.E. Johnson. 1996. The cotranslational integration of membrane proteins into the phospholipid bilayer is a multistep process. *Cell.* 85:369-378.

Esnault, Y., M.-O. Blondel, R. Deshaies, R. Schekman, and F. Képes. 1993. The yeast *SSS1* gene is essential for secretory protein translocation and encodes a conserved protein of the endoplasmic reticulum. *EMBO J.* 12:4083-4093.

Fang, H., and N. Green. 1994. Nonlethal *sec71-1* and *sec72-1* mutations eliminate proteins associated with the Sec63p-BiP complex from *S. cerevisiae*. *Mol. Biol. Cell.* 5:933-942.

Feldheim, D., and R. Schekman. 1994. Sec72p contributes to the selective recognition of signal peptides by the secretory polypeptide translocation complex. *J. Cell Biol.* 126:935-943.

Feldheim, D.A., K. Yoshimura, A. Admon, and R. Schekman. 1993. Structural and functional characterization of Sec66p, a new subunit of the polypeptide translocation apparatus in yeast endoplasmic reticulum. *Mol. Biol. Cell.* 4:931-939.

Finke, K., K. Plath, S. Panzer, S. Prehn, T.A. Rapoport, E. Hartmann, and T. Sommer. 1996. A second trimeric complex containing homologues of the Sec61p complex functions in protein transport across the ER membrane of *S. cerevisiae*. *EMBO J.* 15:1482-1494.

Gerrard, S.R., A.B. Mecklem, and T.H. Stevens. 2000. The yeast endosomal t-SNARE, Pep12p, functions in the absence of its transmembrane domain. *Traffic.* 1:45-55.

Gilmore, R., and G. Blobel. 1985. Translocation of secretory proteins across the microsomal membrane occurs through an environment accessible to aqueous perturbants. *Cell.* 42:497-505.

Gilmore, R., G. Blobel, and P. Walter. 1982a. Protein translocation across the endoplasmic reticulum. I. Detection in the microsomal membrane of a receptor for the signal recognition particle. *J. Cell Biol.* 95:463-469.

Gilmore, R., P. Walter, and G. Blobel. 1982b. Protein translocation across the endoplasmic reticulum. II. Isolation and characterization of the signal recognition particle receptor. *J. Cell Biol.* 95:470-477.

Goder, V., P. Crottet, and M. Spiess. 2000. In vivo kinetics of protein targeting to the endoplasmic reticulum determined by site-specific phosphorylation. *Embo J.* 19:6704-12.

Goder, V., and M. Spiess. 2001. Topogenesis of membrane proteins: determinants and dynamics. *FEBS Lett.* 504:87-93.

Goder, V., and M. Spiess. 2003. Molecular mechanism of signal sequence orientation in the endoplasmic reticulum. *Embo J.* 22:3645-53.

Goldstein, A.L., and J.H. McCusker. 1999. Three new dominant drug resistance cassettes for gene disruption in Saccharomyces cerevisiae. *Yeast.* 15:1541-1553.

Görlich, D., S. Prehn, E. Hartmann, K.-U. Kalies, and T.A. Rapoport. 1992. A mammalian homologue of Sec61p and SecYp is associated with ribosomes and nascent polypeptides during translocation. *Cell.* 71:489-503.

Görlich, D., and T.A. Rapoport. 1993. Protein translocation into proteoliposomes reconstituted from purified components of the ER membrane. *Cell.* 75:615-630.

Goud, B., A. Salminen, N.C. Walworth, and P.J. Novick. 1988. A GTP-binding protein required for secretion rapidly associates with secretory vesicles and the plasma membrane in yeast. *Cell.* 53:753-768.

Green, N., H. Fang, and P. Walter. 1992. Mutants in three novel complementation groups inhibit membrane protein insertion into and soluble protein translocation across the endoplasmic reticulum membrane of *Saccharomyces cerevisiae. J. Cell Biol.* 116:597-604.

Green, N., and P. Walter. 1992. C-terminal sequences can inhibit the insertion of membrane proteins into the endoplasmic reticulum of *Saccharomyces cerevisiae*. *Mol. Cell. Biol.* 12:283-291.

Haigh, N.G., and A.E. Johnson. 2002. A new role for BiP: closing the aqueous translocon pore during protein integration into the ER membrane. *J Cell Biol.* 156:261-70.

Halic, M., T. Becker, M.R. Pool, C.M. Spahn, R.A. Grassucci, J. Frank, and R. Beckmann. 2004. Structure of the signal recognition particle interacting with the elongation-arrested ribosome. *Nature*. 427:808-814.

Hamilton, T.G., and G.C. Flynn. 1996. Cer1p, a novel Hsp70-realted protein required for posttranslational endoplasmic reticulum translocation in yeast. *J. Biol. Chem.* 271:30610-30613.

Hanein, D., K.E.S. Matlack, B. Jungnickel, K. Plath, K.-U. Kalies, K.R. Miller, T.A. Rapoport, and C.W. Akey. 1996. Oligomeric rings of the Sec61p complex induced by ligands required for protein translocation. *Cell.* 87:721-732.

Hann, B.C., and P. Walter. 1991. The signal recognition particle in *S. cerevisiae*. *Cell.* 67:131-144.

Hansen, W., P.D. Garcia, and P. Walter. 1986. In vitro protein translocation across the yeast endoplasmic reticulum. ATP-dependent posttranslational translocation of the prepro-α-factor. *Cell.* 45:397-406.

Hartmann, E., T.A. Rapoport, and H.F. Lodish. 1989. Predicting the orientation of eukaryotic membrane-spanning proteins. *Proc. Natl. Acad. Sci. USA*. 86:5786-5790.

Hartmann, E., T. Sommer, S. Prehn, D. Görlich, S. Jentsch, and T. Rapoport. 1994. Evolutionary conservation of components of the protein translocation apparatus. *Nature.* 348:654-657.

Heinrich, S.U., W. Mothes, J. Brunner, and T.A. Rapoport. 2000. The Sec61p complex mediates the integration of a membrane protein by allowing lipid partitioning of the transmembrane domain. *Cell.* 102:233-44.

Heinrich, S.U., and T.A. Rapoport. 2003. Cooperation of transmembrane segments during the integration of a double-spanning protein into the ER membrane. *Embo J.* 22:3654-63.

Hershey, J.W. 1991. Translational control in mammalian cells. *Annu Rev Biochem.* 60:717-55.

Ito, K., M. Wittekind, M. Nomura, K. Shiba, T. Yura, A. Miura, and H. Nashimoto. 1983. A temperature-sensitive mutant of E. coli exhibiting slow processing of exported proteins. *Cell.* 32:789-97.

Johnsson, N., and A. Varshavsky. 1994. Ubiquitin-assisted dissection of protein transport across membranes. *EMBO J.* 13:2686-2698.

Jungnickel, B., and T.A. Rapoport. 1995. A posttranslational signal sequence recognition event in the endoplasmic reticulum membrane. *Cell.* 82:261-270.

Kalies, K.-U., T.A. Rapoport, and E. Hartmann. 1998. The β-subunit of the Sec61p complex facilitates cotranslational protein transport and interacts with the signal sequence. *J. Cell Biol.* 141:887-894.

Kim, H., Q. Yan, G. Von Heijne, G.A. Caputo, and W.J. Lennarz. 2003. Determination of the membrane topology of Ost4p and its subunit interactions in the oligosaccharyltransferase complex in Saccharomyces cerevisiae. *Proc. Natl. Acad. Sci. USA.* 100:7460-7464.

Knop, M., K. Siegers, G. Pereira, W. Zachariae, B. Winsor, K. Nasmyth, and E. Schiebel. 1999. Epitope tagging of yeast genes using a PCR-based strategy: more tags and improved practical routines. *Yeast.* 15:963-972.

Koch, H.G., T. Hengelage, C. Neumann-Haefelin, J. MacFarlane, H.K. Hoffschulte, K.L. Schimz, B. Mechler, and M. Muller. 1999. In vitro studies with purified components reveal signal recognition particle (SRP) and SecA/SecB as constituents of two independent protein- targeting pathways of Escherichia coli. *Mol. Biol. Cell.* 10:2163-2173.

Liao, S., J. Lin, H. Do, and A.E. Johnson. 1997. Both lumenal and cytosolic gating of the aqueous ER translocon pore are regulated from inside the ribosome during membrane protein integration. *Cell.* 90:31-41.

Luirink, J., C.M. ten Hagen-Jongman, C.C. van der Weidjen, B. Oudega, S. High, B. Dobberstein, and R. Kusters. 1994. An alternative protein targeting pathway in *Escherichia coli*: studies on the role of FtsY. *EMBO J.* 13:2289-2296.

Mandon, E.C., Y. Jiang, and R. Gilmore. 2003. Dual recognition of the ribosome and the signal recognition particle by the SRP receptor during protein targeting to the endoplasmic reticulum. *J Cell Biol.* 162:575-585.

Mason, N., L.F. Ciufo, and J.D. Brown. 2000. Elongation arrest is a physiologically important function of signal recognition particle. *Embo J.* 19:4164-4174.

Matlack, K.E., B. Misselwitz, K. Plath, and T.A. Rapoport. 1999. BiP acts as a molecular ratchet during posttranslational transport of prepro-alpha factor across the ER membrane. *Cell.* 97:553-564.

McCormick, P.J., Y. Miao, Y. Shao, J. Lin, and A.E. Johnson. 2003. Cotranslational protein integration into the ER membrane is mediated by the binding of nascent chains to translocon proteins. *Mol Cell.* 12:329-41.

Miller, J.D., S. Tajima, L. Lauffer, and P. Walter. 1995. The β subunit of the signal recognition particle receptor is a transmembrane GTPase that anchors the α subunit, a peripheral membrane GTPase, to the endoplasmic reticulum. *J. Cell Biol.* 128:273-282.

Mitra, K., C. Schaffitzel, T. Shaikh, F. Tama, S. Jenni, C.L. Brooks, 3rd, N. Ban, and J. Frank. 2005. Structure of the E. coli protein-conducting channel bound to a translating ribosome. *Nature.* 438:318-24.

Monne, M., T. Hessa, L. Thissen, and G. von Heijne. 2005. Competition between neighboring topogenic signals during membrane protein insertion into the ER. *Febs J.* 272:28-36.

Morgan, D.G., J.F. Menetret, A. Neuhof, T.A. Rapoport, and C.W. Akey. 2002. Structure of the mammalian ribosome-channel complex at 17A resolution. *J Mol Biol.* 324:871-886.

Mori, H., and K. Ito. 2001. An essential amino acid residue in the protein translocation channel revealed by targeted random mutagenesis of SecY. *Proc Natl Acad Sci U S A.* 98:5128-5133.

Mothes, W., S.U. Heinrich, R. Graf, I.M. Nilsson, G. von Heijne, J. Brunner, and T.A. Rapoport. 1997. Molecular mechanism of membrane protein integration into the endoplasmic reticulum. *Cell.* 89:523-533.

Mothes, W., S. Prehn, and T.A. Rapoport. 1994. Systematic probing of the environment of a translocating secretory protein during translocation through the ER membrane. *Embo J.* 13:3973-3982.

Müsch, A., M. Wiedmann, and T.A. Rapoport. 1992. Yeast Sec proteins interact with polypeptides traversing the endoplasmic reticulum membrane. *Cell.* 69:343-352.

Mutka, S.C., and P. Walter. 2001. Multifaceted physiological response allows yeast to adapt to the loss of the signal recognition particle-dependent protein-targeting pathway. *Mol Biol Cell.* 12:577-588.

Newitt, J.A., and H.D. Bernstein. 1998. A mutation in the Escherichia coli secY gene that produces distinct effects on inner membrane protein insertion and protein export. *J Biol Chem.* 273:12451-12456.

Ng, D.T.W., J.D. Brown, and P. Walter. 1996. Signal sequences specify the targeting route to the endoplasmic reticulum. *J. Cell Biol.* 134:269-278.

Ogg, S.C., W.P. Barz, and P. Walter. 1998. A functional GTPase domain, but not its transmembrane domain, is required for function of the SRP receptor β-subunit. *J. Cell Biol.* 142:341-354.

Ogg, S.C., M.A. Poritz, and P. Walter. 1992. Signal recognition particle receptor is important for cell growth and protein secretion in *Saccharomyces cerevisiae. Mol. Biol. Cell.* 3:895-911.

Osborne, A.R., T.A. Rapoport, and B. van den Berg. 2005. Protein translocation by the Sec61/SecY channel. *Annu Rev Cell Dev Biol.* 21:529-50.

Panzner, S., L. Dreier, E. Hartmann, S. Kostka, and T.A. Rapoport. 1995. Posttranslational protein transport in yeast reconstituted with a purified complex of Sec proteins and Kar2p. *Cell.* 81:561-570.

Pathak, V.K., P.J. Nielsen, H. Trachsel, and J.W.B. Hershey. 1988. Structure of the β subunit of translational initiation factor eIF-2. *Cell.* 54:633-639.

Pilon, M., K. Romisch, D. Quach, and R. Schekman. 1998. Sec61p serves multiple roles in secretory precursor binding and translocation into the endoplasmic reticulum membrane. *Mol. Biol. Cell.* 9:3455-3473.

Plath, K., W. Mothes, B.M. Wilkinson, C.J. Stirling, and T.A. Rapoport. 1998. Signal sequence recognition in posttranslational protein transport across the yeast ER membrane. *Cell.* 94:795-807.

Plemper, R.K., S. Bohmler, J. Bordallo, T. Sommer, and D.H. Wolf. 1997. Mutant analysis links the translocon and BiP to retrograde transport for ER degradation. *Nature.* 388:891-895.

Powers, T., and P. Walter. 1997. Co-translational protein targeting catalyzed by the Escherichia coli signal recognition particle and its receptor. *Embo J.* 16:4880-4886.

Prinz, A., C. Behrens, T.A. Rapoport, E. Hartmann, and K.U. Kalies. 2000a. Evolutionarily conserved binding of ribosomes to the translocation channel via the large ribosomal RNA. *EMBO J.* 19:1900-1906.

Prinz, A., E. Hartmann, and K.U. Kalies. 2000b. Sec61p is the main ribosome receptor in the endoplasmic reticulum of Saccharomyces cerevisiae. *Biol. Chem.* 381:1025-1029.

Prinz, W.A., L. Grzyb, M. Veenhuis, J.A. Kahana, P.A. Silver, and T.A. Rapoport. 2000c. Mutants affecting the structure of the cortical endoplasmic reticulum in Saccharomyces cerevisiae. *J. Cell Biol.* 150:461-474.

Raden, D., W. Song, and R. Gilmore. 2000. Role of the cytoplasmic segments of Sec61alpha in the ribosome-binding and translocation-promoting activities of the Sec61 complex. *J. Cell Biol.* 150:53-64.

Rapoport, T.A., V. Goder, S.U. Heinrich, and K.E. Matlack. 2004. Membrane-protein integration and the role of the translocation channel. *Trends Cell Biol.* 14:568-75.

Redman, C., and D.D. Sabatini. 1966. Vectorial discharge of peptides released by puromycin from attached ribosomes. *Proc. Natl. Acad. Sci. USA.* 56:608-615.

Redman, C., P. Siekevitz, and G.E. Palade. 1966. Synthesis and transfer of amylase in pigeon pancreatic microsomes. *J. Biol. Chem.* 241:1150-1158.

Rothblatt, J., and R. Schekman. 1989. A hitchhiker's guide to the analysis of the secretory pathway in yeast. *Methods Cell Biol.* 32:3-36.

Rothblatt, J.A., R.J. Deshaies, S.L. Sanders, G. Daum, and R. Schekman. 1989. Multiple genes are required for proper insertion of secretory proteins into the endoplasmic reticulum in yeast. *J. Cell Biol.* 109:2641-2652.

Sabatini, D.D., and G. Blobel. 1970. Controlled proteolysis of nascent polypeptides in rat liver cell fractions. II. Location of the polypeptides in rough microsomes. *J. Cell Biol.* 45:146-157.

Sadler, I., A. Chiang, T. Kurihara, J. Rothblatt, J. Way, and P. Silver. 1989. A yeast gene important for protein assembly into the endoplasmic reticulum and the nucleus has homology to DnaJ, an *Escherichia coli* heat shock protein. *J. Cell Biol.* 109:2665-2675.

Sadlish, H., D. Pitonzo, A.E. Johnson, and W.R. Skach. 2005. Sequential triage of transmembrane segments by Sec61alpha during biogenesis of a native multispanning membrane protein. *Nat Struct Mol Biol.* 12:870-8.

Sato, T., M. Sakaguchi, K. Mihara, and T. Omura. 1990. The amino-terminal structures that determine topological orientation of cytochrome P-450 in microsomal membrane. *EMBO J.* 9.

Shaw, J.M., and J. Nunnari. 2002. Mitochondrial dynamics and division in budding yeast. Trends Cell Biol. 12:178-84.

Siekevitz, P., and G.E. Palade. 1960. A cytochemical study on the pancreas of the guinea pig. V. In vivo incorporation of leucine 14C into chymotrypsinogen of various cell fractions. J. Biophys. Biochem. Cytol. 7:619-631.

Sommer, T., and S. Jentsch. 1993. A protein translocation defect linked to ubiquitin conjugation at the endoplasmic reticulum. Nature. 365:176-179.

Song, W., D. Raden, E.C. Mandon, and R. Gilmore. 2000. Role of Sec61alpha in the regulated transfer of the ribosome-nascent chain complex from the signal recognition particle to the translocation channel. Cell. 100:333-343.

Spear, E.D., and D.T. Ng. 2003. Stress tolerance of misfolded carboxypeptidase Y requires maintenance of protein trafficking and degradative pathways. Mol Biol Cell. 14:2756-2767.

Stirling, C.J., J. Rothblatt, M. Hosobuchi, R. Deshaies, and R. Schekman. 1992. Protein translocation mutants defective in the insertion of integral membrane proteins into the endoplasmic reticulum. Mol. Biol. Cell. 3:129-142.

Tajima, S., L. Lauffer, V.L. Rath, and P. Walter. 1986. The signal recognition particle receptor is a complex that contains two distinct polypeptide chains. J. Cell Biol. 103:1167-1178.

Ulbrandt, N.D., J.A. Newitt, and H.D. Bernstein. 1997. The E. coli signal recognition particle is required for the insertion of a subset of inner membrane proteins. Cell. 88:187-196.

Van den Berg, B., W.M. Clemons, Jr., I. Collinson, Y. Modis, E. Hartmann, S.C. Harrison, and T.A. Rapoport. 2004. X-ray structure of a protein-conducting channel. Nature. 427:36-44.

Von Heijne, G. 1990. The signal peptide. J. Membr. Biol. 115:195-201.

Wach, A., A. Brachat, R. Pöhlmann, and P. Philippsen. 1994. New heterologous modules for classical or PCR-based gene disruptions in Saccharomyces cerevisiae. Yeast. 10:1793-1808.

Wahlberg, J.M., and M. Spiess. 1997. Multiple determinants direct the orientation of signal-anchor proteins: the topogenic role of the hydrophobic signal domain. J Cell Biol. 137:555-62.

Walter, P., and G. Blobel. 1980. Purification of a membrane-associated protein complex required for protein translocation across the endoplasmic reticulum. Proc. Natl. Acad. Sci. USA. 77:7112-7116.

Walter, P., and G. Blobel. 1981. Translocation of proteins across the endoplasmic reticulum. III. Signal recognition protein (SRP) causes signal sequence-dependent and site-specific arrest of chain elongation that is released by microsomal membranes. J. Cell Biol. 91:557-561.

Walter, P., and G. Blobel. 1982. Signal recognition particle contains a 7S RNA essential for protein translocation across the endoplasmic reticulum. Nature. 299:691-698.

Walter, P., I. Ibrahimi, and G. Blobel. 1981. Translocation of proteins across the endoplasmic reticulum. I. Signal recognition protein (SRP) binds to in-vitro-assembled polysomes synthesizing secretory protein. J. Cell Biol. 91:545-550.

Walter, P., R.C. Jackson, M.M. Marcus, V.R. Lingappa, and G. Blobel. 1979. Tryptic dissection and reconstitution of translocation activity for nascent presecretory proteins across microsomal membranes. Proc. Natl. Acad. Sci. USA. 76:1795-1799.

Walter, P., and A.E. Johnson. 1994. Signal sequence recognition and protein targeting to the endoplasmic reticulum membrane. Ann. Rev. Cell Biol. 10:87-119.

Walworth, N.C., and P.J. Novick. 1987. Purification and characterization of constitutive secretory vesicles from yeast. J Cell Biol. 105:163-174.

Waters, M.G., and G. Blobel. 1986. Secretory protein translocation in a yeast cell-free system can occur posttranslationally and requires ATP hydrolysis. J. Cell Biol. 102:1543-1550.

Wiertz, E.J., D. Tortorella, M. Bogyo, J. Yu, W. Mothes, T.R. Jones, T.A. Rapoport, and H.L. Ploegh. 1996. Sec61-mediated transfer of a membrane protein from the endoplasmic reticulum to the proteasome for destruction. Nature. 384:432-438.

Wilkinson, B.M., A.J. Critchley, and C.J. Stirling. 1996. Determination of the transmembrane topology of yeast Sec61p; an essential component of the ER translocation complex. J. Biol. Chem. 271:25590-25597.

Wilkinson, B.M., J.R. Tyson, P.J. Reid, and C.J. Stirling. 2000. Distinct domains within yeast Sec61p involved in post-translational translocation and protein dislocation. J. Biol. Chem. 275:521-529.

Wilkinson, B.M., J.R. Tyson, and C.J. Stirling. 2001. Ssh1p determines the translocation and dislocation capacities of the yeast endoplasmic reticulum. Dev Cell. 1:401-409.

Wilson, C., T. Connolly, T. Morrison, and R. Gilmore. 1988. Integration of membrane proteins into the endoplasmic reticulum requires GTP. J Cell Biol. 107:69-77.

Wittke, S., M. Dunnwald, M. Albertsen, and N. Johnsson. 2002. Recognition of a subset of signal sequences by Ssh1p, a Sec61p-related protein in the membrane of endoplasmic reticulum of yeast Saccharomyces cerevisiae. Mol Biol Cell. 13:2223-2232.

Woolhead, C.A., P.J. McCormick, and A.E. Johnson. 2004. Nascent membrane and secretory proteins differ in FRET-detected folding far inside the ribosome and in their exposure to ribosomal proteins. Cell. 116:725-736.

Zimmermann, R., M. Zimmermann, H. Wiech, G. Schlenstedt, G. Muller, F. Morel, P. Klappa, C. Jung, and W.W. Cobet. 1990. Ribonucleoparticle-independent transport of proteins into mammalian microsomes. J Bioenerg Biomembr. 22:711-23.

Figure 11. L6 and L8 *sec61* mutants cause a higher frequency of respiratory competence loss. (A) Serial dilution experiments were performed as in Fig 8 and 9 except that cells were grown in SD media before plating onto YPD. (B) Mitochondrial morphology in wild-type and *sec61* mutants. Mitochondria are visualized by a mito-GFP reporter. Yeast strains were grown to mid-log phase at 30°C in YPEG media and diluted into YPD media and allowed to grow for 4-8 h at 30°C. Both bright-field and green-fluorescent images of cells are shown.

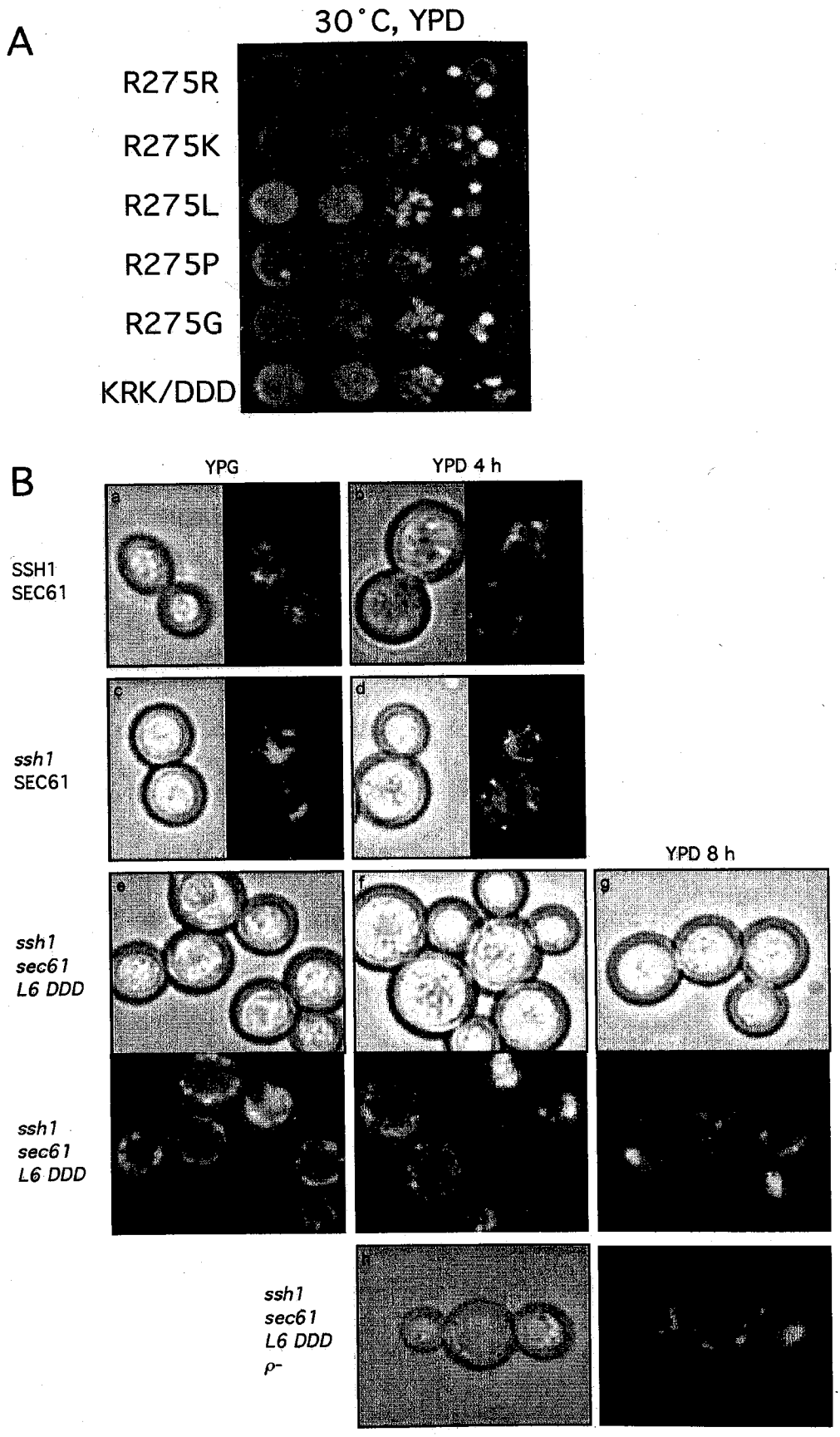
A
30°C, YPD
R275R
R275K
R275L
R275P
R275G
KRK/DDD
B
YPG
YPD 4 h
YPD 8 h
SSH1
SEC61
ssh1
SEC61
ssh1
sec61
L6 DDD
ssh1
sec61
L6 DDD
ssh1
sec61
L6 DDD
ρ-

mitochondria (Fig. 11B) (Shaw and Nunnari, 2002). Eight hours after the shift, *sec61L6DDD*, one of the most severe mutants, shows a clump-like staining of mitochondria. The changed mitochondrial morphology correlates with a loss of respiratory function (Fig. 11B, compare to ρ–) and is known to lead to a loss of mitochondrial DNA. Although the relationship between translocation defects and loss of normal mitochondria function is unclear, this phenotype was also observed for other SRP-pathway mutants (Hann and Walter, 1991; Prinz et al., 2000c). One possibility is that cytosolic accumulation of nontranslocated precursors may reduce the effective concentration of the Hsp70 chaperones that are also required for mitochondrial protein import (Deshaies et al., 1988).

Decreased growth rates correlate with protein translocation defects

RGY401 and its derivatives were maintained on SEG media to select against the accumulation of ρ^- cells. When growth rates were determined after shifting cells into YPD media, the *ssh1Δ* mutant shows a 10-20% decrease in growth rate relative to the wild type strain (Fig. 12A), which is consistent with the initial description of an *ssh1Δ* mutant (Finke et al., 1996). The *sec61R275E ssh1Δ* strain and the *sec61R406E ssh1Δ* strain showed a 2.5-fold decrease in growth rate at 30°C relative to the *ssh1Δ* strain (Fig. 12A).

The *sec61* L6 and L8 mutants were tested for defects in translocation of the SRP-dependent substrate dipeptidylaminopeptidase B (DPAPB) and the SRP-independent substrate carboxypeptidase Y (CPY). To facilitate detection of DPAPB, selected RGY401 derivatives were transformed with a low copy plasmid that encodes DPAPB-HA (Ng et al., 1996). Wild type and mutant cultures were pulse labeled with ^{35}S amino acids after cells were shifted into SD media for 0-24 h (Fig. 12B). Integration of the type II membrane protein DPAPB into the RER is accompanied by the addition of 7 to 8 N-linked oligosaccharides, resulting in an increase of

Figure 12. Translocation defects in *sec61* mutants over time. (A) Wild type yeast (RGY402, solid squares) and *ssh1Δ* mutants expressing wild type Sec61p (solid circles), *sec61R275E* (open squares) or *sec61R406E* (triangles) were grown to mid log phase at 30°C in SEG media. The cultures were diluted into YPD media at 0 h and allowed to grow for 8-12 h at 30°C. (B) Wild-type and mutants were pulse labeled to evaluate integration of DPAPB-HA after 1, 2, 4, 8 or 24 h of growth in SD media. As needed, cell cultures were diluted with fresh SD media to maintain an A_{600} of less than 0.8. DPAPB-HA immunoprecipitates were resolved by PAGE in SDS. The glycosylated (D) and nonglycosylated (p-D) forms of DPAPB-HA are labeled. (C) Integration of DPAPB-HA in wild type yeast (RGY402, filled squares) and *ssh1Δ* mutants expressing wild type Sec61p (filled circles), *sec61R275E* (triangles) or *sec61R406E* (open squares) at each time point were quantified with a BioRad FX Molecular Imager and plotted.

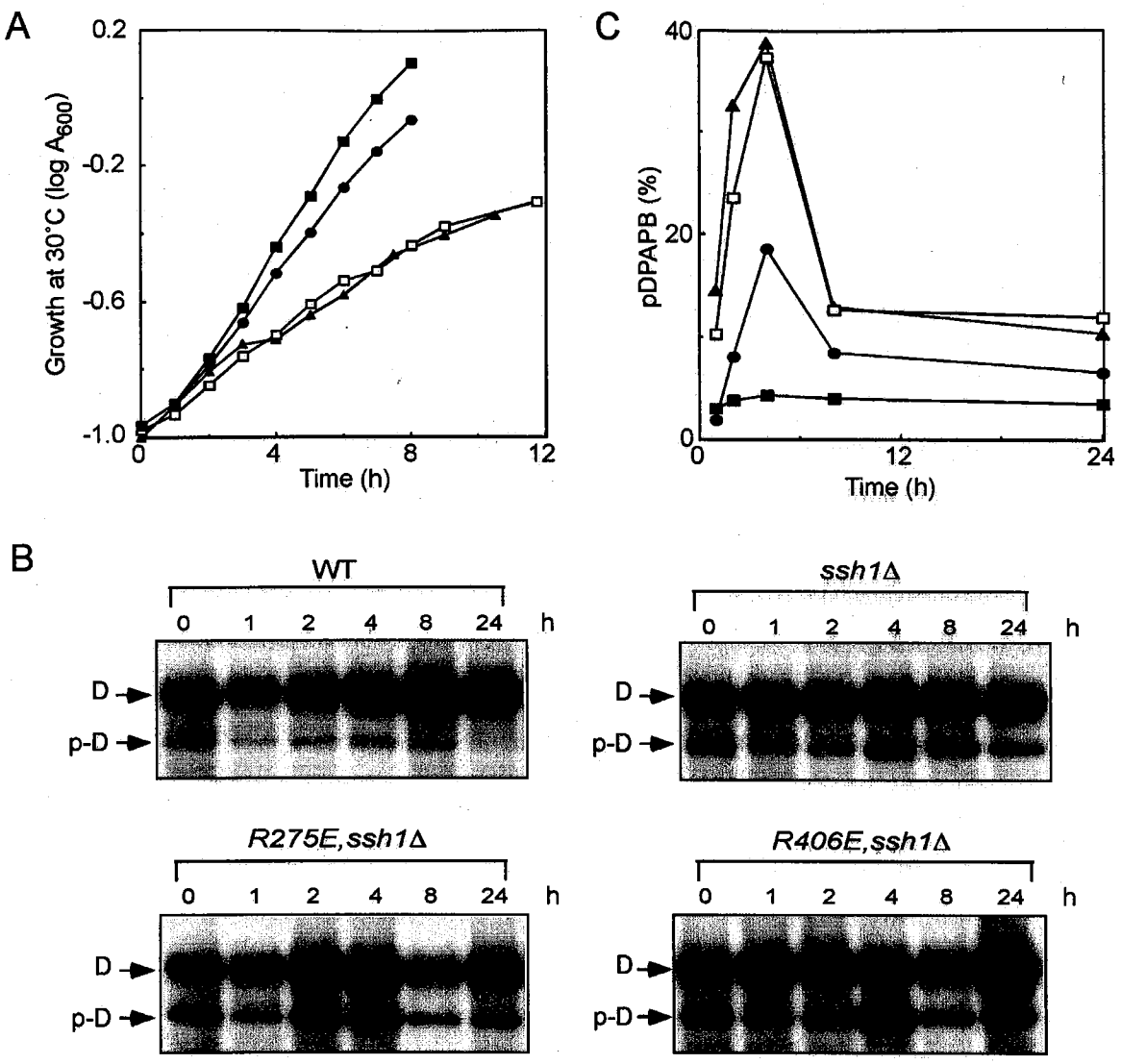
A
0.2
-0.2
-0.6
-1.0
Growth at 30°C (log A_{600})
0
4
8
12
Time (h)
C
40
20
0
pDPAPB (%)
0
12
24
Time (h)
B
WT
0 1 2 4 8 24 h
D
p-D
ssh1Δ
0 1 2 4 8 24 h
D
p-D
R275E,ssh1Δ
0 1 2 4 8 24 h
D
p-D
R406E,ssh1Δ
0 1 2 4 8 24 h
D
p-D

molecular weight from the precursor form (p-D) to the ER form (D) of DPAPB-HA (Fig. 12B). While most of DPAPB-HA was integrated into the ER in wild-type cells, a significant percentage of non-translocated DPAPB-HA was observed in *ssh1*Δ and *ssh1*Δ*sec61* mutants. The precursor percentages of DPAPB-HA were quantified and plotted in Fig. 12C. DPAPB integration in wild type cells was efficient at all time points after shift to SD media (Fig. 12C, filled squares). The quantification revealed a reduction in DPAPB translocation in the *ssh1Δ* mutant that was greatest 4 h after transfer into SD media (Fig. 12C, filled circles). Importantly, the percentage of non-translocated DPAPB (15-20% at 4 h) was 4-fold lower than previously reported for an *ssh1Δ* strain (Wilkinson et al., 2001). Transport defects for the L6 (triangles) and L8 (open squares) *sec61ssh1Δ* mutants were more significant relative to *ssh1Δ* mutant and reached a peak 4 h after cells were transferred into the SD media and declined thereafter.

The sec61 L6 and L8 mutants were then tested for translocation defects in the presence or absence of Ssh1p. Unglycosylated DPAPB-HA synthesized by tunicamycin treated cells (wt +TM) serves as a mobility marker for the non-translocated precursor (p-D) (Fig. 13A). Expression of Ssh1p suppresses the translocation defect caused by point mutations in L8 (Fig 13A), consistent with the lack of a growth defect. Non-glycosylated CPY obtained by labeling cells in the presence of tunicamycin was used as a mobility marker for prepro-CPY (Fig. 13B). As expected, there was little or no production of the Golgi (p2) or mature vacuolar forms of CPY during the 7 min pulse-labeling period. Translocation of CPY was similar in the wild type and the *ssh1Δ* strain, consistent with the observation that the Ssh1p heterotrimer is not incorporated into the Sec complex. Although point mutations in L8 do not cause a translocation defect when expressed in an *SSH1* strain, there was a substantial reduction in CPY translocation when the

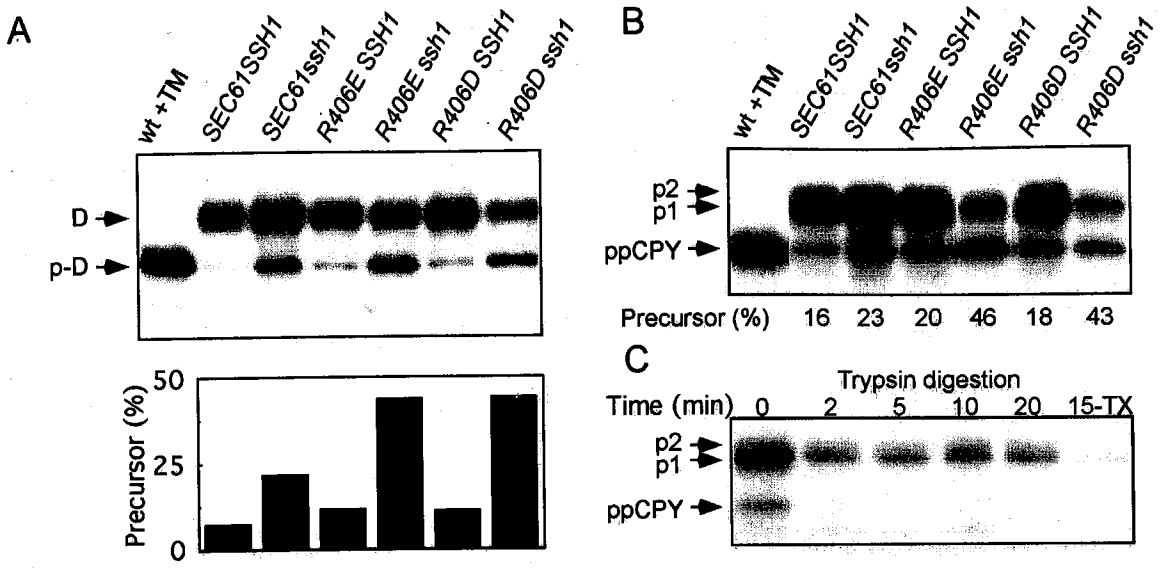

Figure 13. Translocation defects in *sec61* mutants are suppressed by expression of Ssh1p. (A, B) Wild type and mutant yeast cultures were pulse-labeled for 7 min at 30°C after 4 h of growth in SD media at 30°C. One sample of wild type cells was treated with tunicamycin (wt + TM) for 30 min prior to pulse-labeling. DPAPB-HA (A) and CPY (B) immunoprecipitates were resolved by PAGE in SDS. The ER (p1), Golgi (p2) and precursor (ppCPY) forms of CPY and the glycosylated (D) and nonglycosylated (p-D) forms of DPAPB-HA are labeled. Translocation of CPY or integration of DPAPB-HA was quantified with a BioRad FX Molecular Imager. (C) Pulse-labeled *sec61L6DDD* spheroplasts were osmotically lysed and centrifuged at 0.5Kg to remove unbroken cells. Spheroplast lysates were incubated on ice with trypsin (100 μg/ml) as indicated. The lane designated 15-TX contained trypsin plus Triton X-100. Trypsin was inactivated with PMSF prior to immunoprecipitation.

sec61 mutants were tested in the *ssh1Δ* strain (Fig. 13B). Endo H digestion experiments confirmed that the protein designated as ppCPY was the precursor, and not comigrating mature CPY (data not shown). Conceivably, a defect in N-linked glycosylation could cause the accumulation of non-glycosylated p1CPY. To address this possibility, spheroplasts prepared from the *sec61L6DDD* mutant were pulse labeled for 7 min prior to osmotic lysis. As shown in Fig. 13C, the majority of p1CPY was trypsin-resistant in the absence of detergent, unlike ppCPY which was accessible to the protease. As observed for DPAPB integration (Fig. 12C), the maximal defect in CPY translocation was observed 4 h after transfer of cells into SD media (not shown). Suppression of a CPY transport defect in the *SSH1* strain is unlikely to occur by transport of CPY through an Ssh1p translocon (Wittke et al., 2002), suggesting that reduced translocation of CPY in the L8 *sec61* mutants arises by an indirect mechanism.

A larger collection of the L6 and L8 *sec61* mutants were assayed for defects in translocation of DPAPB-HA, CPY and Gas1p (Fig. 14). Between 30 and 50% of the DPAPB was not integrated in each of the *sec61ssh1Δ* mutants that were tested. Deficiencies in CPY translocation showed significantly greater variation, with some substitutions (e.g. R275F and R275V) causing only minor defects relative to the parental *ssh1Δ* strain. A second SRP-independent substrate (Gas1p) was analyzed to determine if the L6 and L8 *sec61* mutants have defects in translocation of other substrates that utilize the posttranslational translocation pathway. The percentage of Gas1p that was not translocated during the 7 min pulse was much lower than observed for CPY. Taken together with the genetic evidence presented in Figs 9-11, these data suggest that mutations in L6 and L8 preferentially interfere with the SRP-dependent translocation pathway.

Figure 14. Differential effect of Sec61p mutations upon SRP-dependent and SRP-independent translocation pathways. Integration of DPAPB-HA and translocation of CPY and Gas1p was evaluated by pulse labeling of wild type and mutant yeast strains that were grown for 4 h in SD media at 30°C. Pulse labeling and immunoprecipitation of proteins was conducted as in Fig. 13.

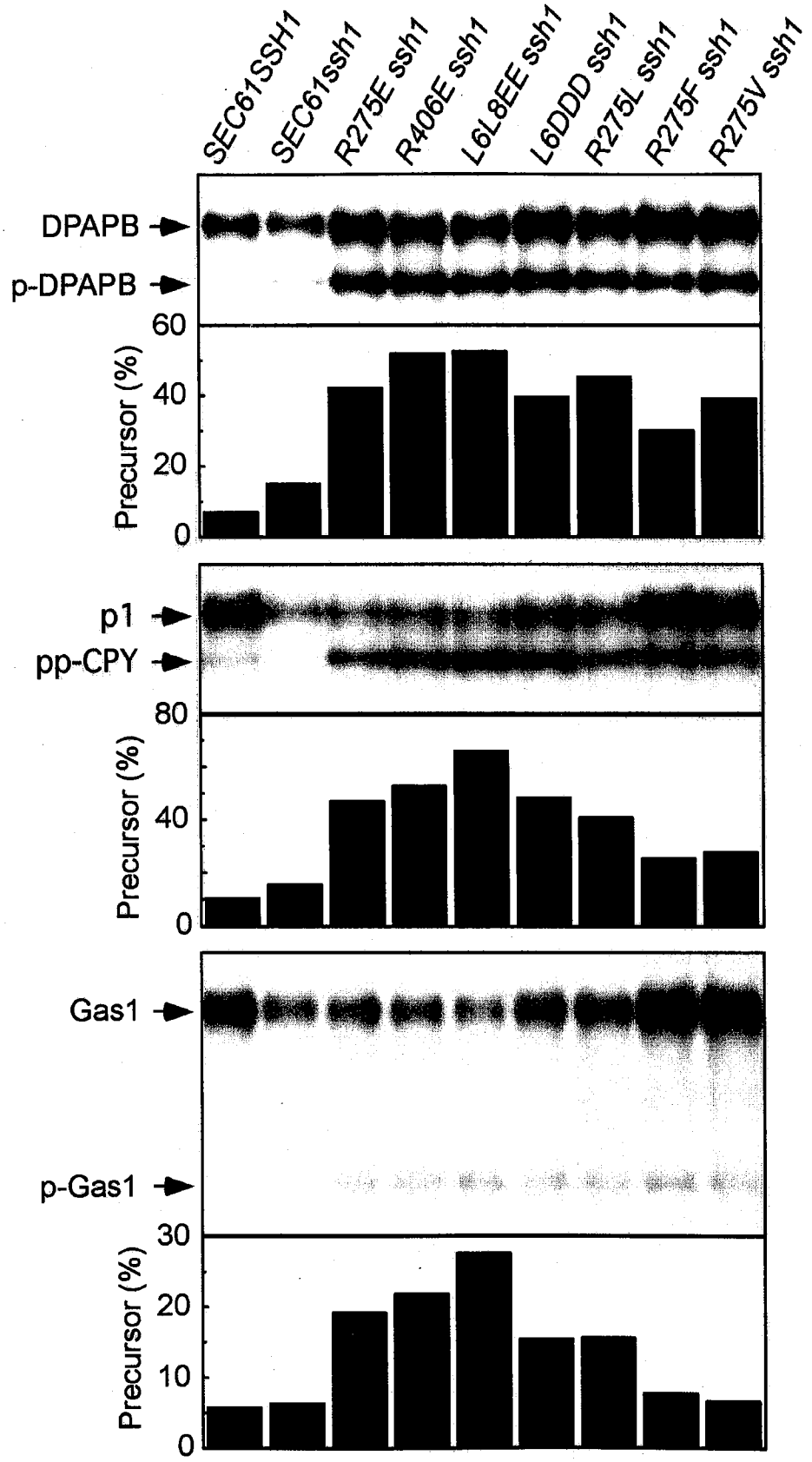
SEC61SSH1
SEC61ssh1
R275E ssh1
R406E ssh1
L6L8EE ssh1
L6DDD ssh1
R275L ssh1
R275F ssh1
R275V ssh1
DPAPB
p-DPAPB
Precursor (%)
60
40
20
0
p1
pp-CPY
Precursor (%)
80
40
0
Gas1
p-Gas1
Precursor (%)
30
20
10
0

Impact of *sec61* mutations on protein dislocation and precursor accumulation

A mutation that reduces folding of Sec61p should inhibit all protein transport pathways that are mediated by the translocon due to a reduction in the cellular content of the Sec61 heterotrimer. Identical amounts of total protein extracts of yeast cells were resolved by PAGE in SDS for a subsequent protein immunoblot using antibodies specific for Sec61p (Fig. 15A). Similar amounts of Sec61p were expressed in the wild type and L6 and L8 *sec61* mutants. Migration differences between lanes are explained by increases in the number of acidic residues in the mutant proteins. Thus, the translocation defects are not explained by a reduction in the cellular content of Sec61p.

Dislocation of unfolded proteins from the ER lumen back into the cytosol for degradation by the proteasome is thought to occur through the Sec61 complex (Wiertz et al., 1996). Degradation of the well characterized degradation substrate CPY^*_{HA} was monitored using a cycloheximide-chase procedure (Spear and Ng, 2003), as the apparent rate of dislocation determined using this method should not be perturbed by the kinetic delay in CPY^*_{HA} translocation (Fig. 15B). The p1 form of CPY^*_{HA} was degraded rapidly with a calculated half life of less than 30 min in all strains, suggesting that mutations in L6 and L8 of Sec61p do not interfere with the dislocation pathway. Mutations in gene products that are required for CPY^*_{HA} dislocation typically increase the half time of degradation to roughly 1 h (Spear and Ng, 2003).

Cytoplasmic precursors (pre-Kar2p, prepro-CPY and prepro-α factor) that are translocated through the Sec complex are readily detected by protein immunoblot analysis when *sec62* or *lhs1* mutants are analyzed at a semi-permissive temperature (Baxter et al., 1996; Hamilton and Flynn, 1996). Protein immunoblot analysis of total cell extracts prepared from the L6 and L8 *sec61* mutants revealed a single immunoreactive species for CPY (Fig. 16A). Mature

Figure 15. Sec61 stability and dislocation activity in *sec61* mutants. All experiments were conducted after 4 h of growth in SD media at 30°C. (A) Equal amounts of total protein (25 μg) were resolved by PAGE in SDS for protein immunoblot analysis using a C-terminal specific antibody to Sec61p. (B) Degradation of CPY*$_{HA}$ in L6 and L8 *sec61* mutants. Cell extracts prepared at 30 min intervals after cycloheximide addition were resolved by PAGE in SDS. Non-translocated ppCPY*$_{HA}$ and translocated p1CPY*$_{HA}$ were detected using anti-HA antibodies. Protease digestion experiments confirmed that p1CPY*$_{HA}$, but not ppCPY*$_{HA}$, was in a membrane-enclosed compartment (not shown). Protein immunoblots were quantified by densitometry. The apparent half-life ($t_{1/2}$) of p1CPY*$_{HA}$ determined according to a first order decay process is plotted below representative time courses.

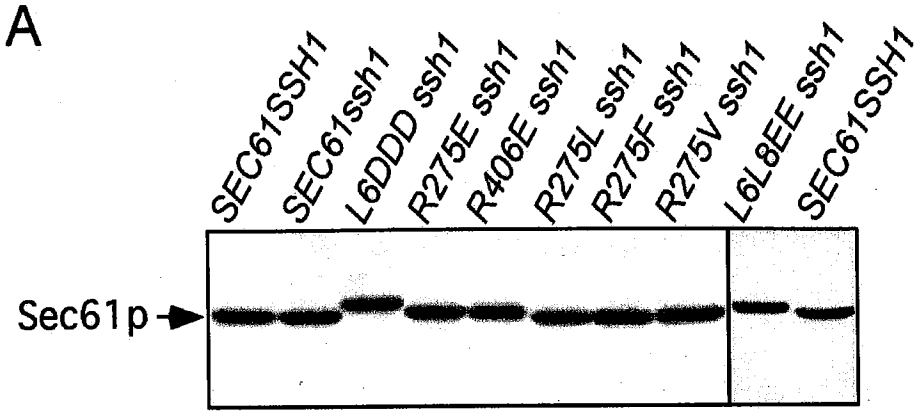
A
SEC61SSH1
SEC61ssh1
L6DDD ssh1
R275E ssh1
R406E ssh1
R275L ssh1
R275F ssh1
R275V ssh1
L6L8EE ssh1
SEC61SSH1
Sec61p

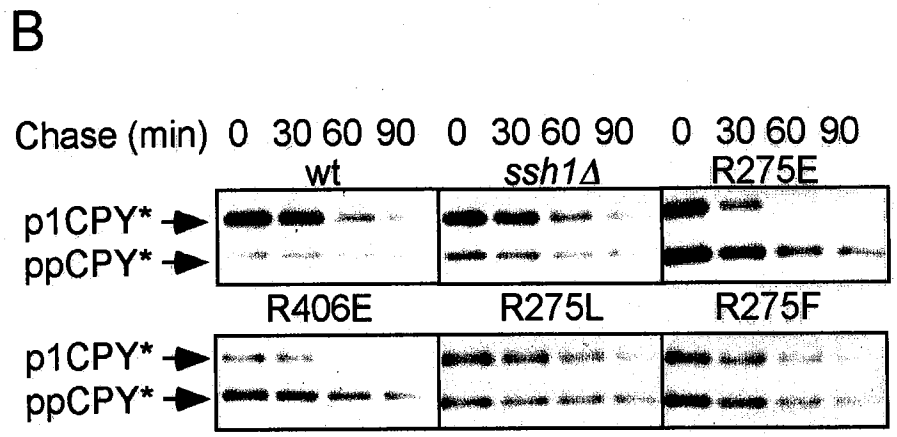
B
Chase (min) 0 30 60 90 0 30 60 90 0 30 60 90
wt
ssh1Δ
R275E
p1CPY*
ppCPY*
R406E
R275L
R275F
p1CPY*
ppCPY*

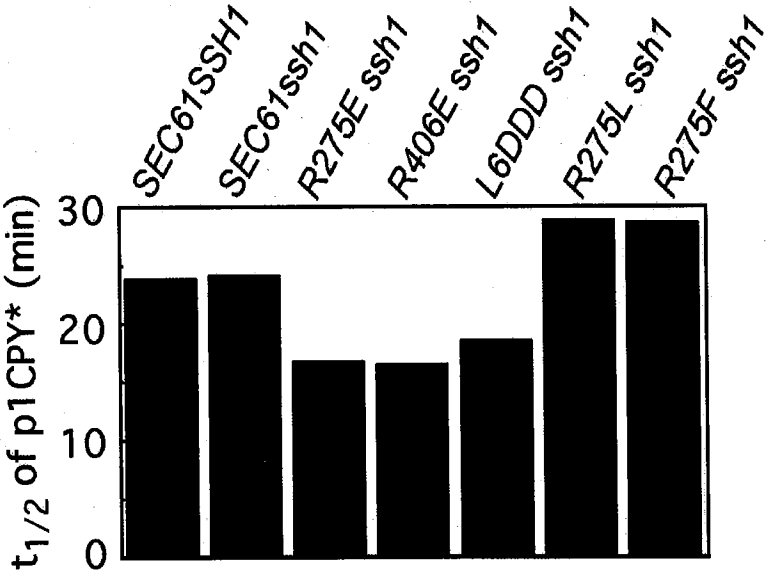
SEC61SSH1
SEC61ssh1
R275E ssh1
R406E ssh1
L6DDD ssh1
R275L ssh1
R275F ssh1
t1/2 of p1CPY* (min)
30
20
10
0

CPY comigrates with prepro-CPY due to cleavage of the propeptide in the vacuole. Deglycosylation of mature CPY with Endo H resolved prepro-CPY from deglycosylated mature CPY. Prepro-CPY was only faintly visible in the Endo H digested lanes demonstrating that the majority of the CPY precursor detected in a 7 min pulse-labeling experiment is subsequently translocated into the ER.

Additional evidence supporting a minor kinetic delay in transport of SRP-independent precursors was obtained by pulse-chase analysis of Gas1p biosynthesis (Fig. 16B). Although the Gas1p precursor was detected after the 7 min pulse, the majority of the precursor was translocated into the ER during the subsequent 10-min chase (Fig. 16B). These results suggest that there is a reduction in transport rate for precursors that utilize the Sec complex.

Protein immunoblots showed that the non-translocated DPAPB-HA precursor accumulates in the *sec61* mutants after 4 h of growth in SD media (Fig. 17A). Cellular accumulation of pDPAPB-HA was elevated 2 to 3-fold relative to the *ssh1Δ* mutant and reached a maximal value 6-8 h after the *sec61* mutants were transferred into SD media (Fig. 17B). We next asked whether the non-translocated DPAPB was soluble or membrane-associated. Differential centrifugation of spheroplast lysates achieved a partial resolution of the pDPAPB-HA from DPAPB-HA (Fig. 18A). As expected, DPAPB-HA was recovered in the P13 fraction that contains vacuoles. RER membranes, as detected using antibodies to the oligosaccharyltransferase subunit Ost1p, were enriched in the P0.5 and P13 fractions (not shown). The precursor (pDPAPB-HA) was not in the cytosol fraction (S100) but instead sedimented at low and intermediate speeds. Subsequent centrifugation of the P13 fraction on a sucrose step gradient demonstrated that the precursor was membrane associated since it did not sediment through a 1.6 M sucrose cushion (Fig. 18B). In contrast to mature DPAPB-HA, the

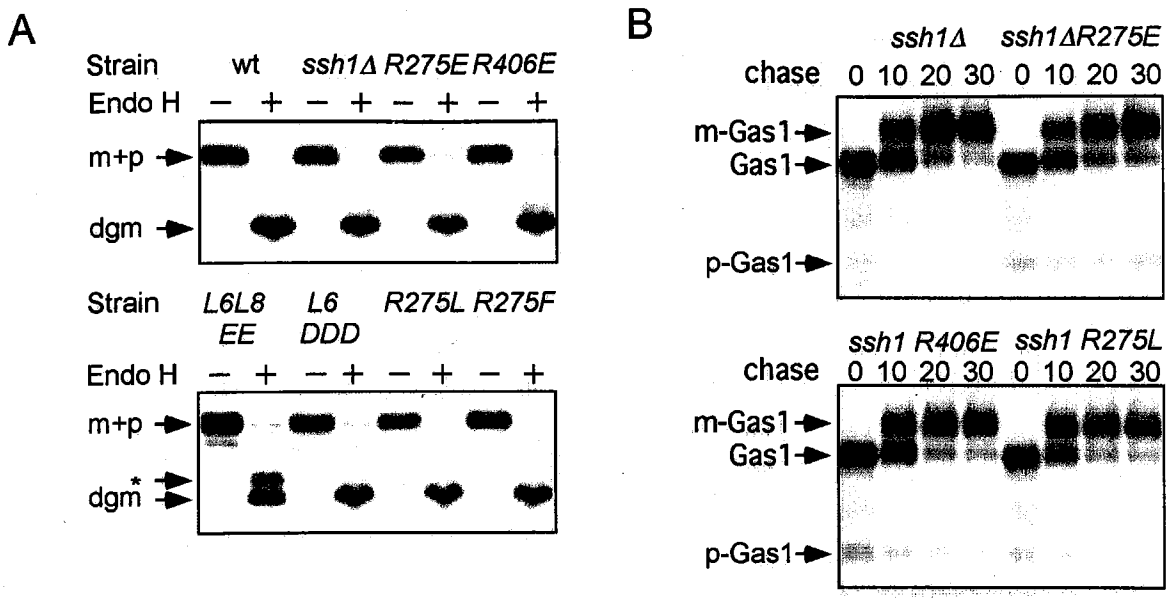

Figure 16. Kinetic delay in posttranslational translocation pathway. (A) Total cell extracts were prepared for PAGE in SDS with or without prior digestion by Endo H. Deglycosylated mature CPY (dgm) is resolved from vacuolar CPY (m) and non-translocated preproCPY (p). The asterisk designates an incomplete Endo H digestion product. (B) Yeast cultures were pulse-labeled for 7 min and chased for 10, 20 or 30 min. The non-translocated precursor (p-Gas1), the translocated ER-form (Gas1) and the mature form (m-Gas1) of Gas1p are labeled.

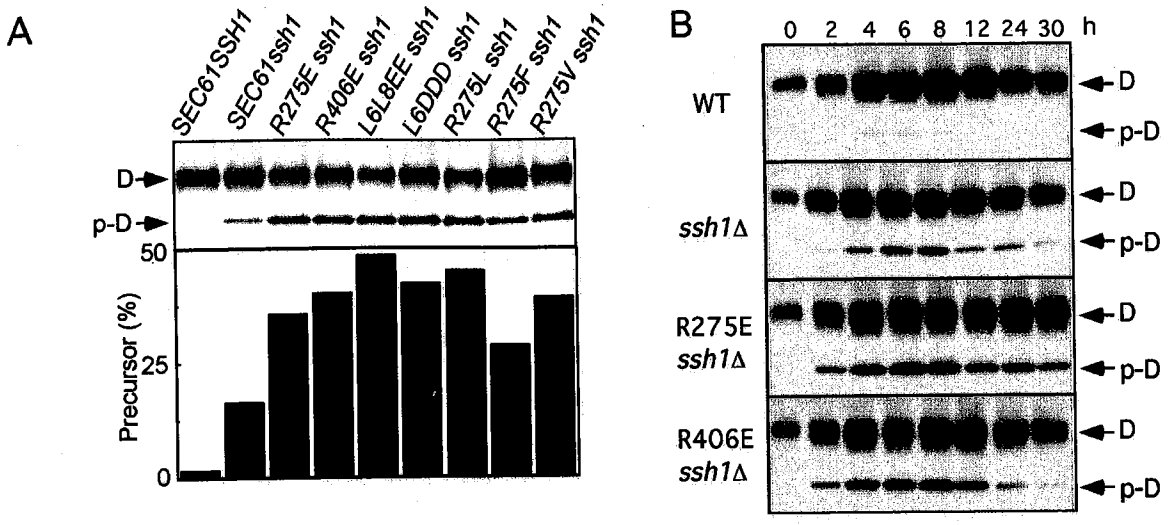

Figure 17. Precursor accumulation in *sec61* mutants. (A, B) Protein immunoblot detection of p-DPAPB-HA (p-D) and mature DPAPB-HA (D) in total cell extracts resolved by PAGE in SDS. Protein immunoblots were quantified by densitometry. Total cell extracts were prepared from wild type yeast and mutants after 4 h (A) or the designated times of growth (B) in SD media at 30°C. As needed, cell cultures were diluted with fresh SD media to maintain an A_{600} of less than 0.8.

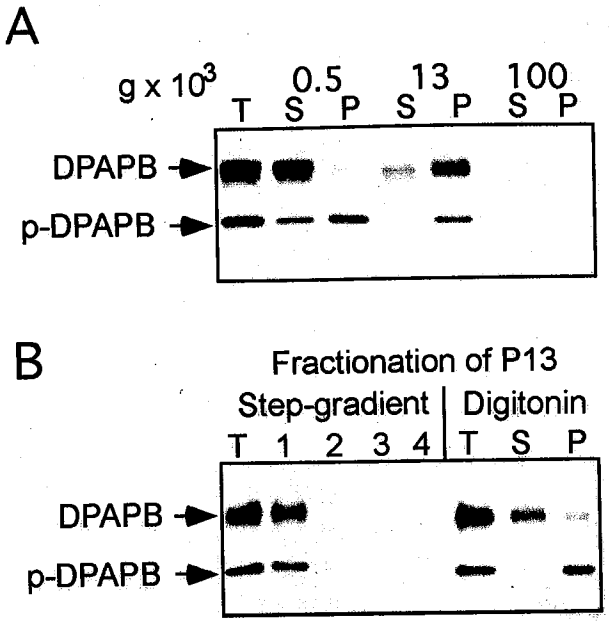

Figure 18. DPAPB precursor protein forms a membrane-associated aggregate.

(A) Differential centrifugation of spheroplast lysates prepared from the *sec61L6DDDssh1Δ* mutant. Total lysates (T), supernatant (S) and pellet (P) fractions were obtained after centrifugation at 0.5 Kg, 13 Kg and 100 Kg. (B) The P13 fraction (T) was resuspended in buffer A (50 mM Hepes pH 7.5, 150 mM KOAc, 5 mM $Mg(OAc)_2$, 1 mM DTT) adjusted to 250 mM sucrose and applied to a sucrose step gradient in buffer A with 1.6 M and 2 M sucrose layers. Following centrifugation for 1 h at 100 Kg, the gradient was resolved into the following fractions: (1) 0.25 sample load plus 0.25/1.6 M interface, (2) 1.6M sucrose layer plus 1.6/2 M interface, (3) 2 M sucrose layer, (4) pellet. The P13 fraction (T) was solubilized in 3% digitonin, 500 mM KOAc and centrifuged at 100 Kg for 1 h to obtain supernatant (S) and pellet (P) fractions.

precursor was insoluble in the non-ionic detergent digitonin (Fig. 18B), suggesting that it is incorporated into a membrane-associated aggregate. These results suggest that pDPAPB-HA molecules that are not translocated by the SRP-dependent pathway rapidly adopt a translocation incompetent conformation.

Defects in Ribosome Binding

Microsomal membranes that were isolated from the *ssh1Δ* strain as well as several L6 and L8 *sec61ssh1*Δ mutants were treated with puromycin and high salt to remove endogenous membrane bound ribosomes. The resulting ribosome-stripped microsomes (PK-RM) were assayed for ribosome-binding activity in a physiological ionic strength buffer (Fig. 19A and 19B). PK-RM prepared from the *ssh1Δ* strain bind ribosomes in a saturable manner (Fig. 19A, filled circles) with a binding affinity (K_d=5.5±0.5 nM) that is in good agreement with previous reports (Prinz et al., 2000a; Prinz et al., 2000b). The negative reciprocal of the slope of a Scatchard plot is proportional to the K_d, so a decrease in the absolute value of the slope corresponds to a decrease in binding affinity. Mutagenesis of R275 to aliphatic or acidic residues (Fig. 19A) caused a minor reduction in apparent ribosome binding affinity (R275L, K_d=13.1±0.3 nM; R275E, K_d=15.7±3.2 nM; R275V K_d=20.7±3.5 nM). The ribosome binding affinity of the triple mutant (L6DDD) was similar (K_d=17±2.6 nM), suggesting that basic residues in L6 are not the primary determinants for the ribosome-Sec61p interaction. Point mutations in L8 (Fig. 19B) that caused mild growth defects also reduced the ribosome binding affinity by 2-3 fold (K396D, K_d=18.2±1.7 nM; R406H, K_d=11.3±1.5 nM). Less conservative substitutions at R406 caused a more significant decrease in ribosome binding affinity (R406D, K_d=37.4±10.6 nM; R406W, K_d=54.2±9.8 nM; RRL6L8EE, K_d=38.2 ±7.7 nM).

The reduction in ribosome binding affinity caused by several L8 *sec61* mutations was accompanied by an apparent increase in ribosome binding sites, suggesting that the residual binding activity might be non-specific. To address this possibility, wild type and mutant Sec61 heterotrimers were purified from yeast strains expressing an affinity tagged derivative (His_6-FLAG-Sbh1p) of the Sbh1p subunit of the Sec61 complex. All three subunits of Sec61 complex were detected in the purified Sec61 complex (not shown), suggesting the stability of Sec61 complex is not affected by the affinity tag or the purification process. The ribosome binding affinity of purified Sec61 translocons was determined after reconstitution into liposomes (Fig. 19C). Proteoliposomes prepared with wild type Sec61p and a loop 6 mutant had similar binding affinities for the 80S ribosome (wild type K_d=6.5±1.7 nM; R275E, K_d=2.3±0.4 nM). In contrast, proteoliposomes prepared using *sec61* R406E or *sec61 L6L8*EE had a dramatically reduced capacity and affinity for the ribosome (Fig. 19C) even though the proteoliposomes contained comparable amounts of Sec61p (not shown). A marked reduction in ribosome binding sites in L8 *sec61* proteoliposomes suggests that dissociation of the channel into 3-4 Sec61 complexes is unlikely to be the reason for increased number of binding sites in PK-RM prepared from L8 *sec61* mutants. The Sec61p-ribosome interaction was also monitored in detergent solution using a cosedimentation assay (Prinz et al., 2000a). Wild type and mutant Sec61p heterotrimers, as detected using anti-FLAG sera (Fig. 19D) or antibody to Sec61p (not shown), were recovered in the supernatant fraction in the absence of added ribosomes. Purified wild type Sec61p heterotrimers and two different L6 mutants (R275E and R275L) quantitatively co-sedimented with ribosomes in this assay (Fig. 19D). Cosedimentation of the L8 mutant (R406E) and the L6L8 double mutant (RRL6L8EE) with the ribosome was undetectable using anti-FLAG sera

(Fig. 19D) or antibody to Sec61p (not shown). The identity of the protein or proteins responsible for the residual ribosome binding activity of PK-RM isolated from the L8 mutants is not known.

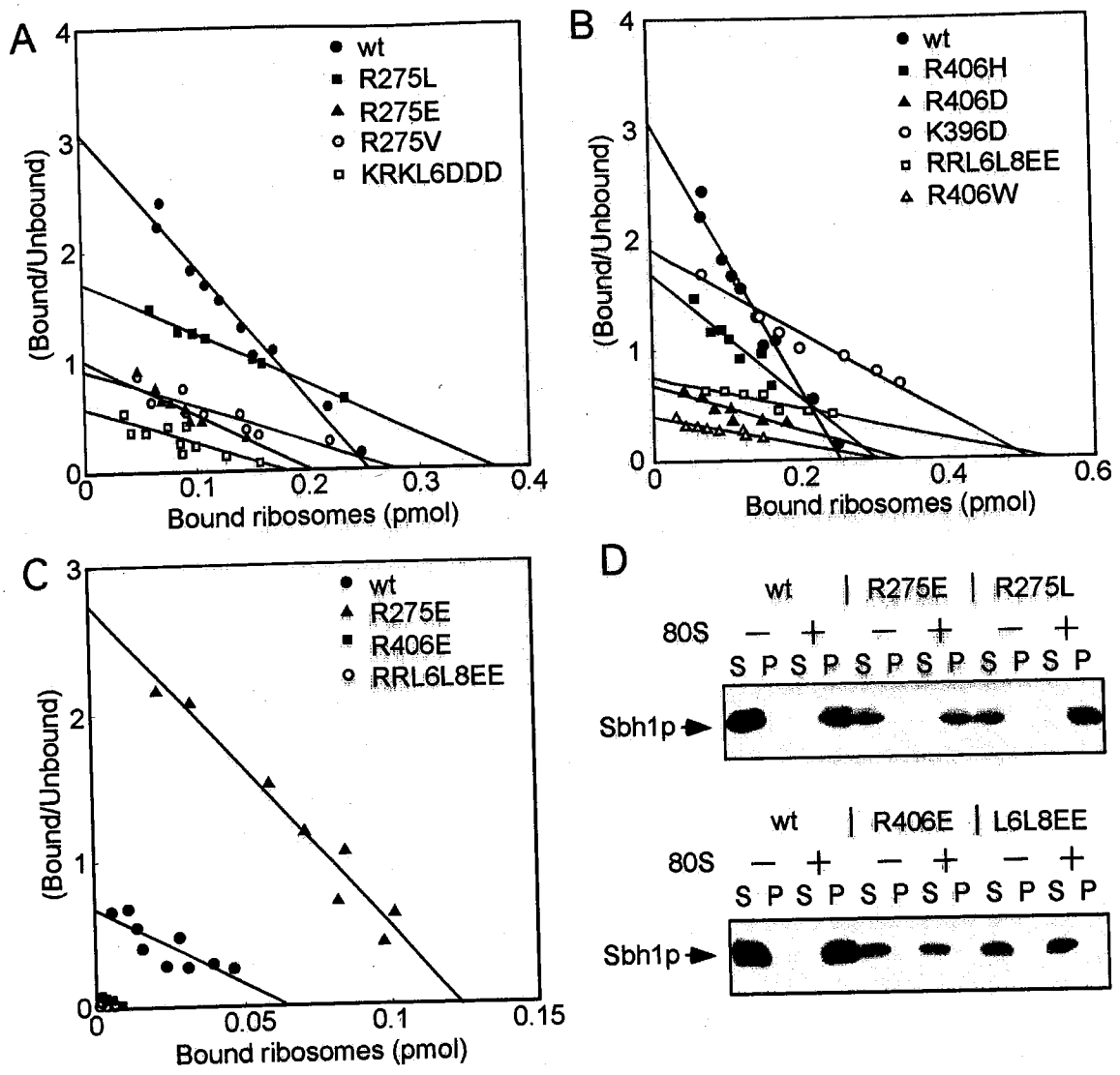

Figure 19. Binding of ribosomes to yeast PK-RM and Sec61 proteoliposomes. (A-C) Scatchard plots of ribosome binding to PK-RM (A, B) or Sec61p proteoliposomes (C) isolated from wild type (*SEC61ssh1Δ*) or L6 (A, C) and L8 (B, C) *sec61ssh1Δ* mutants. (D) Sec61 heterotrimers (150-300 fmol) purified from wild type and selected L6 and L8 mutants were incubated in the presence or absence of 900 fmol of yeast ribosomes prior to centrifugation to obtain supernatant (S) and pellet (P) fractions. Following PAGE in SDS, Sbh1p was detected using anti-FLAG antibodies.

Discussion

Isolation of a novel class of *sec61* mutants

Alleles of *sec61* that selectively interfere with the cotranslational translocation pathway have not been described previously, in part because expression of Ssh1p suppresses the growth and translocation defects. Two temperature sensitive *sec61* alleles (*sec61-2* and *sec61-3*) encode unstable proteins that are degraded at the restrictive temperature (Sommer and Jentsch, 1993), hence these mutants do not display selective defects in translocation or dislocation at the restrictive temperature (Plemper et al., 1997; Stirling et al., 1992). A screen for cold-sensitive *sec61* mutants yielded several strains (*sec61-8*, *sec61-10*, *sec61-110*) that were primarily defective in transport of substrates that utilize the posttranslational translocation pathway (Pilon et al., 1998).

Cytosolic loops of Sec61p are critical for cotranslational translocation

Mutagenesis of yeast Sec61p can be interpreted in the context of the recently solved X-ray structure of *M. jannashii* SecYEβ because the length, and to a lesser extent, the sequence of L6 and L8 are well conserved between the archae and eukaryotic translocation channels. The amphipathic H2 α-helix in SecE (γ-subunit, homologous to Sss1p) defines the interface between the membrane and the cytosol (Van den Berg et al., 2004). L6 and L8 of SecY project ~20Å into the cytosol from the presumed membrane surface (Fig. 20A). Four (K273, R275, G276 and Q277) of the five residues in L6 that were selected for mutagenesis are located at the tip of the loop between two β-strands, while the fifth residue (K284) is located near the polar head group region of the membrane bilayer (Fig. 20B). Examination of the corresponding residues (R239 and K241) in *M. jannashii* SecYEβ reveals that the positively charged side chains of K273 and R275 in Sec61p are exposed and oriented towards the cytosol. In contrast, the side chain on

A243 (Q277 in Sec61p) is oriented towards the membrane surface, which likely explains why point mutations at this site do not cause growth defects. Point mutations at G276 (G242 in *M. jannashii*) that cause growth defects in *S. cerevisiae* might do so by introducing a negative charge (G276E) or by reducing the flexibility of L6 (e.g. G276P). G276 may be important for the conformation of the seven-residues loop connecting two β strands in L6.

Four of the eight residues selected for mutagenesis in L8 of Sec61 are located in the tip of a loop that connects two α-helical segments (Fig. 20B). The importance of K405 and R406 in Sec61p is readily explained by the orientation and location of the corresponding side chains (F359 and K360) in *M. jannashii* SecY (Fig. 20B). Interestingly, replacement of K405 with phenylalanine (as in *M. jannashii* SecY) did not cause growth or translocation defects (not shown) indicating that basic or bulky hydrophobic residues are tolerated at this site. The top view of SecYEG shows that the side chains of four residues in L8 (R389, D390, K393, E407) that did not cause growth defects upon mutagenesis (Fig. 20C, yellow side chains) are closer to the membrane surface and directed away from the proposed translocation pore in the SecY subunit (Van den Berg et al., 2004). When viewed from the top, the critical residues in L6 and L8 are in three separate clusters separated by 15-20 Å (Fig. 20D).

Point mutations in L6 and L8 of Sec61p interfere with RNC transfer to the translocation channel

How might single amino acid substitutions in L6 and L8 of Sec61p interfere with translocation of SRP-dependent substrates? The non-additive nature of the translocation defects displayed by the RRL6L8EE *sec61* mutant suggests that the R275E and R406E mutations affect different steps in a single pathway, not parallel pathways, leading to cotranslational translocation of SRP-dependent substrates. Attachment of a ribosome-nascent chain complex to the

Figure 20. Point mutations in L6 and L8 define a contact surface for cytoplasmic ligands of the Sec61 complex. (A) A ribbon diagram of SecYEG complex showing the three subunits (SecY, green; SecE, cyan and SecG, magenta) as viewed from within the plane of the membrane. The L6 (blue) and L8 (white) regions in SecY are highlighted. The SecY residue that aligns with a Sec61 residue subjected to mutagenesis is designated by a colored side chain; mutagenesis of red, but not yellow, side chains caused growth defects. (B) An expanded view of panel A showing that the critical residues in Sec61p are located at the tips of L6 and L8. (C) A top-view of the SecYEG complex. The subunits, loops and mutagenized residues are colored as in A. The dimerization interface for the SecYEG complex is formed by the TM span of SecE (cyan chain). The asterisk designates the proposed translocation pore in SecYEG that is plugged by the short TM2a helix. (D) An expanded top-view of the L6 and L8 regions. SecE is hidden to simplify the image. The figure was created with MacPyMOL software using SEC YEG structure (PDB 1RHZ).

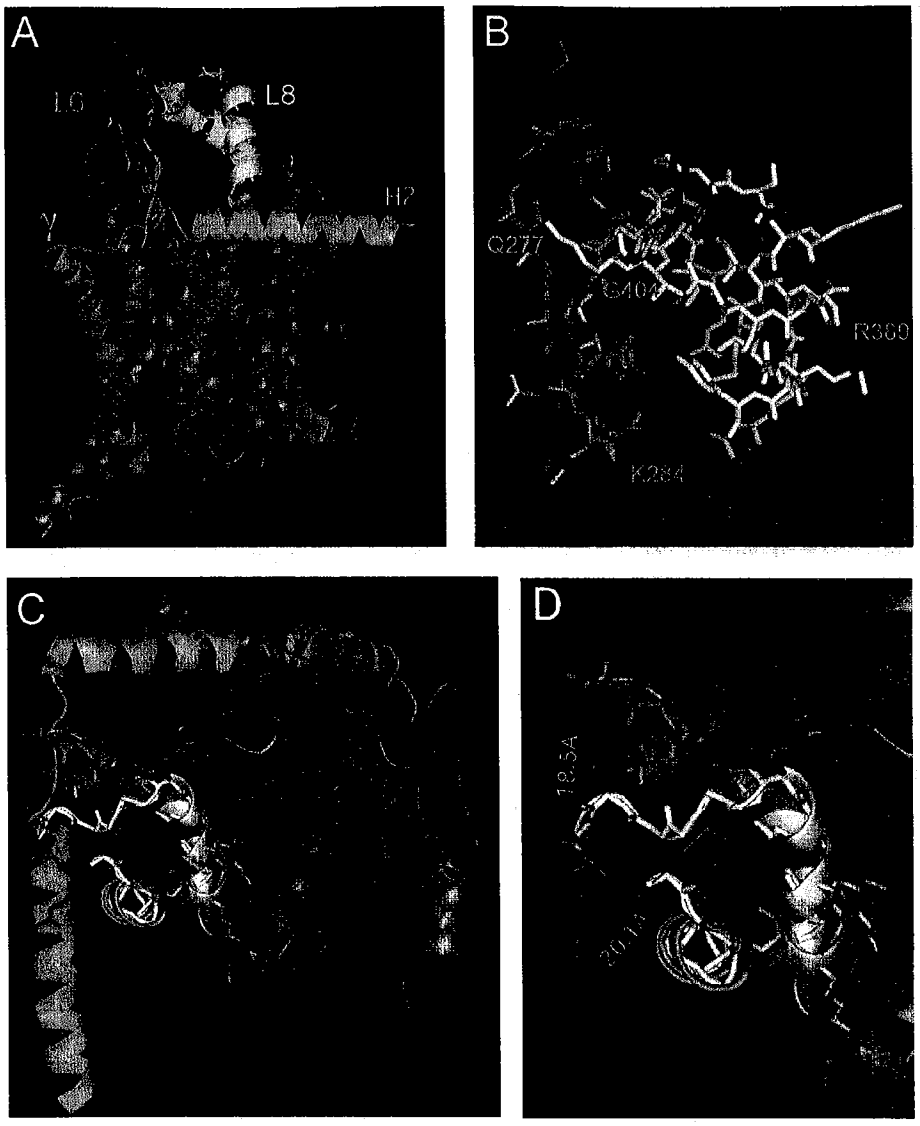
A
L6
L8
H2
γ
B
Q27
G404
R360
K284
C
D
1.85Å

translocation channel is a multi-step process that is regulated by the SRP and SR GTPases and is dependent upon critical interactions between Sec61p, the ribosome and the signal sequence (Jungnickel and Rapoport, 1995; Song et al., 2000). There are at least two steps in this reaction pathway that are likely dependent upon cytoplasmic segments of the Sec61 complex. The two steps correspond to recognition of an unoccupied translocon by a post-targeting intermediate, and docking of the ribosome onto the channel. A stable post-targeting intermediate (SR-SRP-RNC complex) is formed when SRP-RNCs are incubated with microsomes or proteoliposomes that lack a functional Sec61 complex (Song et al., 2000). The binding sites for SRP54 on the large ribosomal subunit overlap with the Sec61 binding sites, hence SRP must dissociate from the ribosome prior to Sec61 attachment (Halic et al., 2004). Previously we proposed that a direct interaction between the post-targeting intermediate and a vacant Sec61 complex facilitates transfer of the RNC to the translocation channel following dissociation of SRP54 from the signal sequence (Song et al., 2000). Cytosolic loops of Sec61p would be the optimal marker for an unoccupied translocon, as these segments will be occluded upon attachment of a ribosome to the translocation channel (Morgan et al., 2002). Residues in L6 of Sec61p are excellent candidates for such a recognition determinant, as point mutations in L6 (e.g. R275E) interfere with the cotranslational protein translocation pathway without causing a significant reduction in ribosome binding affinity. Although current models for the cotranslational translocation pathway typically depict an interaction between the SR and the Sec61 complex, biochemical evidence to support this conjecture is scant. Study of the interaction between residues in L6 of Sec61p and SRP, the SR or a translating ribosome may reveal how the L6 mutants affect the cotranslational translocation pathway.

An analysis of RNC-translocon interactions (Jungnickel and Rapoport, 1995) has indicated that the initial binding of an RNC to the Sec61 complex is sensitive to salt, and precedes signal sequence insertion into the translocation pore. Point mutations that reduce the affinity between the translocation channel and the ribosome should reduce the efficiency of RNC attachment to the translocon by destabilizing this intermediate. RNCs can bind to protease-inactivated Sec61 complexes that lack detectable affinity for non-translating ribosomes (Raden et al., 2000), hence signal sequence insertion into the translocation pore is not obligatorily dependent upon intimate ribosome-channel contact. This may explain why certain point mutations in L8 (R406E) do not cause a complete block in the cotranslational translocation pathway. Three-dimensional EM reconstructions of the ribosome-Sec61 complex and the RNC-Sec61 complex have revealed the presence of a 15Å gap between the channel and the ribosome which is bridged by four stalk-like connections (Beckmann et al., 2001; Morgan et al., 2002). Four connections per translocon would be consistent with the presence of three to four Sec61 heterotrimers per channel and this would imply that a single structural element in Sec61p forms the stalk-like connections. Notably, the diameter of the ribosome-channel connections observed by electron microscopy (~20Å (Morgan et al. 2002)) is very similar to the diameter of the SecY domain formed by the L6 and L8 loops (Fig. 20C). Contact points on the ribosome for the Sec61 complex correspond to several large subunit proteins (L25, L26 and L35) and specific 25S rRNA segments (Beckmann et al., 2001; Morgan et al., 2002). Inhibition of ribosome binding to the mammalian Sec61 complex by the canine 28S rRNA, but not by the 18S rRNA, supports the conclusion that specific protein-rRNA contacts contribute to the evolutionarily conserved binding of the ribosome to Sec61p/SecY (Prinz et al., 2000a). Here, we observed that point mutations in surface exposed residues in L8 cause dramatic reductions in ribosome-binding

activity, suggesting that salt bridges between the basic side chains on Sec61p and the phosphodiester backbone of the 25S rRNA are critical for ribosome attachment. The Sec61 channel is likely formed by three to four Sec61 complexes. Oligomerization of three to four Sec61p complexes in the channel may provide a high affinity binding site for the ribosome. Simultaneous loss of three to four basic residues in the binding sites may explain how a single amino acid substitution in L8 causes a dramatic reduction in ribosome-binding activity.

Extensive mutagenesis of *E. coli* SecY has shown that R357 (R406 in Sec61p) is a crucial residue for the translocation activity of SecYEG (Mori and Ito, 2001). Suppression of the translocation defect of the *E. coli* SecY R357E mutant by "superactive alleles of SecA" has been interpreted as evidence that a functional SecA binding site maps to the C5 region (L8) of SecY. However, other SecY point mutations (A363T) in L8 selectively interfere with the Ffh/FtsY dependent integration of inner membrane proteins (Newitt and Bernstein, 1998). Clearly, this region of the translocation channel is an evolutionarily conserved segment that is critical for interaction with cytosolic effectors of the translocation pathway.

Secondary defects in posttranslational translocation

Kinetic delays in transport of the SRP-independent substrates CPY and Gas1p were observed when the *sec61* mutants were grown in rich media. Expression of Ssh1p eliminates the posttranslational transport defects caused by the *sec61* mutants suggesting that cytosolic accumulation of SRP-dependent substrates interferes with one or more steps in the posttranslational targeting pathway. Accumulation of non-translocated precursors in the cytosol may reduce the effective concentration of Hsp70 chaperones that deliver precursors like preproCPY to the Sec complex. Posttranslational translocation via the Sec complex of substrates

that are normally transported by a cotranslational pathway could also cause kinetic delays in transport of posttranslational substrates by increasing precursor flux through the Sec complex.

Shared phenotypes with SRP pathway mutants

A comparison of the phenotypes of the L6 and L8 *sec61* mutants with those described for SRP targeting pathway mutants is informative. The 4-5 fold decrease in growth rate that is caused by repressing expression of SRP54 or SRα in *S. cerevisiae* (Hann and Walter, 1991; Ogg et al., 1992) is more severe than the 2-3 fold reductions in growth rate that are caused by point mutations in the cytosolic loops of Sec61p. The simplest interpretation of this difference is that point mutations in L6 and L8 do not eliminate the SRP-dependent targeting of RNCs to the RER, but instead interfere with the efficient transfer and attachment of the RNC to the translocation channel. The rate at which the L6 and L8 *sec61* mutants acquire a petite phenotype is less pronounced than the rapid and complete conversion of *srp54Δ* strains to a ρ- phenotype (Hann and Walter, 1991). Although the mechanistic link between a defect in cotranslational protein translocation and subsequent loss of mitochondrial respiration remains undefined, the morphologies of the cortical ER and the mitochondria are grossly perturbed when temperature sensitive SRα mutants are shifted to the restrictive temperature (Prinz et al., 2000c). Here we also observed an alteration in mitochondrial morphology when the *sec61* L6 and L8 mutants were shifted from SEG media to SD media. A third characteristic of the L6 and L8 *sec61* mutants is the transient nature of the translocation defect. Gene product depletion experiments using the GAL1/GAL10 promoter have shown that repression of SRP54 or SRα synthesis is accompanied by a severe, yet transient defect in translocation of SRP-dependent substrates (Hann and Walter, 1991; Ogg et al., 1992). Adaptation of yeast cells to the elimination of the SRP-dependent targeting pathway occurs by induction of cytosolic chaperones and reductions in

the protein synthesis rate (Mutka and Walter, 2001). The L6 and L8 *sec61* mutants described here likely adapt by a comparable mechanism.

CHAPTER IV

Cytosolic exposure of transmembrane spans and lumenal domains during in vivo integration of membrane proteins

Introduction

Membrane protein integration into the endoplasmic reticulum (ER) is more complex than secretory protein translocation because the nascent polypeptide has domains that are ultimately exposed to the phospholipid bilayer in addition to the ER lumen and cytosol. Recognition of the first transmembrane (TM) span by the signal recognition particle (SRP), targeting of the SRP-ribosome nascent chain complex (RNC) to the SRP receptor (SR) and GTP-dependent delivery of the RNC to the protein translocation channel occur by reactions that are analogous to those characterized for secreted proteins (Do et al., 1996; Heinrich et al., 2000; Wilson et al., 1988). The final topology of membrane protein integration is determined by the insertion orientation (N_{cyt}- C_{lum} or N_{lum}- C_{cyt}) of the initial TM span, which is influenced by the charge distribution of the flanking residues (Beltzer et al., 1991) in accord with the "positive inside" rule (Hartmann et al., 1989). In addition, integration in the type I topology (N_{lum}- C_{cyt}) is favored for unusually long hydrophobic TM spans (Wahlberg and Spiess, 1997), while rapid folding of an N-terminal domain that precedes the first TM span favors a type II (N_{cyt}- C_{lum}) orientation (Denzer et al., 1995).

Site-specific incorporation of photoactivatable amino acid analogues (Heinrich et al., 2000; Heinrich and Rapoport, 2003; McCormick et al., 2003; Mothes et al., 1997; Sadlish et al., 2005) or fluorescent reporters (Haigh and Johnson, 2002; Liao et al., 1997; Woolhead et al., 2004) into nascent membrane proteins that are encoded by termination codon-deficient mRNA molecules has allowed an in vitro mechanistic analysis of membrane protein integration.

Photocrosslinking experiments have shown that the Sec61 heterotrimer has a primary binding site for a TM span (Heinrich and Rapoport, 2003; Sadlish et al., 2005) that is now thought to be identical to the signal-sequence binding (SSB) site formed by TM2b and TM7 of Sec61p (Plath et al., 1998). The X-ray crystal structure of the closed-conformation of the M. *jannaschii* SecYEβ complex (Van den Berg et al., 2004) suggests that the lumenal domain of a type II membrane protein is threaded through an hourglass-shaped transport pore in Sec61, while the TM span occupies the SSB site adjacent to the lateral gate of the translocon that is formed by TM2b, TM3, TM7 and TM8 of Sec61 (Rapoport et al., 2004). Prior to nascent chain termination the TM span exits the SSB site to enter an environment where it contacts phospholipids, Sec61α and in some cases the TRAM protein (Heinrich et al., 2000; McCormick et al., 2003). Integration of a membrane protein with two or more TM spans is considerably more complex, as individual TM spans must sequentially move from the transport pore to the SSB site, and exit through the lateral gate of the channel into the membrane bilayer (Heinrich and Rapoport, 2003; Sadlish et al., 2005). Conformational changes in the Sec61 heterotrimer that facilitate the lateral moment of TM spans between these three distinct environments and mediate the gating of the lumenal transport pore in SecY/Sec61p/Sec61α are not well understood. Three-dimensional reconstructions of eukaryotic ribosome-channel complexes are of insufficient resolution to provide structural details concerning the open conformation of a Sec61 heterotrimer (Beckmann et al., 2001; Morgan et al., 2002).

Photocrosslinking analysis of in vitro-assembled integration intermediates does not yield kinetic information about the mechanism of membrane protein integration because reporter photoactivation typically occurs minutes to hours after polypeptide elongation is complete. Consequently, the environment detected by the fluorescent reporters or photocrosslinking probes

may represent an equilibrium distribution of accessible endpoints, rather than the most probable probe location during elongation of the polypeptide. The accessible endpoints are defined by the length, in amino acid residues, and conformation of the nascent polypeptide between the reporter group and the peptidyl-transferase site on the ribosome. Based upon the possibility that one or more steps in membrane protein integration could be slow relative to the in vivo rate of protein synthesis, we employed an experimental approach that would provide in vivo kinetic information during integration of membrane proteins. Ubiquitin translocation assay (UTA) reporters were first developed by Johnnson and Varshavsky (1994) to analyze the in vivo kinetics of protein translocation in yeast. Here, we have used UTA reporters derived from the type II membrane protein dipeptidylaminopeptidase B (DPAPB) to investigate the in vivo kinetics of integration of DPAPB and model polytopic membrane proteins.

Results

UTA reporters for membrane protein integration

The ubiquitin translocation assay (UTA) reporters consist of a signal sequence, a spacer segment, an Ub domain, a linker sequence and a reporter domain (Fig. 21A). Rapid cotranslational folding of the Ub domain permits cleavage after Gly76 (Fig. 21A, arrow) by Ub-specific proteases (UBPs) to liberate the reporter domain in the cytosol (Johnsson and Varshavsky, 1994). If polypeptide transport through Sec61p initiates before the Ub sequence emerges from the ribosome, folding of the Ub domain will not occur in the cytosol hence the reporter will not be cleaved. Since a folded Ub domain blocks reporter transport through the translocon even when the UBP processing site is deleted (Johnsson and Varshavsky, 1994), reporter cleavage does not need to be cotranslational. Partitioning of nascent polypeptides between the cotranslational and posttranslational translocation pathways in the yeast *S. cerevisiae* is governed by the relative hydrophobicity of the signal sequence (Ng et al., 1996), with SRP selecting proteins with more hydrophobic signals for transport by the cotranslational pathway. Three factors that influence the efficiency of UTA reporter cleavage are therefore the hydrophobicity of the signal sequence, the length of the spacer segment and mutations in gene products (e.g. SRP54) that mediate the cotranslational targeting pathway (Johnsson and Varshavsky, 1994). UTA reporters derived from proteins that are translocated by the posttranslational targeting pathway are cleaved efficiently in vivo regardless of the spacer length (Johnsson and Varshavsky, 1994) (Fig. 21B, III). In contrast, reporter cleavage decreases as the spacer length is increased for UTA reporters that are targeted as RNCs by SRP to the Sec61 complex (Fig. 21B, I and II). A long spacer allows translocon gating by RNCs to occur before

Figure 21. The ubiquitin translocation assay (UTA) reporters can be used to monitor the in vivo kinetics of protein translocation. (A) The five elements in a UTA reporter are: (a) a signal sequence, (b) a spacer segment, (c) an Ub domain, (d) a linker sequence and (e) a reporter domain. Rapid folding of the Ub domain permits cleavage after Gly76 (arrow) by cytosolic Ub-specific proteases (UBPs) to liberate the reporter domain in the cytosol. (B) Processing of the UTA reporter depends on the signal sequence and the length of spacer. If RNC gating of the Sec61 complex occurs before the Ub domain has emerged from the ribosome, folding of the Ub domain will not occur in the cytosol. Reporter cleavage decreases as the spacer length is increased for UTA reporters that are targeted as RNCs by SRP to the Sec61 complex (compare I and II). In contrast, UTA reporters that contain signal sequences from proteins that are translocated by the posttranslational targeting pathway (III) are cleaved efficiently in vivo regardless of the length of the spacer (Johnsson and Varshavsky, 1994).

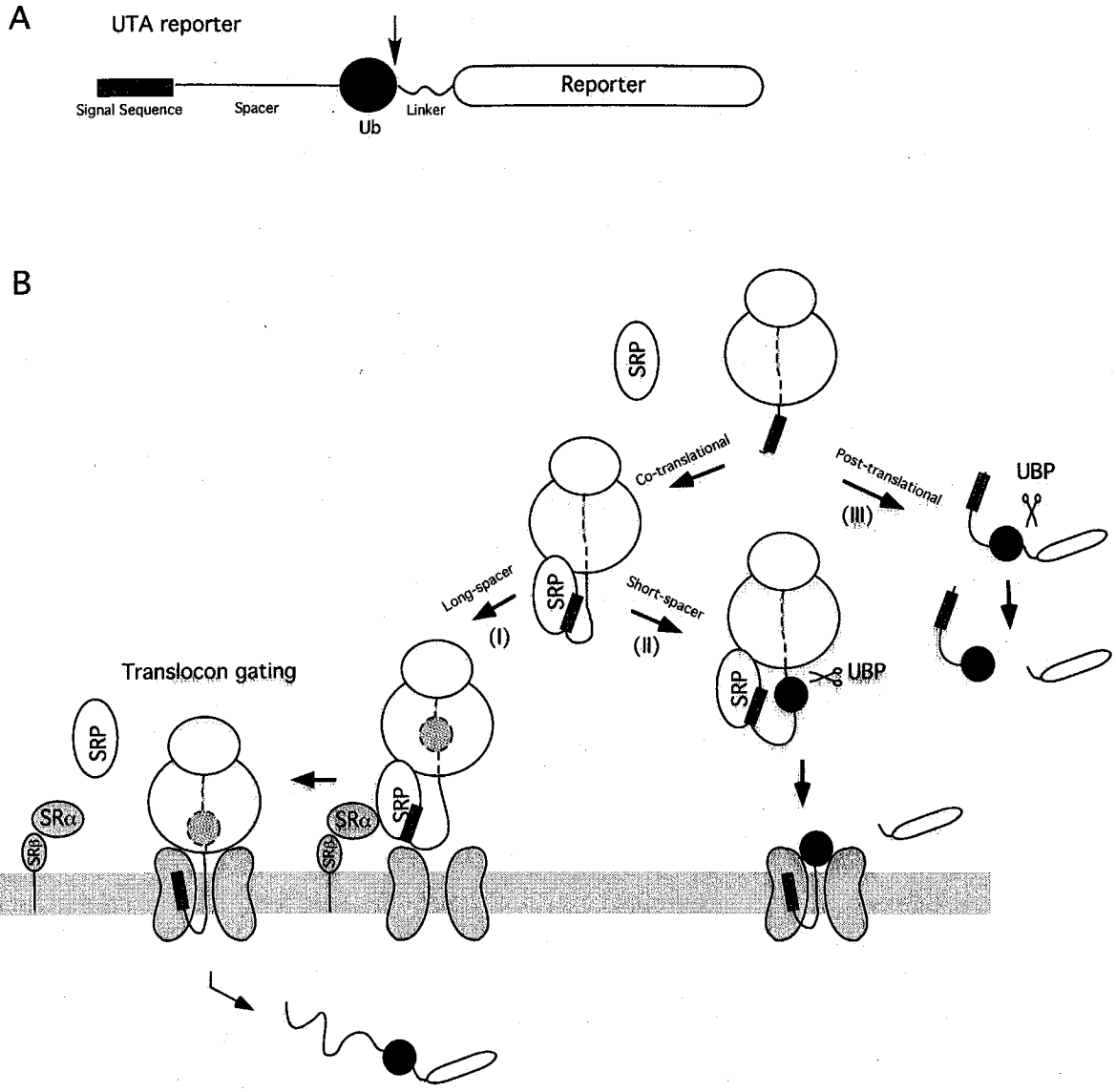
A
UTA reporter
Signal Sequence
Spacer
Ub
Linker
Reporter
B
SRP
Co-translational
Post-translational
(III)
UBP
Long-spacer
(I)
Short-spacer
(II)
Translocon gating
SRα
SRβ

the Ub domain emerges from the ribosome. In this study, the in vivo kinetics of translocon gating is studied using UTA reporters with different spacer lengths.

The signal and spacer segments of the DPA series of UTA reporters (Fig. 22A) consist of 94 to 310 residues of DPAPB sequence, with the reporter name (e.g. DPA49) designating the length of the spacer segment between the TM span of DPAPB (residues 30-45) and the N-terminal residue of the Ub domain. Point mutations (I3G and I13G) were introduced into the Ub domain to produce a previously characterized folding-defective mutant (ub*) to determine whether DPA49 is integrated in the Type II (N_{cyt}- C_{lum}) topology. Since folding of the Ub domain is a prerequisite for UBP cleavage (Johnsson and Varshavsky, 1994), integrated and non-integrated forms of intact DPA49-ub* can be immunoprecipitated with anti-HA antibodies from pulse-labeled yeast cells (Fig. 22B). Cultures labeled in the presence of glycosylation inhibitor tunicamycin (Tm) provide a marker for the unglycosylated (49*) reporter. The majority (92%) of DPA49-ub* was glycosylated at both N-X-T/S sites (Fig. 22B) indicating that the reporter is integrated as a type II (N_{cyt}-C_{lum}) membrane protein.

Wild-type yeast and *ssh1*Δ mutants expressing wild-type Sec61p or the *sec61* L6 and L8 mutants were transformed with DPA series of UTA reporters. Wild-type and mutant cultures were grown in SEG media to mid-log phase, and pulse labeled with ^{35}S- amino acids 4 h (Fig. 22C-E) or 24 h (not shown) after cells were shifted into SD media. As shown here for DPA49, DPA103 and DPA149 (Fig. 22C- E, wt), glycosylated intact (g49, g103, g149) and proteolytically cleaved (U-HA) forms of the reporter were detected upon expression in wild type yeast. Quantification of reporter cleavage (Fig. 23B, filled squares) revealed a striking dependence upon the length of the spacer segment. Little intact reporter (< 20%) was detected when DPA49 was tested, while insertion of longer spacer segments (DPA149 or DPA265) did

not significantly reduce cleavage below that observed for DPA103. The gating window is defined as the minimal spacer length required for reporter cleavage to decrease to the plateau value. At this spacer length the majority of the reporters from the ribosome have gated the translocon before the Ub domain emerges. For most DPA RNCs, gating of the Sec61 channel occurred as the spacer was increased from 49 to 94 residues. The plateau value for DPA cleavage (28%) was greater than the percentage of non-integrated DPA49-ub*, hence roughly 20% of the DPA reporters are integrated by a posttranslational pathway. If translocon gating does not occur before the nascent polypeptide reaches a critical length, the nascent chain enters the posttranslational targeting pathway.

Kinetic delays in translocon gating in *sec61* mutants

How do mutations in protein translocation components affect the kinetics of the RNC targeting and translocon gating steps for DPA RNCs? A rapid and complete blockade of the SRP-targeting pathway can be achieved by shifting a temperature sensitive SRP receptor mutant (*srp102*K51I, (Ogg et al., 1998)) to the restrictive temperature (37°C). As shown in Fig. 23A, translocation of DPAPB in the *srp102* mutant is blocked at the restrictive temperature. Cleavage of the DPA265 reporter in the *srp102* mutant was virtually complete at 37°C (Fig. 23A, 23B closed diamond) but not at 25°C (Fig. 23A, 23B open diamond).

The pulse-labeling experiments revealed an increase in the reporter cleavage as well as traces of the unglycosylated forms of the reporters in the *ssh1*Δ strain (Fig. 22C-E). Elimination of the auxiliary Ssh1p translocon (e.g. *ssh1ΔSEC61*) increased the plateau value for reporter cleavage consistent with a decrease in the number of protein translocation channels (Finke et al., 1996). However, elimination of Ssh1p translocons did not significantly delay translocon gating by the DPA RNCs (Fig. 23B, closed circles). Point mutations in the cytoplasmic loops of

Figure 22. Kinetics of DPA reporter integration. (A) The DPA series of UTA reporters contain the following five elements: (a) the N-terminal cytoplasmic domain of DPAPB (gray box, DPA_{1-29}); a TM span (black box, DPA_{30-45}); (b) 49-265 residue spacer segments (diagonal hatch) derived from the lumenal domain of DPAPB; (c) a Ub domain; (d) a 42 residue linker (vertical hatch) with a processing site (arrowhead) for a Ub-specific protease; (e) Ura3p with a triple-HA tag (stippled box). Sites for N-linked glycosylation (Y) are indicated. (B) Wild-type yeast expressing a folding-impaired reporter (DPA49-ub*) were pulse labeled in the presence or absence of tunicamycin (Tm). HA-immunoprecipitates were resolved by SDS-PAGE. Glycosylated (g49*) and non-glycosylated (49*) DPA49-ub* are indicated by labeled arrows. The percent integration of the reporter in the N_{cyt}-C_{lum} topology corresponds to (100 x g49*/g49* + 49*) in untreated (-Tm) cells. (C, D, E) Yeast strains expressing the DPA49 (C), DPA103 (D) or DPA149 (E) reporters were grown to mid-log phase at 30°C in SEG media, transferred into SD media and pulse labeled after 4 h of growth. Intact glycosylated (e.g. g49) and non-glycosylated (e.g. 49) reporter and the processed reporter (U-HA) are indicated by labeled arrows.

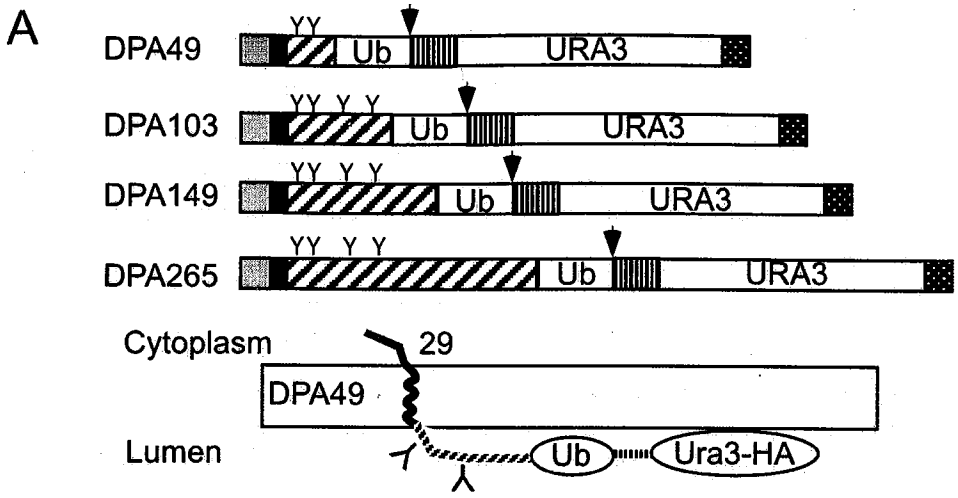
A
DPA49
DPA103
DPA149
DPA265
YY
Y
Ub
URA3
Cytoplasm
29
DPA49
Lumen
Ub
Ura3-HA

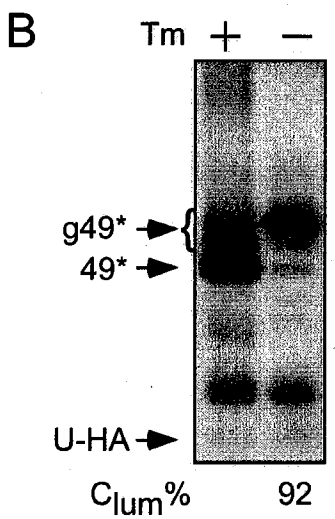
B
Tm
+
−
g49*
49*
U-HA
Clum%
92

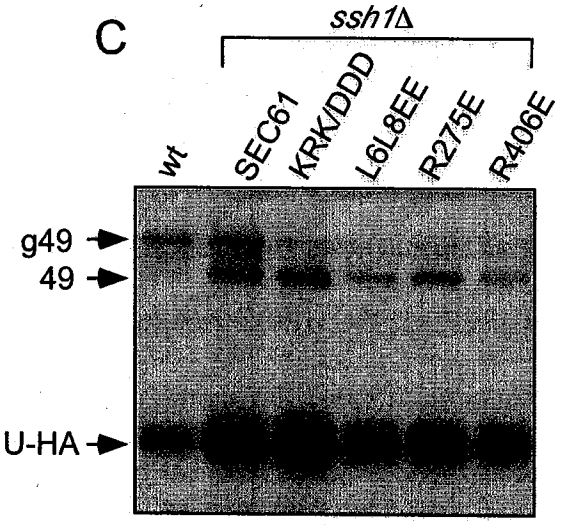
C
ssh1Δ
wt
SEC61
KRK/DDD
L6L8EE
R275E
R406E
g49
49
U-HA

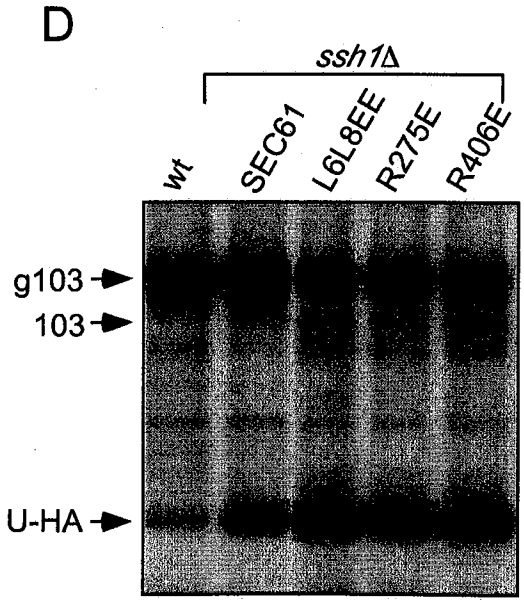
D
ssh1Δ
wt
SEC61
L6L8EE
R275E
R406E
g103
103
U-HA

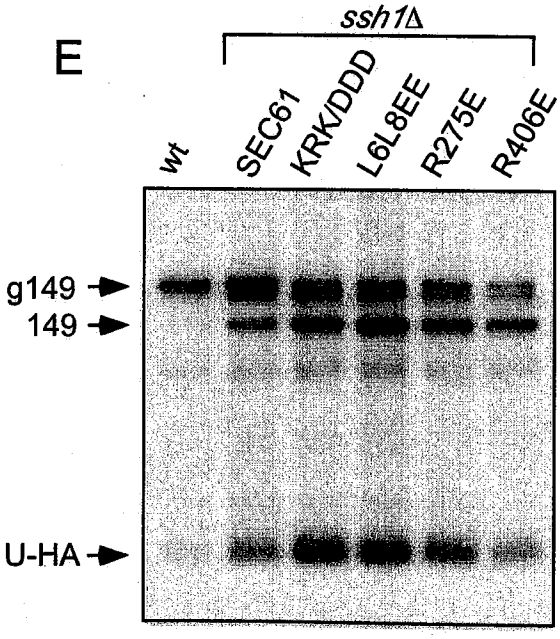
E
ssh1Δ
wt
SEC61
KRK/DDD
L6L8EE
R275E
R406E
g149
149
U-HA

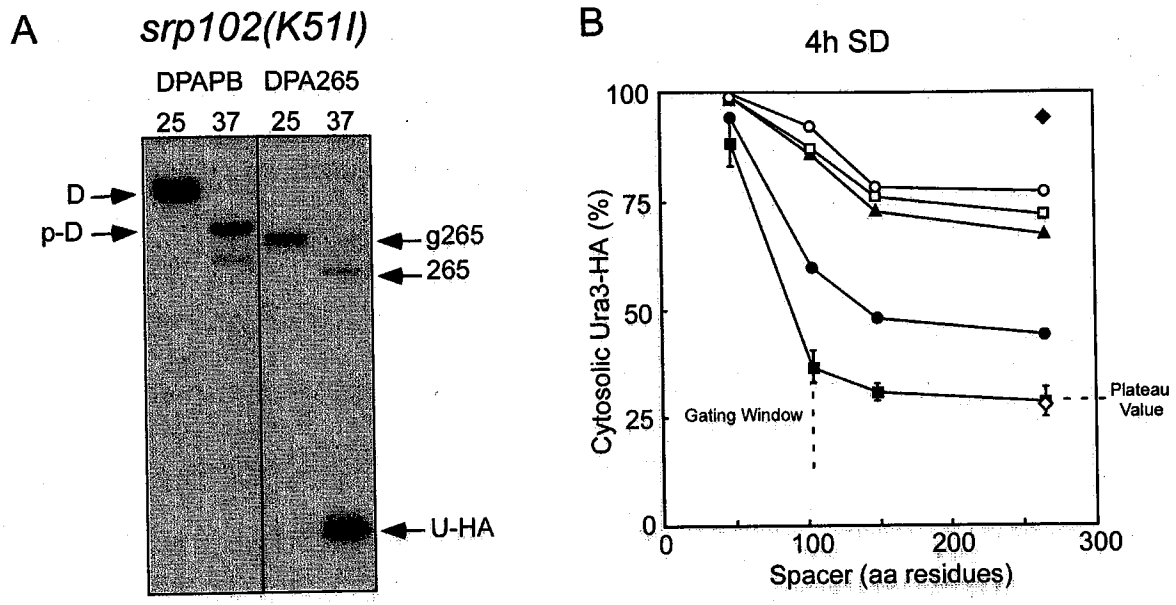

Figure 23. Delayed translocon gating in the *sec61* L6 and L8 mutants at peak time. (A) The *srp102(K51I)* mutant expressing DPAPB-HA or DPA265 was pulse labeled at 25°C, or after 3 h of growth at 37°C. Immunoprecipitates of DPAPB-HA or DPA265 were resolved in SDS-PAGE. (B) With the exception of the *srp102(K51I)* strain, all yeast strains were pulse-labeled at 30°C after 4h of growth in SD media. Cleavage of the DPA reporters was quantified as described in the Materials and Methods. Reporter cleavage (% cytosolic Ura3-HA) is expressed as a function of spacer length for the following strains: wild-type (filled squares), *srp102(K51I)* (25°C, open diamond; 37°C, filled diamond), *ssh1*Δ (filled circles), *ssh1*Δ *sec61R275E* (filled triangles), *ssh1*Δ *sec61R406E* (open squares), *ssh1*Δ *sec61R275E R406E* (open circles). Standard deviation of the reporter cleavage in wild-type strains was calculated from three sets of experimental data. For the definition of gating window, see text.

Sec61p (L6 and L8 *sec61* mutants) cause a severe but transient defect in the integration of DPAPB in an *ssh1Δ* background roughly 4 h after a culture is shifted from a nutrient poor (SEG) to a richer (SD) growth media (Cheng et al., 2005). Pulse-labeling experiments of the *sec61* mutants revealed a dramatic increase in reporter cleavage as well as the unglycosylated forms of the reporters (Fig. 22C-E). Non-integrated DPAPB accumulates as a membrane-associated aggregate in the *sec61* mutants (Cheng et al., 2005), which likely explains the presence of uncleaved non-glycosylated DPA reporters. Regardless of spacer length, DPA reporter cleavage was elevated in the L6 and L8 *sec61* mutants (Fig. 23B, open circles, squares and triangles). The gating kinetics of the Sec61 complex were retarded in the L6 and L8 *sec61* mutants relative to the wild type strain, as reporter cleavage decreased across a wider range of spacer lengths.

After 24h of growth in SD media (Fig. 24B), wild-type cells display identical kinetics of translocon gating. A decrease in reporter cleavage is observed for the *ssh1* null strain (Fig. 24B, closed circles), which shows a similar rate of translocon gating by RNCs relative to wild-type strain. The L6 and L8 *sec61* mutants show roughly a 10% decrease in the cleavage of DPA149 and DPA265. Again, the translocon gating by RNCs was retarded in *sec61* mutant strains at 24h. However, *sec61* mutants in *SSH1* background display a marked decrease in reporter cleavage (Fig. 24B, open triangles). This result agrees with the theory that the Ssh1 complex rescues the translocation defects in the L6 and L8 sec61 mutants by providing an auxiliary translocon for the cotranslational pathway.

Yeast *srp54Δ* mutants are viable (Hann and Walter, 1991) and adapt to the loss of the SRP targeting pathway by a complex response that includes increased expression of cytosolic chaperones and a decreased rate of protein synthesis (Mutka and Walter, 2001). In contrast to the *sec61* L6 and L8 mutants (Fig. 22), unglycosylated forms of intact reporters are not detected

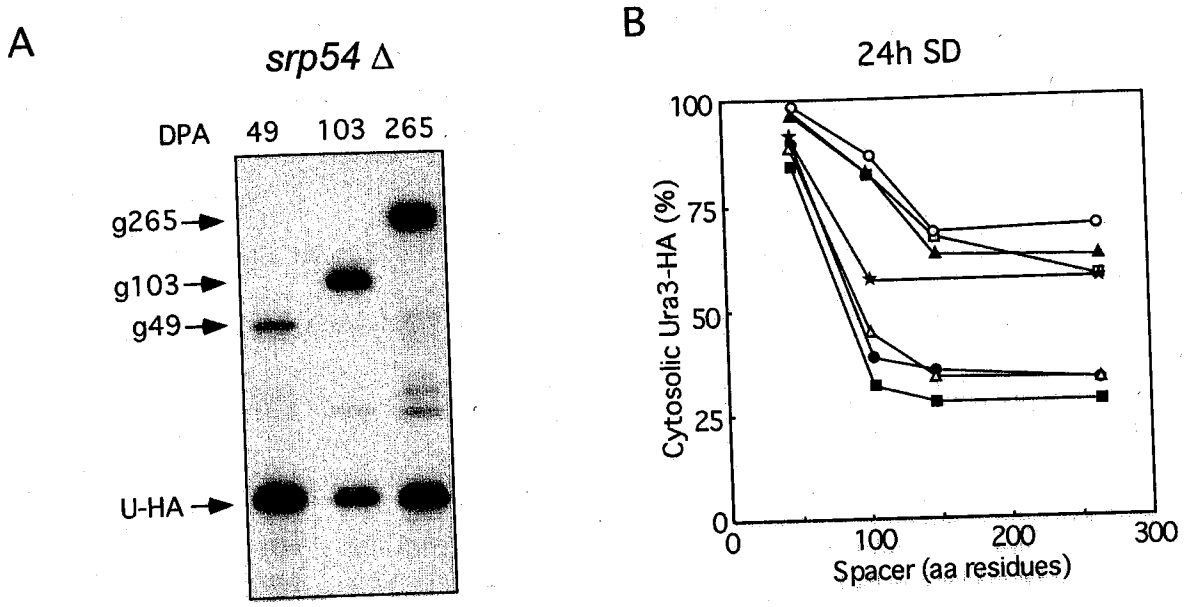

Figure 24. Translocon gating in *srp54Δ* and the *sec61* L6 and L8 mutants after adaptation. (A) The *srp54*Δ mutant expressing DPA series of UTA reporters was pulse labeled at 30°C in SD media. (B) With the exception of the *srp54*Δ strain, all yeast strains were pulse-labeled at 30°C after 24h of growth in SD media. Cleavage of the DPA reporters was quantified as in Fig 22. Reporter cleavage (% cytosolic Ura3-HA) is expressed as a function of spacer length for the following strains: wild-type (filled squares), *srp54*Δ (stars), *ssh1*Δ (filled circles), *ssh1*Δ *sec61R275E* (filled triangles), *ssh1*Δ *sec61R406E* (open squares), *ssh1*Δ *sec61R275E R406E* (open circles), *SSH1sec61R275E R406E* (open triangles).

in the *srp54Δ* strain, which is consistent with efficient translocation in the *srp54Δ* strain after adaptation. Interestingly, the *srp54D* strain shows high, yet incomplete reporter cleavage. (Fig. 24A, 24B stars), suggesting that DPAPB integration in the *srp54D* strain following adaptation is not solely dependent upon a posttranslational pathway. The rapid translocon gating by RNCs in the *srp54D* strain suggests that the delay observed in *sec61* mutants is not due to a slow SRP-dependent targeting step.

After 24h of growth in SD media, the L6 and L8 *sec61* mutants display relatively minor defects in DPAPB integration (Cheng et al., 2005), yet show an elevated level of DPA265 cleavage (Fig. 25). For both wild type and mutant strains, DPA reporter cleavage (%) was greater than the DPAPB precursor accumulation (Fig. 25). We conclude that roughly 20% of DPAPB is integrated by a posttranslational pathway in vivo. Prior to adaptation the posttranslational targeting pathway for DPAPB is readily saturated, hence pDPAPB accumulates in the cytosol of the *sec61* mutants as shown in Fig. 14. Adaptation of the L6 and L8 *sec61* mutants, like the *srp54Δ* strain, appears to occur by an enhanced ability of pDPAPB to enter a posttranslational translocation pathway (Fig. 25, compare 4 and 24 h columns). Together, these results indicate that DPA series of UTA reporters can be used to investigate the in vivo kinetics of membrane protein integration.

Delayed gating of the translocon by DPA RNCs

As reported previously (Johnsson and Varshavsky, 1994) and confirmed here using the Suc2-34 and Suc2-60 reporters (Fig. 26A, 26B), translocon gating by the invertase (Suc2) signal sequence is rapid. Moreover, the DPA spacer segment in Suc2-296 does not interfere with rapid translocon gating (Fig. 26A, 26B, quantified in 26D, circles). The spacer length dependence for the DPA and Suc2 reporters is strikingly different (Fig. 26D, filled squares). Delayed translocon

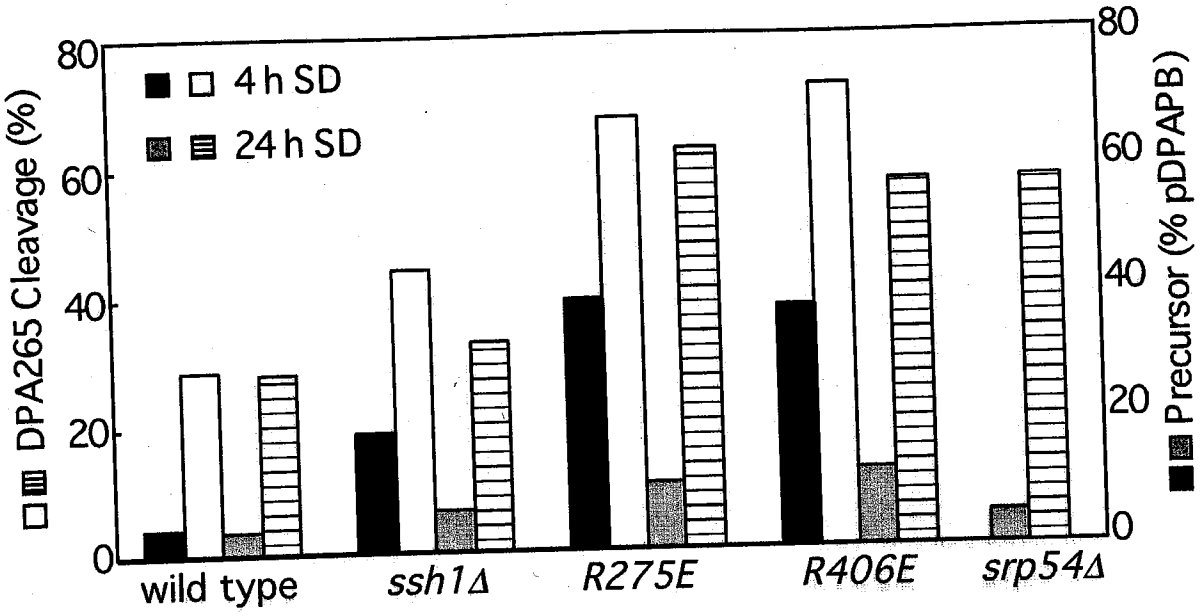

Figure 25. A comparison of DPA265 reporter cleavage and DPAPB-HA integration in wild-type and mutant strains. Data for DPAPB-HA integration is taken from Fig. 11. (Cheng et al., 2005).

gating by DPA-RNCs relative to Suc2-RNCs might be explained by slow targeting of the DPA-RNC to the translocon. Reducing the protein synthesis rate should allow additional time for a slow early step, resulting in a decreased percentage of reporter cleavage. Pulse labeling of cells in the presence of sufficient cycloheximide to reduce ^{35}S methionine incorporation by 4-fold did not significantly alter the spacer-length dependence of reporter cleavage (Fig. 26C, quantified in Fig. 26D). We conclude the slow step in translocon gating likely occurs after the DPA-RNC has been targeted to the Sec61 complex.

The DPA Nub reporter (Fig. 26A) was constructed to test whether the N terminal 34 residues of ubiquitin (Nub) acquires sufficient secondary structure to interfere with reporter translocation prior to emergence of the entire Ub domain from the ribosome. Complex formation between ubiquitin fragments (Nub and Cub) is the basis for the split-ubiquitin procedure for detecting protein-protein interactions (Johnsson and Varshavsky, 1994). If a folded Nub domain interferes with lumenal domain transport, reporter cleavage for DPA-Nub should be similar to DPA49. Quantification of DPA-Nub cleavage indicates that the Nub domain serves as a relatively inert spacer segment (Fig. 26D, open square), so it seems likely that the entire Ub domain must emerge before reporter domain translocation is prevented. Thus, 125-170 residues of the nascent polypeptide following the TM span (49-94 residue spacer plus 76 residue Ub domain) are exposed to the cytosol before the translocon is gated by a DPA-RNC.

Ribosome dynamics during integration of a polytopic membrane protein

Once the translocon is gated by an RNC synthesizing a polytopic membrane protein, downstream TM spans might act as extra "spacer segments" in the ubiquitin translocation assay. However, if exit of TM spans from the channel into the lipid bilayer is slow relative to the rate of protein synthesis, a loop of non-translocated protein could form on the cytoplasmic face of the

Figure 26. Kinetics of translocon gating by Suc2 and DPAPB RNCs. (A) Diagrams of DPA-Nub and the Suc2 series of UTA reporters. In DPA-Nub, the N-terminal 34 residues of the Ub domain are inserted between tandem copies of the 49 residue DPA spacer segment. In the Suc2 series, the signal sequence of Suc2p (black box, $Suc2_{1-19}$) is followed by spacer segments derived from Suc2p (horizontal hatch) and DPAPB (diagonal hatch). The remaining elements of the reporter are identical to the DPA series. (B, C) Yeast expressing either the Suc2 series (B) or the DPA series (C) of UTA reporters were pulse-labeled in the absence or presence of 0.5 μg/ml of cycloheximide (CHX). The volume of labeled cells and the exposure times for the autoradiograms were doubled to compensate for a 4-fold reduction in protein synthesis in CHX-treated cells. Intact reporters and processed products (U-HA) are indicated by labeled arrows. (D) Reporter cleavage is expressed as a function of spacer length for the Suc2 series (circles), DPA-Nub (open square) and DPA series (- CHX, squares; +CHX, triangles) of UTA reporters.

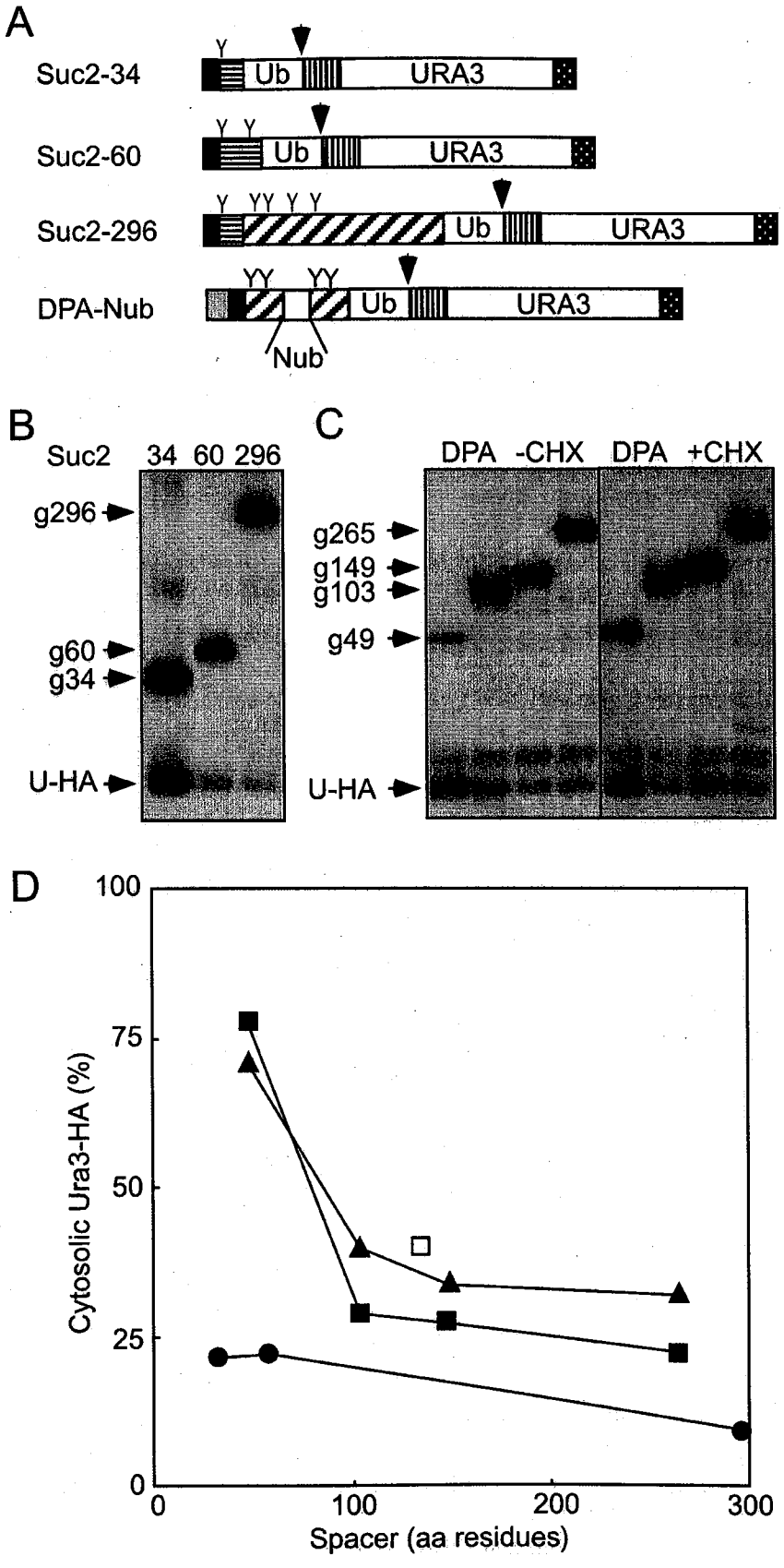
A
Suc2-34
Ub
URA3
Suc2-60
Ub
URA3
Suc2-296
Ub
URA3
DPA-Nub
Ub
URA3
Nub
B
Suc2
34 60 296
g296
g60
g34
U-HA
C
DPA -CHX DPA +CHX
g265
g149
g103
g49
U-HA
D
Cytosolic Ura3-HA (%)
100
75
50
25
0
0
100
200
300
Spacer (aa residues)

membrane. To investigate the dynamics of the ribosome-channel junction during integration of a polytopic membrane protein, the DPAPB TM span and flanking sequences were triplicated to obtain the 3TM series of reporters (Fig. 27A). Charged residues were introduced into the segments flanking TM2 to favor integration of this TM in the N_{lum}- C_{cyt} orientation.

The folding defective ub* derivatives were analyzed to determine whether these constructs are integrated in the 3TM N_{Cyt}-C_{lum} orientation (Fig. 27C). Incomplete glycosylation of the N-X-T/S sites in the spacer domain is responsible for the doublet of glycosylated reporters (g49* and g265*). Although 87% of the 3TM265ub* was integrated in the correct topology, the fidelity of reporter orientation was lower for 3TM49ub*. Intact 3TM reporters as well as the cleaved URA3-HA domain were detected upon expression in wild type cells (Fig. 27B). The spacer length dependence for 3TM reporter cleavage was initially calculated by defining the spacer as being the segment between the C-terminal end of TM1, and the start of the Ub domain (Fig. 27D, open circles). A comparison to the results obtained with the DPA reporters (Fig. 27D, squares) indicates that TM2, TM3 and the intervening loops do not act as spacer segments to decrease 3TM reporter cleavage. When the spacer length is defined as the distance between TM3 and the Ub domain, the translocon gating window is wider than that observed for the DPA series (Fig. 27D, filled circles). These results indicate that a surprisingly large segment of the lumenal domain of a polytopic integral membrane protein is transiently exposed to the cytosol during integration.

Impact of loop size on translocon gating by TM3

Delayed gating of the Sec61 complex by TM1, and slow exit of TM spans into the membrane bilayer could contribute to prolonged cytosolic exposure of the 3TM reporter domain. We tested whether expansion of the lumenal loop (L1) by 128 residues or the cytoplasmic loop

Figure 27. Cytoplasmic exposure of transmembrane spans and lumenal segments during integration of a polytopic membrane protein. (A) A diagram of the predicted topology, loop size, and location of glycosylation sites (Y) in the 3TM49 reporter. The remaining elements of the reporter, including the spacer segments, are identical to the DPA series. (B) Yeast cells expressing the 3TM series of reporters were pulse-labeled in the absence or presence of tunicamycin (Tm). Glycosylated intact reporters (g49-g265), unglycosylated intact reporter (49) and the cleaved reporter domain (U-HA) are labeled. (C) Pulse-labeling of yeast expressing the 3TM49-ub* or 3TM265-ub*reporters. The % integration of the reporter in the N_{cyt}-C_{lum} topology was calculated as in Fig. 21. (D) Reporter cleavage (% cytosolic Ura3-HA) is expressed as a function of spacer length for the DPA series (filled squares) and 3TM series (filled circles) of UTA reporters. Reporter cleavage for the 3TM reporters was re-plotted with the spacer segment defined as the length in amino acid residues between the C-terminal end of TM1 and the Ub domain (open circles).

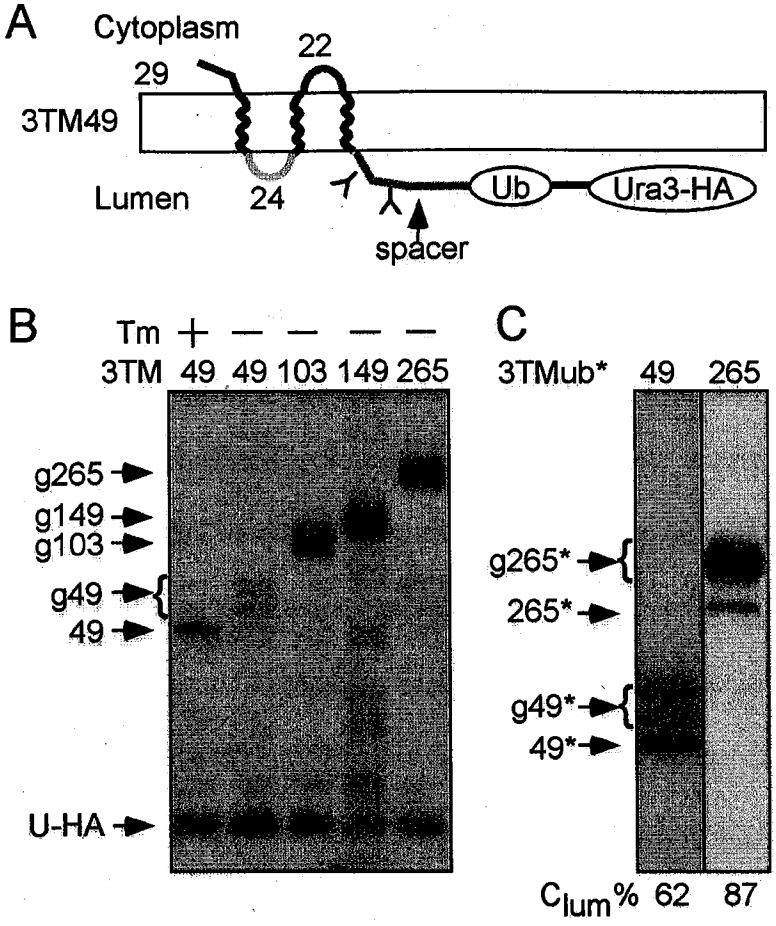
A
Cytoplasm
22
29
3TM49
Lumen
24
Ub
Ura3-HA
spacer
B
Tm + − − − −
3TM 49 49 103 149 265
g265
g149
g103
g49
49
U-HA
C
3TMub* 49 265
g265*
265*
g49*
49*
Clum% 62 87
D
Cytosolic Ura3-HA (%)
100
75
50
25
0
0 100 200 300 400
Spacer (aa residues)

(L2) by 104 residues could overcome slow steps in 3TM integration (Fig. 28A). The L1-IN reporters are more efficiently integrated in the 3TM (N_{cyt}-C_{lum}) topology than the L2-IN or 3TM reporters (Fig. 28B). Expansion of L1 also caused a significant reduction in reporter cleavage relative to the 3TM series (Fig. 28C, 28D, triangles and circles). The expanded L1 loop is identical in length and sequence to the 149-residue spacer segment in DPA149. Thus, the L1-insertion allows translocon gating to occur before TM2 emerges from the ribosome, just as a spacer segment of this length allows translocon gating in DPA149. However, subsequent events in the integration of the L1-IN reporter still favor cytosolic exposure of the Ub domain, as reporter cleavage decreases as the spacer segment is increased from 49 to 149 residues. Expansion of the cytosolic loop (L2) had a subtle, but interesting effect on the spacer-length dependence of reporter cleavage (Fig. 28C and 28D). In comparison to the 3TM reporter, the plateau value for L2-IN cleavage was reached at a shorter spacer length (L3-IN103) suggesting that L2 expansion facilitates more rapid gating of the channel by TM3.

Translocon gating by (N_{cyt}-C_{lum}) TM spans

The N-terminal 68 residues of the 3TM reporter were replaced with $Suc2_{1-79}$ (Fig. 29A, S2TM) to determine whether rapid translocon gating by the invertase signal sequence would eliminate the cytosolic exposure of the Ub domain. Signal sequence cleaved (c49*) and uncleaved (49*) forms of S2TM49ub* were detected when cells were labeled in the presence of tunicamycin (Fig. 29B + Tm). In the absence of tunicamycin, the major glycoform of the reporter has three N-linked oligosaccharides indicating that both pairs of N-X-T/S sites are simultaneously exposed to the ER lumen in the majority (71%) of the reporter molecules. As observed for several other ub* derivatives (Fig. 27B and 28B), the fidelity of reporter integration was higher with the longer spacer segment (Fig. 29B). In contrast to the 3TM series,

S2TM reporter cleavage decreased gradually as the spacer was elongated from 49 to 265 residues (Fig. 29C, 29D squares), indicating delayed translocon gating by the final TM span. The combination of the cleavable Suc2 signal sequence and a minimal lumenal domain retards subsequent events in reporter integration. The SL1-IN reporters were constructed to determine whether extension of the N-terminal lumenal segment by an additional 116 residues would overcome the inhibitory effect of the Suc2 signal sequence (Fig. 29A). The SL1-IN reporters were efficiently integrated in the 2TM (N_{lum}-C_{lum}) orientation regardless of spacer length (Fig. 29B). Expansion of the N-terminal lumenal domain significantly reduced reporter cleavage relative to the 3TM series (Fig. 27) and to the S2TM series (Fig. 29C, 29D). Nonetheless, the Ub domain is transiently exposed to the cytosol if the spacer segment is short.

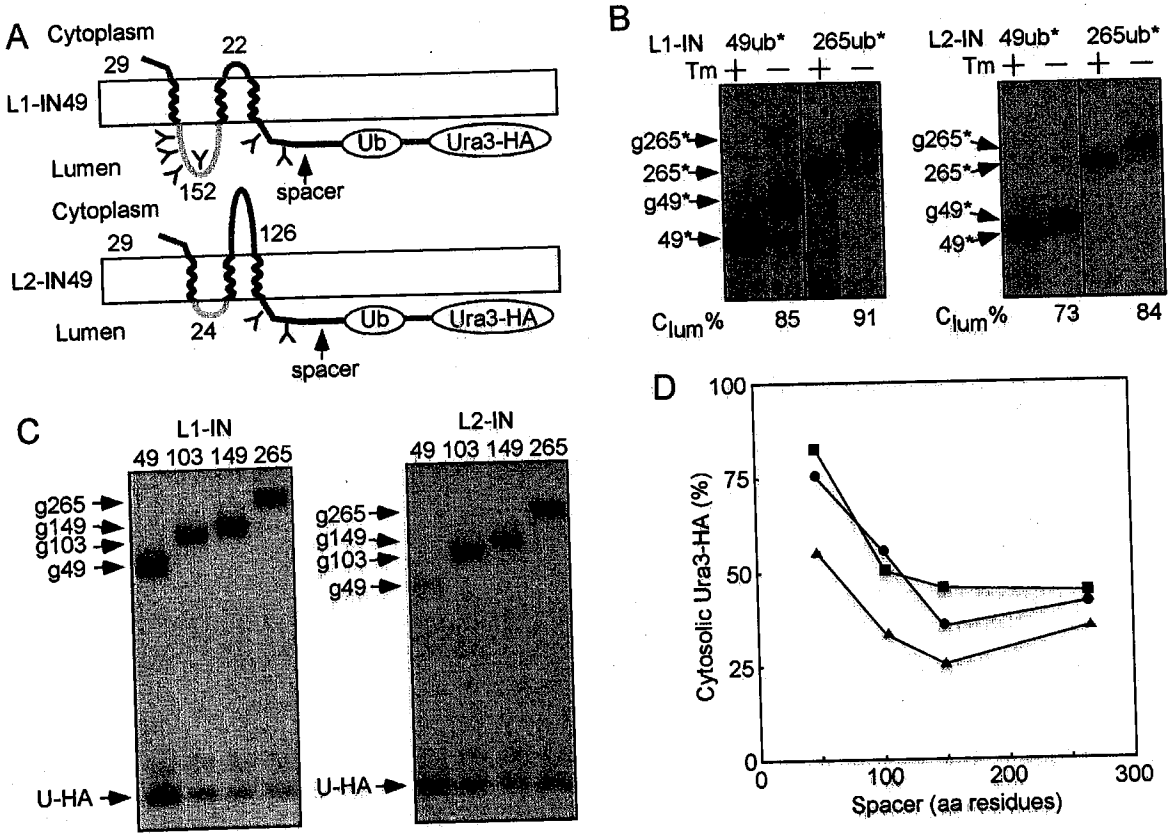

Figure 28. Effect of loop insertions on UTA reporter cleavage. (A) Diagrams of the predicted topology, loop size, and location of glycosylation sites (Y) in the L1-IN49 and L2-IN49 reporters. The remaining elements of the reporter, including the spacer segments, are identical to the 3TM series. (B) Wild type yeast expressing the folding-impaired UTA reporters were pulse labeled in the presence or absence of tunicamycin (Tm). The percent integration of the reporter in the N_{cyt}-C_{lum} topology was calculated as in Fig. 21. (C) Pulse-labeling of wild-type yeast expressing the L1-IN and L2-IN series of UTA reporters. Glycosylated full-length reporters (g49-g265), and processed products (U-HA) are labeled. (D) Reporter cleavage is expressed as a function of spacer length for the 3TM (circles, taken from Fig. 23), L1-IN (triangles) and L2-IN (squares) series of UTA reporters.

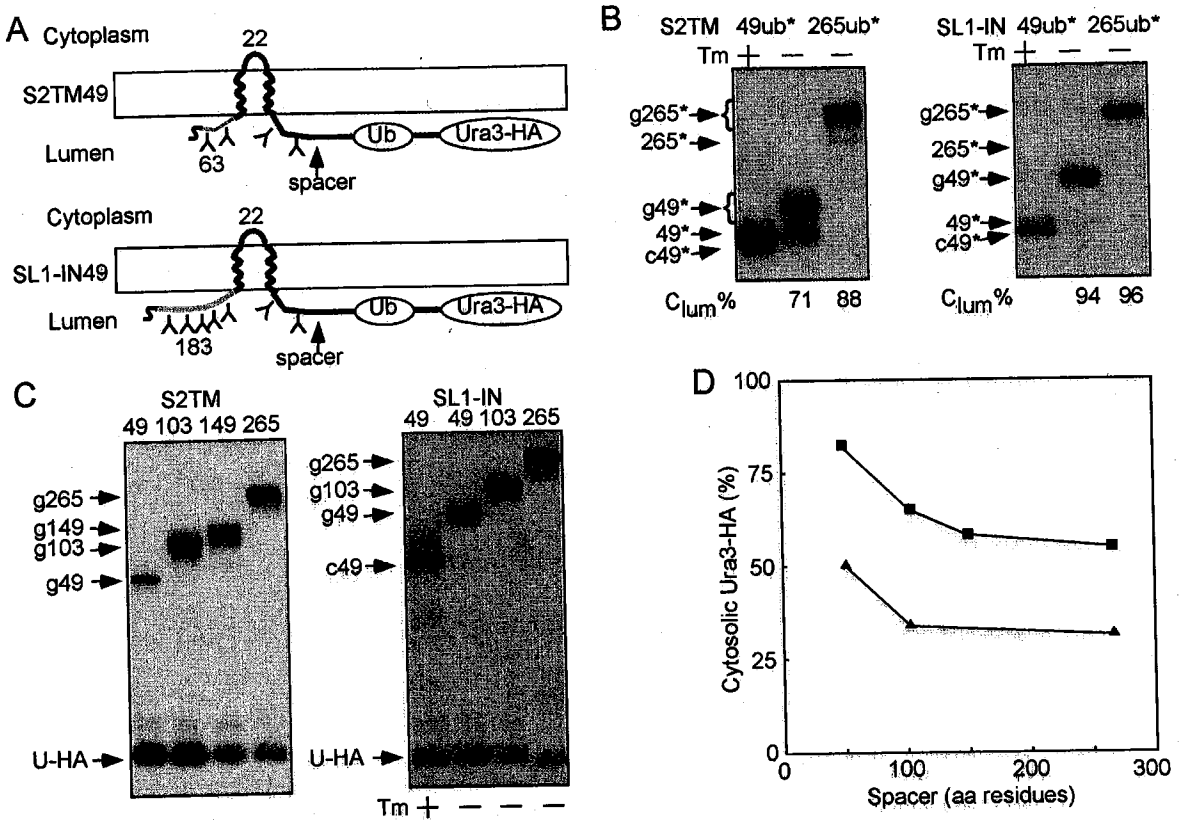

Figure 29. Targeting of membrane proteins by the Suc2 signal sequence. (A) Diagrams of the predicted topology, lumenal domain length, and location of glycosylation sites (Y) in the S2TM and SL1-IN49 reporters (see Methods for reporter construction). The N-terminal invertase signal sequence is designated by the S. (B) Pulse labeling of yeast cultures expressing the folding-impaired reporters in the presence or absence of tunicamycin (Tm). In the presence of Tm, cleavage of Suc2p signal sequence yielded the polypeptide designated as c49. The percent integration of the reporter in the N_{cyt}-C_{lum} topology was calculated as in Fig. 21. (C) Pulse-labeling of wild-type yeast expressing the S2TM and SL1-IN series of UTA reporters in the presence or absence of tunicamycin (Tm). Glycosylated full-length reporters (g49-g265), and processed products (U-HA) are labeled. (D) Reporter cleavage is expressed as a function of spacer length for the S2TM (squares) and SL1-IN (triangles) series of UTA reporters.

Discussion

Few previous studies have investigated the kinetics of membrane protein integration in vivo (Goder et al., 2000; Goder and Spiess, 2003). Here, we have used UTA reporters derived from the type II integral membrane protein DPAPB to analyze cotranslational integration of membrane proteins into the yeast endoplasmic reticulum. Yeast SRP reduces polypeptide elongation rates in vivo, thus extending the time window for RNC targeting to the translocon (Mason et al., 2000). In wild type cells, SRP recognition of DPA RNCs is inefficient as roughly 20% of DPAPB nascent chains reach a critical size that mandates entry into a posttranslational targeting pathway. The posttranslational targeting pathway for DPAPB is saturable, resulting in a low basal level of untranslocated precursor in wild type cells and increased pDPAPB in the *sec61* L6 and L8 mutants prior to adaptation (Cheng et al., 2005).

Rapid cotranslational folding of the Ub domain in the cytoplasm prevents translocation of downstream segments and allows reporter cleavage (Johnsson and Varshavsky, 1994). These properties allow the calculation of nascent polypeptide length when a translocon is gated by an RNC translating a UTA reporter. Gating of the translocon by the majority of Suc2 RNCs initiates after 110 (Johnsson and Varshavsky, 1994), but is completed before, 130 residues of polypeptide emerge from the polypeptide exit tunnel on the large ribosomal subunit (19 residue signal sequence + 13 to 33 residue spacer + 76 residue Ub domain). Translocon gating by the majority of DPA RNCs occurs after 170, but before 220 residues of polypeptide emerge from the ribosome. While translocon gating by DPA RNCs occurs within a narrow window, it is not synchronous, but is instead stochastic. The calculated nascent polypeptide lengths for translocon gating are in apparent conflict with a considerable amount of data obtained using in vitro experimental systems. Secretory RNCs assembled using termination codon-deficient mRNAs

can gate the mammalian Sec61 complex when as few as 50-60 residues of polypeptide emerge from the ribosome (Connolly et al., 1989; Crowley et al., 1993; Jungnickel and Rapoport, 1995). Interactions between nascent integral membrane proteins and the translocon are also detected shortly after the first TM span emerges from the ribosome (Heinrich et al., 2000; Heinrich and Rapoport, 2003; McCormick et al., 2003; Mothes et al., 1997; Sadlish et al., 2005). Moreover, the yeast RNC-translocon complex that has been visualized by cryoelectron microscopy was assembled using a truncated DPAPB mRNA that encodes the N-terminal 120 residues of DPAPB (Beckmann et al., 2001). We propose that the nascent polypeptide length defined by the in vitro experiments defines the minimal transit path for the polypeptide between the peptidyltransferase site on the ribosome and the SSB site in the Sec61 heterotrimer. Our results indicate that one or more of the events that precede translocon gating are slow relative to the in vivo rate of polypeptide elongation in a eukaryotic cell (~ 5 residues/second) (Hershey, 1991; Pathak et al., 1988), hence the minimal transit path does not accurately describe the ensemble of nascent polypeptide conformations that exist during secretory protein translocation or membrane protein integration within the cell. The conformational changes in Sec61p that allow signal sequence insertion into the SSB site and opening of the lumenal gate are good candidates for rate limiting steps in translocon gating that are revealed by in vivo analysis using UTA reporters, yet are not detected when elongation arrested RNCs are targeted to the Sec61 complex in vitro.

Signal sequences for secretory proteins are inserted into the SSB site of Sec61p in the N_{cyt}-C_{lum} orientation to allow translocation of the nascent polypeptide through the hourglass shaped pore in Sec61p. The TM span in a type II integral membrane protein also adopts the N_{cyt}-C_{lum} orientation, yet we observe a considerable delay in translocon gating by DPA RNCs relative to Suc2 RNCs. Compared to a cleavable signal sequence, a TM span usually has a longer and more

hydrophobic core, which would favor the translocation of the N-terminus (Sato et al., 1990; Wahlberg and Spiess, 1997). A recent in vivo analysis of membrane protein integration in mammalian cells suggests that the TM span of a Type II protein is initially inserted in the N_{lum}-C_{cyt} orientation (Goder and Spiess, 2003). The rate at which TM spans invert to adopt the type II orientation is increased by the addition of positively charged residues that precede the TM span and decreased as the TM span in lengthened (Goder and Spiess, 2003). Although TM span inversion can occur during a surprisingly long time window (~50 sec), the DPA TM sequence favors a more rapid inversion (< 20 sec) based upon the model proteins analyzed by Goder and Spiess. A 10 sec delay to allow the DPA span to adopt the type II orientation in the translocon could account for cytoplasmic accumulation of the Ub domain in the DPA reporters.

Current models for the integration of polytopic integral membrane proteins describe an orderly and stepwise integration of membrane spanning segments, translocation of lumenal loops and retention of cytoplasmic loops in a process that is intimately coupled to elongation of the nascent polypeptide. Analysis of the 3TM series of UTA reporters revealed an unanticipated cytoplasmic exposure of reporter domains that follow TM3, which like the DPA TM span, is integrated in the N_{cyt}-C_{lum} orientation. Instead of acting as spacer segments that reduce cytosolic exposure of Ub domain, TM2 and TM3 enhance exposure of the reporter domain. Several slow steps contribute to the delay in translocation of the reporter domain. By the time the 3TM RNCs are targeted to the translocon, TM2 has probably emerged from the large ribosomal subunit (Fig. 30a). Insertion of TM1 into the SSB site in the N_{lum}-C_{cyt} orientation without inversion (Fig. 30b) leads to reporter misorientation. Based upon the translocon-gating window defined by the DPA reporters, TM3 also emerges from the ribosome before the translocon is gated by TM1 (Fig. 30c). Before TM3 can insert into the SSB site in the N_{cyt}-C_{lum} orientation to re-gate the transport

pore after synthesis of L2 (Fig. 30g), the following events are thought to occur: TM1 exits Sec61p through the lateral gate (Fig. 30d), TM2 moves from the transport pore into the SSB site (Fig. 30e) and TM2 exits Sec61p through the lateral gate (Fig. 30f). Continued elongation of the polypeptide during these steps results in cytoplasmic exposure of the lumenal domain. Based upon the crystal structure of the SecYEβ complex (Van den Berg et al., 2004), the cytoplasmic face of the Sec61p transport pore is not large enough to accommodate a folded Ub domain, hence the loop of untranslocated polypeptide must be extruded laterally into the cytoplasm. One difference between this model, and previous models for membrane protein integration (Rapoport et al., 2004; Sadlish et al., 2005), is that we explicitly indicate that the lateral movement of TM spans between the transport pore, SSB site and the phospholipid bilayer are slow relative to the rate of nascent polypeptide elongation.

The simultaneous extra-ribosomal exposure of TM2 and TM3 likely explains why the 3TMUb*49 construct shows a reduced efficiency of integration in the 3TM N_{cyt}-C_{lum} orientation. If the residues flanking TM2 had not been changed to favor insertion in the N_{lum}-C_{cyt} orientation, misorientation could be explained by competition between adjacent topogenic sequence elements (Monne et al., 2005). We observed a higher percentage of misorientation for the Ub*49 derivative than the Ub*265 derivative for the 3TM and L2-IN series of reporters. Cytoplasmic folding of the URA3 domain in the ub* derivatives may interfere with reporter integration when the spacer segments are short.

The 25 residue loops in the 3TM reporter are not unusually short for multi-pass integral membrane proteins. Expansion of L1 by 128 residues reduced extra-ribosomal exposure of TM2 and TM3 during the time window for TM1 insertion (Fig. 30c), and this led to a significant decrease in the percentage of misoriented Ub* derivatives. Secondly, expansion of L1 likely

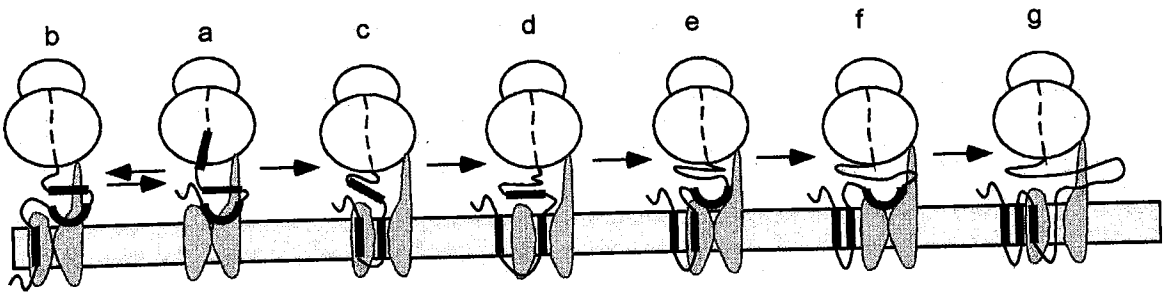

Figure 30. Cytosolic exposure of TM spans and lumenal domains during in vivo integration of a polytopic membrane protein. Intermediates a, c, d and e represent four channel conformations that differ with respect to the presence (c and e) or absence (a and d) of a TM span in the SSB site, and an open (c and d) or closed (a and e) transport pore.

allows partitioning of TM1 into the bilayer prior to entry of TM2 into the transport pore, thereby facilitating more rapid transfer of TM2 into the SSB site (Fig. 30e). Lateral exit of hydrophobic TM spans is energetically favorable, and occurs before termination of protein synthesis (Heinrich and Rapoport, 2003).

Expansion of the L2 loop does not prevent extra-ribosomal exposure of TM2 prior to translocon gating, hence misorientation of the ub* derivatives was similar to the 3TM series. Expansion of L2 reduces the delay associated with TM3 gating of the pore resulting in a spacer length dependence curve that resembles the DPA series. How can we explain the residual delay in reporter translocation displayed by the L2-IN reporters? Fluorescence quenching experiments have shown that the lumenal gate of the translocon is closed during synthesis of a cytosolic loop (Liao et al., 1997). Gating of the translocon by a TM3 and TM1 are mechanistically similar as both segments are inserted into the channel in the N_{cyt}-C_{lum} orientation. Contact between TM3 and the SSB site permits insertion of a polypeptide hairpin that gates the transport pore (Fig. 30g), and is dependent upon egress of TM2 through the lateral gate. Presumably, TM2 is primed for lateral exit by the time TM3 emerges from the ribosome. Site-specific photocrosslinking studies have begun to reveal how the translocon is gated by a TM span in the type II orientation (Sadlish et al., 2005).

Replacement of TM1 with the invertase signal sequence provided a second strategy to eliminate the delay in translocon gating caused by the type II orientation of TM1. This approach did not result in decreased reporter cleavage when the L1 domain was short (e.g. 59 residues in S2TM). Even though the invertase signal sequence allows more rapid translocon gating, TM2 and TM3 emerge from the ribosome within the gating window (110 to 130 residues for Suc2-RNCs), and this leads to an elevated percentage of misoriented reporters when the spacer

segment is short. Elevated cleavage of the S2TM reporters indicates that the close spacing between the cleavable signal sequence and the TM spans causes an additional delay in channel gating by the TM3 segment. The normal fate for an N-terminal signal sequence is to remain bound to Sec61p until cleaved by signal peptidase, hence the invertase signal sequence may impede exit of TM2 through the lateral gate. Signal sequence cleavage is not an early event during nascent polypeptide transport. For example, cleavage of the preprolactin signal sequence does not occur until 120-140 residues of polypeptide emerge from the ribosome (Gilmore and Blobel, 1985; Mothes et al., 1994). Expansion of the lumenal domain to 185 residues virtually eliminated misorientation of the Ub* derivatives because the translocon gating step was completed before synthesis of the TM spans. Expansion of the lumenal domain accelerates one of more of the slow steps in membrane protein integration. Presumably, cleavage of the signal sequence allows unobstructed movement of the TM2 segment from the channel pore into the lateral gate, thereby minimizing the time required for channel gating upon exposure of TM3.

Extensive cytosolic exposure of TM spans and lumenal domains could have a negative impact on the fidelity of membrane protein integration if cells do not possess a mechanism to prevent premature folding of a lumenal domain or aggregation of TM spans in the cytosol. C-terminal reporter domains can reduce the fidelity of membrane protein integration in *S. cerevisiae* (Green and Walter, 1992; Kim et al., 2003), particularly when the reporter domain is derived from a cytosolic protein. Long loops or pauses during translation may allow the preceding segments to achieve the correct topology before the following domains emerge from the ribosome. Chemical differences in the protein-folding environment of the ER lumen and the cytosol may bias against cytosolic folding of lumenal protein domains. In addition, cytosolic chaperones may assist in the

cotranslational integration of membrane proteins that are composed of multiple closely spaced TM spans.